POLITECNICO DI MILANO

DEPARTMENT OF ELECTRONICS, INFORMATION AND BIOENGINEERING

DOCTORAL PROGRAM IN BIOENGINEERING

Dynamic cardiovascular control of arterial blood pressure and heart rate in response to central volume variations and anesthesia.

Doctoral dissertation of:

Guadalupe Dorantes Méndez

Advisor:
PhD Manuela Ferrario

Tutor:
Prof. Maria Gabriella Signorini

Supervisor of the PhD Program:
Prof. Maria Gabriella Signorini

XXV Cycle
2013

Ph.D. Thesis in Biomedical Engineering

Guadalupe Dorantes Méndez
Department of Electronics, Information and Bioengineering
Politecnico di Milano
Piazza Leonardo da Vinci, 32
20133 Milano, Italy
e-mail: guadalupe.dorantes@polimi.it

Dynamic cardiovascular control of arterial blood pressure and heart rate in response to central volume variations and anesthesia.

Doctoral dissertation of:

Guadalupe Dorantes Méndez

Advisor:
PhD Manuela Ferrario

Tutor:
Prof. Maria Gabriella Signorini

Supervisor of the PhD Program:
Prof. Maria Gabriella Signorini

XXV Cycle
2013

Learn from yesterday, live for today, hope for tomorrow.

The important thing is not to stop questioning.

Albert Einstein

Dedicated to my parents

and my brothers

Acknowledgements

ABSTRACT

The arterial and cardiopulmonary baroreflexes are important mechanisms for short-term blood pressure regulation, and there is evidence about the clinical relevance of the analysis of these mechanisms. Since changes in the characteristics of baroreflex function can reflect alterations in autonomic control of the cardiovascular system, the analysis of baroreflex responses can provide valuable information in clinical management.

Maintenance of arterial blood pressure (ABP) to prevent hypotension and preservation of organ perfusion are the main challenges faced by the clinicians during hemodynamic monitoring in major surgery as well as in the intensive care unit. In this context, the aim of this thesis is to assess arterial and cardiopulmonary baroreflexes during perioperative maneuvers through mathematical models, in order to provide quantitative indices that may contribute to the characterization of hemodynamic status of patients and give additional information that could help, for instance, to support the decision making process of anesthesiologists, constantly faced with the challenge of identifying the optimal strategy to stabilize volumes and pressures during surgery.

The maneuvers that were explored in this thesis were oriented to study alterations due to anesthesia and variations in central volumes, in particular in the venous return. In fact, intraoperative fluid infusion is meant to restore cardiac output. In addition, the lower body negative pressure (LBNP) procedure produces a decrease in venous return, and it is meant as a model of hemorrhage. Finally, long duration bed rest is a model of cardiovascular deconditioning.

In particular, the novel contribution of this thesis lies therefore on the analysis approaches used to assess arterial and cardiopulmonary baroreflexes from non invasive or minimally invasive recordings and in the application to different experimental conditions.

The analysis approaches used in this thesis consisted in a) mathematical techniques for estimation of arterial baroreflex sensitivity, considering causality in the relationship between systolic blood pressure (SBP) and heart rate (HR); b) black box models for the assessment of the role of arterial and cardiopulmonary baroreflex control on HR and the role of cardiopulmonary baroreflex control of afterload and heart contractility; and c) a system identification model of total peripheral resistance baroreflexes.

Briefly this works shows that critical patients as uncontrolled hypertensive patients have a larger drop in ABP during the induction of general anesthesia and a lower

baroreflex sensitivity than non-hypertensive patients, consistent with this pathological condition. Moreover, the prediction model of RR was able to show the involvement of cardiopulmonary baroreflex in mediating the regulation of vascular resistance during the rapid onset of mild LBNP, and in varying HR according to a "reverse" Bainbridge mechanism. The cardiopulmonary contribution tends to become even smaller in simulated weightlessness conditions.

The results of the analysis addressed in this thesis reinforce the opinion that the assessment of arterial and cardiopulmonary baroreflexes provides additional information to guide therapy and anesthesia in the perioperative period, in order to avoid hypotensive episodes or unstable cardiovascular condition.

SUMMARY

Cardiovascular control relies on a number of complex interacting feedback mechanisms that depend on information from several sensor sites. The information on the state of the system is processed in the central autonomic control centre in the brain. This control centre generates autonomic nervous system outflow that is conveyed to the cardiovascular system by parasympathetic and sympathetic pathways which, in most instances, elicit opposite actions to maintain homeostasis. Arterial and cardiopulmonary baroreflex systems play an important role in the maintenance of blood pressures on a time scale of seconds to minutes.

The primary role of the arterial baroreflex is the rapid adjustment of blood pressure around an existing mean level. After baroreceptor signals have entered the tractus solitaries of the medulla, secondary signals inhibit the vasoconstrictor center of the medulla and excite the vagal parasympathetic center. The net effects are vasodilation of the veins and arterioles throughout the peripheral circulatory system, decreased heart rate (HR) and strength of heart contraction. Therefore, excitation of the baroreceptors by high pressure in the arteries causes the arterial pressure to decrease because of both a decrease in peripheral resistance and a decrease in cardiac output (CO). Conversely, low pressure has opposite effects, causing the pressure to rise back toward normal.

Cardiopulmonary baroreceptors sense changes in central blood volume and pressure and modulate efferent sympathetic neural outflow and vascular resistance (Mancia et al., 1983; Middlekauff et al., 1995; Hainsworth et al., 1991; Ray et al., 2000).

Modeling of short term cardiovascular variability can provide powerful insights into autonomic nervous system control of circulation (Pagani et al., 1986). Therefore, mathematical models have been developed in order to disentangle baroreflex regulation processes.

In the context of hemodynamic monitoring, which can be defined as the assessment of the dynamic interactions of hemodynamic variables in response to a defined perturbation (Pinsky et al., 2005), securing hemodynamic stability, during major surgery and in the intensive care unit (ICU), is one of the main challenges faced by the clinicians, where maintenance of blood pressure and prevention of organ perfusion deficiencies are the primary goals. Thus, analysis of autonomic nervous system control of circulation during common interventions such as anesthesia induction and administration of fluids may lead to improve maintenance of blood pressure stability and patients' outcome.

In order to explore the baroreflex responses to changes in circulating volume, analysis of fluid infusion during major surgery was performed. Volume depletion during surgery represents a challenge. For this reason, fluid removal was analyzed through a physiological model of lower body negative pressure (LBNP), which involves the application of reduced atmospheric pressure to supine resting subjects from the iliac crests caudally. Application of negative pressure to the lower body redistributes fluid from the upper body to the lower extremities, allowing for the study of hemodynamic responses to central hypovolemia (Convertino et al., 2001; Cooke et al., 2004). Responses to long duration bed rest were assessed as well. Simulated microgravity by head down bed rest (HDBR) leads to cardiovascular deconditioning with the associated reductions in blood pressure regulation during orthostatic stress. Several factors contribute to the diminished ability to maintain blood pressure in bed rest: reductions in plasma volume (Convertino et al., 1996; Buckey et al., 1996), diminished baroreflex control of HR (Sigaudo-Roussel et al., 2002), and/or reduced vascular resistance (Moffitt et al., 1998).

The main goal of this thesis is to assess arterial baroreflex, cardiopulmonary baroreflex and the role of both baroreflexes in specific conditions such as anesthesia induction, during changes in central blood volumes elicited by fluid infusion or LBNP maneuvers and during long duration bed rest. In particular, the specific aims are:

1. To quantify the causal interactions between HR and ABP in patients undergoing general anesthesia for major surgery, in particular during anesthesia induction with a bolus of propofol, and to evaluate the possible effects of propofol and of preparatory maneuvers on ABP autonomic control, in normotensive and hypertensive patients.

2. To identify arterial and cardiopulmonary baroreflex control of HR and sympathetic mediated heart rate variability (HRV) responses to mild, rapid and short duration

LBNP cycles, by black box modelling of HRV, and to shed light on the possible occurrence of the "reverse" Bainbridge Reflex.

3. To explore the response of cardiopulmonary baroreflex control of afterload and ventricular contractility to changes in venous return through fluid infusion maneuvers during major surgery and during orthostatic challenge by LBNP, in spontaneous conditions and under the effects of cardiovascular deconditioning (i.e., during an LBNP experiment before and on day 50 of bed rest.)

Arterial baroreflex control during anesthesia induction

To achieve the first aim of this thesis the evaluation of baroreflex gain is performed by means of well-known techniques and it is considered as an important tool in clinical practice in the assessment of autonomic control of the cardiovascular system in normal and disease states. In addition, this evaluation may help to understand the hemodynamic side effects of anesthetic drugs, which may be caused by direct action on the heart and the peripheral vasculature, or by alterations of cardiovascular regulation (La Rovere et al., 2008). Despite the importance of understanding the underlying physiological mechanism and its clinical value, quantification of the effects of anesthetic drugs on the cardiovascular control under general anesthesia is not fully elucidated yet, and in particular in hypertensive patients.

In this study 10 non hypertensive (NH) and 7 chronic hypertensive (CH) patients undergoing major surgery, with American Society of Anesthesiologists (ASA) classification score greater than I were enrolled in the study. A Granger causality test was performed to verify the causal relationship between RR and systolic blood pressure (SBP), and four different mathematical methods were used to estimate the baroreflex sensitivity (BRS): 1) ratio between autospectra of RR and SBP, 2) transfer function, 3) sequence method and 4) bivariate closed loop model. Three different surgical epochs were considered: awake, post-induction and post-intubation. A comparison of BRS trends in CH patients with respect to NH patients was performed as well.

The first goal was to compare BRS following anesthesia induction via propofol and after intubation to pre-induction baseline values through a systematic and mathematically robust analysis. This permits to evaluate the potential blunting of baroreflex control of HR and its residual responsiveness under anesthesia and during mechanical ventilation, prior to

the beginning of surgery. The second goal was to quantify and track the trend in BRS following anesthesia induction as well as the switch from spontaneous to mechanical ventilation, and to assess different trends in a hypertensive population when compared to normotensive patients.

In NH patients, propofol administration caused a decrease in arterial blood pressure (ABP), due to its vasodilatory effects, and a reduction of BRS, while HR remained unaltered with respect to baseline values before induction. A larger decrease in ABP was observed in CH patients when compared to NH patients, whereas HR remained unaltered and BRS was found to be lower than in the NH group at baseline, with no significant changes in the following epochs when compared to baseline.

The absence of significant changes in average HR values was found to be accompanied by a significant decrease of the total RR spectral power and of the spectral low frequency (LF, 0.04 - 0.15 Hz) component. The decrease in RR variance may be explained by the aforementioned diminished sympathetic outflow, and the maintenance of HR could be explained by the counterbalance of the positive chronotropic effects of propofol to the change in sympathetic nervous activity, which is expected to cause a deceleration of the heart rhythm. Specifically, ligand-gated ion channels are likely to be one of the major sites of action of anesthetic agents, and the GABA and ionotropic glutamate (NMDA) receptors are known to be affected by anesthetic drugs.

To our knowledge, this was the first study in which the autonomic response to propofol sedation in CH and NH patients was compared. The analysis of BRS through a mathematically rigorous procedure in the perioperative period could result in the availability of additional information to guide anesthesia in uncontrolled hypertensive patients, which resulted prone to a higher rate of hypotension events occurring during sedation.

Arterial and cardiopulmonary baroreflex control on heart rate

The second aim of this study was to quantify the role of arterial and cardiopulmonary baroreflex control on HR and sympathetic mediated and respiratory sinus arrhythmia mediated HRV responses to mild, rapid onset and short duration LBNP cycles, and secondly to investigate the possibility of "reverse" Bainbridge reflex.

The "reverse" Bainbridge reflex implies that a reduction in venous return would cause an unloading (deactivation) of cardiopulmonary baroreceptors and thus initiate a reflex-induced decrease in HR. In theory, a "reverse" Bainbridge reflex would decelerate the beat in conditions of poor diastolic filling. A "reverse" Bainbridge reflex may be elicited by non hypotensive hypovolemia induced by mild LBNP (Cooke et al., 2004; Cristal et al., 2012).

In order to explain short term control mechanisms of HR and ABP, previous models and results were taken into consideration, in particular, the model for RR prediction from SBP oscillations and respiration (Baselli et al., 1994; Aletti et al., 2009) and the results from the work of Aletti et al. (2012), which showed arterial baroreflex is the main player in the mediation of total peripheral resistance (estimated by means of diastolic blood pressure variability) during incremental levels of LBNP before and after bed rest. In order to complete these investigations about arterial and cardiopulmonary baroreflex, the analysis of the HR contribution in maintaining cardiac output in the same conditions is fundamental.

In this thesis the model of RR prediction (Baselli et al., 1994) was improved by including the relationship between CVP and RR with the aim to elucidate the cardiopulmonary baroreflex modulation of RR variability and to investigate the presence of a "reverse" Bainbridge.

The black box model included three components: arterial baroreflex modulation of RR variability ($RR_{/SBP}$), the cardiopulmonary baroreflex modulation of RR variability, which encompasses the "reverse" Bainbridge reflex ($RR_{/CVP}$) and the respiratory sinus arrhythmia ($RR_{/RESP}$). Impulse responses of the model components were constructed using Laguerre expansion and the least square error method.

The data analyzed in this study are a subset of data collected during the Women's International Space Simulation for Exploration (WISE-2005). The subset consisted of seven healthy women that underwent LBNP maneuver with increasing levels (0, 10, 20, 30 mmHg). The experiment was completed once before entry into bed rest and then repeated again on day 50 of HDBR.

CVP was progressively decreased with increasing LBNP intensities in both conditions (pre-HDBR and during HDBR), whereas HR significantly increased only during HDBR at high LBNP intensities, as expected.

The "Reverse" Bainbridge effect was elicited during mild LBNP cycles, but its limited relevance tends to disappear in the presence of cardiovascular deconditioning due to prolonged bed rest (see figure 3.5).

HRV appeared to be mainly caused by the arterial baroreflex, since contribution of SBP variability to the prediction of RR variability ($RR_{/SBP}$) was largely predominant in all experimental conditions both before and during bed rest, while CVP contributed little to the identification of RR variability and to its spectral decomposition; results that are consistent with (Aletti et al., 2012). We can conclude that the rapid onset of mild LBNP does involve the cardiopulmonary baroreflex in mediating the regulation of vascular resistance, and also affects HR according to a "reverse" Bainbridge mechanism; however, this small contribution tends to become even smaller in simulated weightlessness conditions.

Regarding the estimation of BRS gain, a decrease in LF power with increasing levels of LBNP was found before and on day 50 of HDBR, suggesting a progressive impairment of arterial baroreflex with high levels of LBNP, which is more relevant with the combined effect of bed rest.

For the feedforward mechanism no changes were reported. This is expected because the mechanical coupling between HR (i.e., CO) and ABP should not be altered by bed rest, while the main changes are known to affect neural regulation of cardiovascular function.

Cardiopulmonary baroreflex control of afterload and heart contractility

An explorative study was carried out to disentangle the contribution of cardiopulmonary baroreflex control of afterload and heart contractility in two different protocols with different signals recordings and setting in order to study the effects of central volume variations.

Two identification models were applied for the prediction and spectral decomposition of beat-by-beat fluctuations of stroke volume (SV) and pulse pressure (PP) as an extension of a previously proposed model (Aletti et al., 2009). The PP signal was used as a surrogate of SV.

In the first protocol data from subjects that participated in the LBNP experiment before and during HDBR were analyzed (see previous aim). Estimated gain of

cardiopulmonary baroreflex control of ventricular contractility decreased as expected by a reduction in venous return, in both conditions (before and during HDBR), but only in some subjects, with no significant differences. A higher contribution of diastolic blood pressure (DBP) into PP variability was reported, while small contribution of CVP was observed with no evident trend during the LBNP experiment. Results using a SV prediction model showed also a decrease in gain of cardiopulmonary baroreflex control of ventricular contractility, and contribution of DBP and CVP in SV variability prediction also were predominant and smaller respectively.

The different trends among subjects may be due to the signal quality, since model estimation requires stationary signals with few artifacts. Moreover, SV signal is not a direct measure but estimated from ABP signal by the device. Thus longer time series could provide stationary signal subset suitable for a better model estimation. Moreover, ad hoc protocols with direct measurements, such in animal experiments, may clarify these preliminary results.

For the study of the hemodynamic response to an increase in venous return, fluid infusion maneuver in patients undergoing major surgeries was analyzed. Segments of 3 minutes before and after fluid infusion from 10 maneuvers were considered for analysis.

A decrease in RR interval after fluid infusion revealed a possible Bainbridge reflex, i.e. hypervolemia-induced tachycardia; however, no significant changes were found in the frequency domain to support this finding, as in (Barbieri et al., 2002), where a decrease in high frequency (HF) of RR was reported.

The increase of gain of cardiopulmonary baroreflex control of ventricular contractility, hinted that the cardiopulmonary baroreflex enhanced ventricular contractility to improve cardiac performance when the circulating volume was increased, but this trend was observed only in some patients.

The significant increase in the contribution of CVP to PP variability prediction after fluid infusion suggests that the role of cardiopulmonary baroreflex control of ventricular contractility increases with fluid infusion maneuver, whereas the role of afterload modulation of cardiac ejection decreases.

Summary of achievements and contribution to the literature

The results presented in this thesis have been partially published. In particular the analyses on the effects of propofol on baroreflex were reported in the work Dorantes et al. (2013a) and conference procedings (Dorantes et al., 2011; Ferrario et al., 2011; Dorantes et al., 2012a; Dorantes et al., 2012b). The results from LBNP protocols have been presented at a conference (Dorantes et al., 2013b) and are ready to be submitted to an international journal.

Conclusion

The results illustrated in this thesis showed that the assessment of arterial and cardiopulmonary baroreflexes may provide useful information that could be used as a powerful tool in hemodynamic monitoring of patients.

Quantification of contribution of the role of baroreflexes could provide additional information to interpret variability of central volumes under stress conditions such as anesthesia and clinical maneuvers, and could aid in the administration of the proper therapy to ensure hemodynamic stability and to prevent unexpected and potentially harmful blood pressure drops. However, future studies and clinical protocols are needed in order to standardize and validate these results in a larger population. For the validation, invasive data from animal studies in controlled experiments may prove to be more useful than working on patient data characterized by large variability. However, the goal would remain to develop reliable indices for guiding therapy in clinical settings such as the operative room or the ICU. In addition, further development could entail the evaluation of nonlinear models, exploring closed-loop nonlinear analysis of ABP variability.

Abbreviations

ABP: Arterial blood pressure

AIC: Akaike Information Criterion

AR: Autoregressive

BRS: Baroreflex sensitivity

CH: Chronic hypertensive

CO: Cardiac output

CVP: Central venous pressure

DBP: Diastolic blood pressure

HDBR: Head down bed rest

HF: High frequency

HR: Heart rate

HRV: Heart rate variability

ICU: Intensive care unit

LBNP: Lower body negative pressure

LF: Low frequency

MAP: Mean arterial pressure

NH: Non hypertensive

OR: Operative Room

PP: Pulse pressure

SBP: Systolic blood pressure

SV: Stroke volume

TPR: Total peripheral resistance

Contents

CHAPTER 1

Introduction

In this chapter, the physiology of autonomic control of circulation is described. In particular, the role of arterial and cardiopulmonary baroreflex is addressed. In the context of cardiovascular hemodynamic monitoring, a description of some monitoring systems of arterial blood pressure (ABP) used in the Operative Room (OR) is shown, since this thesis treats data from major surgeries. The development of mathematical models aimed at obtaining a deeper insight into baroreflex functioning and its interactions with other control mechanisms is briefly described as well. Finally, the objectives of this thesis are described at the end of this chapter.

1.1 Cardiovascular regulatory system: arterial and cardiopulmonary baroreflex

The cardiovascular system is responsible for transporting oxygen, nutrients, hormones and cellular waste products throughout the body. This system is comprised of the heart and the circulatory system. Peripheral circulation is regulated to distribute cardiac output (CO) to the various organs and tissues according to their individual metabolic or functional needs while the maintenance of ABP is within a relatively narrow range.

The neural control of the circulation operates through parasympathetic efferents that innervate the heart and a small number of blood vessels, limiting their influence largely to the control of cardiac function, and sympathetic efferents that innervate the heart, blood vessels, adrenal glands, and kidneys, providing for widespread direct and indirect control of cardiac and vascular function (Guyenet et al., 2006). There are three main classes of sympathetic neurons: barosensitive, thermosensitive and glucosensitive. The barosensitive sympathetic efferents are under the control of arterial baroreceptors. This large group of efferents has a dominant role in both short-term (i.e. seconds to minutes) and long-term (i.e. hours and days) ABP regulation. Figure 1.1 shows the ABP control mechanisms at different time intervals after onset of a disturbance to the arterial pressure.

The three mechanisms that show responses within seconds are the baroreceptor feedback mechanism, the central nervous system ischemic mechanism, and the chemoreceptor mechanism. After any acute fall in pressure, as might be caused by severe hemorrhage, the nervous mechanisms elicit a constriction of the veins and provide transfer of blood into the heart, an increase of heart rate (HR) and contractility of the heart to provide greater pumping capacity, and a constriction of most peripheral arterioles to impede flow of blood out of the arteries (Guyton et al., 2006); all these effects occur almost instantly to raise the ABP back to survival range. When the pressure suddenly rises too high, the same control mechanisms operate in the reverse direction, again returning blood pressure back toward normal.

This thesis is focused on the study of baroreflex involved in short-term regulation and control of the cardiovascular system, particularly on arterial and cardiopulmonary baroreflex control of HR.
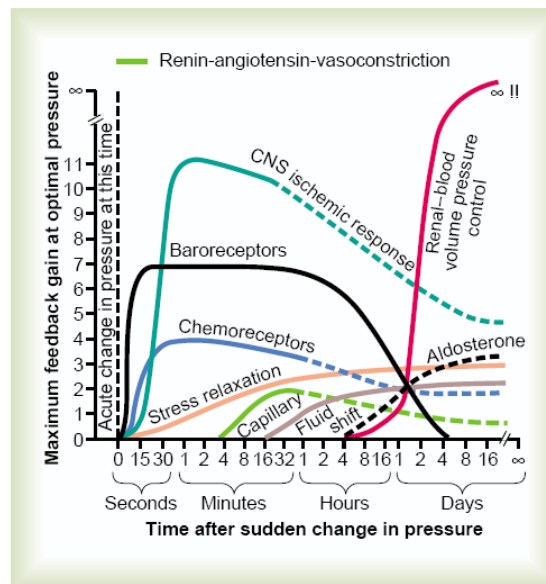
Figure 1.1. Arterial pressure control mechanisms at different time intervals after onset of a disturbance to the arterial pressure. Reprinted from (Guyton et al., 2006).

1.1.1 Baroreceptors

Baroreceptors are mechanosensitive nerve endings that respond to deformation or strain of the vessel walls in which they are located. Pressure is sensed by the baroreceptors in a multi-step process that includes pressure-mechanical deformation in the vessel wall followed by mechano-electrical transduction in the receptors themselves (Brown et al., 1980). Mechanosensitive ion channels are present on baroreceptor nerve endings, and the influx of sodium and calcium through these channels is responsible for depolarization of baroreceptors during increased arterial pressure (Chapleau et al., 2001).

Baroreceptors in the aortic arch and carotid sinuses are known as high pressure baroreceptors, whereas cardiopulmonary baroreceptors in the atria, ventricles, vena cava, and pulmonary vasculature are often referred to as volume receptors or low pressure baroreceptors (Freeman et al., 2006).

Arterial baroreceptors

The cell bodies of carotid sinus and aortic arch baroreceptor neurons are located in petrosal and nodose ganglia, respectively. Signals from the carotid baroreceptors are transmitted through very small Hering's nerves to the glossopharyngeal (cranial nerve IX) nerves in the high neck, and then to the nucleus tractus solitarius (NTS) in the medulla

oblongata (Aicher et al., 1990). Signals from the aortic baroreceptors in the arch of the aorta are transmitted through the vagus (cranial nerve X) nerves also to the same NTS of the medulla oblongata (figure 1.2). At this level numerous neurotransmitters (serotonin, acetylcholine,…) appear to be present in ganglio, and to be involved in the neuronal conduction process (Zhuo et al., 1997). After the baroreceptor signals arrive to the NTS of the medulla, the NTS evokes changes in efferent sympathetic and parasympathetic outflow to the heart and blood vessels that adjust CO and vascular resistance to return ABP to its original baseline. Thus, increases in ABP stimulate afferent baroreceptor discharge, causing reflex inhibition of efferent sympathetic outflow to the blood vessels and heart and activation of parasympathetic outflow to the heart. The resultant decreases in vascular resistance, stroke volume (SV), and HR will reduce ABP back to baseline. Conversely, decreases in ABP, and decreased stretch of the baroreceptors, increase sympathetic neural activity and decrease parasympathetic neural activity, resulting in increased HR, SV, and peripheral resistance; this returns ABP toward the normal level (Guyton et al., 2006; Thomas et al., 2011). If the fall in ABP is very large, increased sympathetic neural activity to veins is added to the above responses, causing contraction of the venous smooth muscle and reducing venous compliance. Decreased venous compliance shifts blood to increase central blood volume, increasing right atrial pressure and, in turn, SV. Figure 1.3 shows a description of arterial baroreceptor control of the circulation.

The baroreflex is somewhat more sensitive to decreases in pressure than to increases, and is more sensitive to sudden changes in pressure than to more gradual changes. The baroreceptors respond extremely rapidly to changes in ABP; indeed, the rate of impulse firing increases in the fraction of a second during each systole and decreases again during diastole.

Cardiopulmonary baroreceptors

Cardiopulmonary baroreceptors are located in the cardiac atria, at the junction of the great veins and atria, in the ventricular myocardium, and in pulmonary vessels. Their nerve fibers run in the vagus nerve to the NTS, with projections to supramedullary areas as well. These baroreceptors sense changes in central blood volume and pressure and, modulate efferent sympathetic neural outflow and vascular resistance (Mancia et al., 1983; Middlekauff et al., 1995; Hainsworth et al., 1991; Ray et al., 2000). Elevations in central

blood volume increase vagal afferent nerve firing, reflexively decreasing sympathetic nerve activity (SNA), while unloading (i.e., decreasing the stretch) of the cardiopulmonary receptors by reducing central blood volume evoke profound increases in sympathetic nerve activity and decreased parasympathetic nerve activity to the heart and blood vessels. In addition, the cardiopulmonary reflex interacts with the baroreceptor reflex.

Cardiopulmonary stimulation is thought to have direct inhibitory influence on medullary vasoconstrictor centers, leading to reciprocal effects on parasympathetic and sympathetic outflow: increased afferent nerve traffic reduces efferent sympathetic outflow and is thought to increase efferent parasympathetic action.

The outputs of cardiopulmonary receptors are modified by changes in central venous pressure (CVP). CVP changes are elicited by venous volume shifts, such as those occurring shortly after postural changes, or venous volume changes in response to stimuli of longer duration. Cardiopulmonary receptor loading or unloading initiates reflex changes in peripheral resistance, blood pressure and HR. Reflex HR changes due to cardiopulmonary receptor perturbation are not as pronounced in some cases as changes elicited by arterial baroreceptors (Desai et al., 1997). Therefore, cardiopulmonary baroreceptors have been shown to be very responsive to CVP (Desai et al., 1997; Raymundo et al., 1989), the cardiopulmonary baroreflex responds to a change in CVP by inducing an opposite change in total peripheral resistance (TPR) (Raymundo et al., 1989).

The cardiopulmonary baroreflex control of ventricular contractility has not been clarified yet, since a change in CVP could induce a same directional change in ventricular contractility so as to maintain CVP, much like the Bainbridge effect. On the other hand, a change in CVP could cause an opposite change in ventricular contractility in order to blunt the forthcoming change in ABP due to the altered preload, much like the cardiopulmonary baroreflex control of TPR.

Low pressure receptors in the cardiopulmonary region also influence HR through the Bainbridge reflex, which refers to the increase in HR secondary to an increase in central blood volume. The Bainbridge reflex has been demonstrated in canines and baboons with low resting HR, and an intravenous saline infusion (Vatner et al., 1981). However, Bainbridge reflex in humans is a matter of debate.

It is commonly thought that receptors sensing central venous and pulmonary venous pressures modulate the baroreflexes on HR and TPR in a way to protect the heart against excessive preloads and afterloads.

The cardiopulmonary reflex also exerts important longer-term neurohumoral control over cardiovascular function. Direct cardiopulmonary influence on vasopressin (antidiuretic hormone, ADH) and atrial natriuretic peptide release allows for low-pressure modulation of renal fluid-electrolyte balance.

Maneuvers that alter cardiac and pulmonary filling volumes, such as postural change and exercise, elicit reflex alterations in sympathetic nervous activity to specific organs through cardiopulmonary baroreceptors.
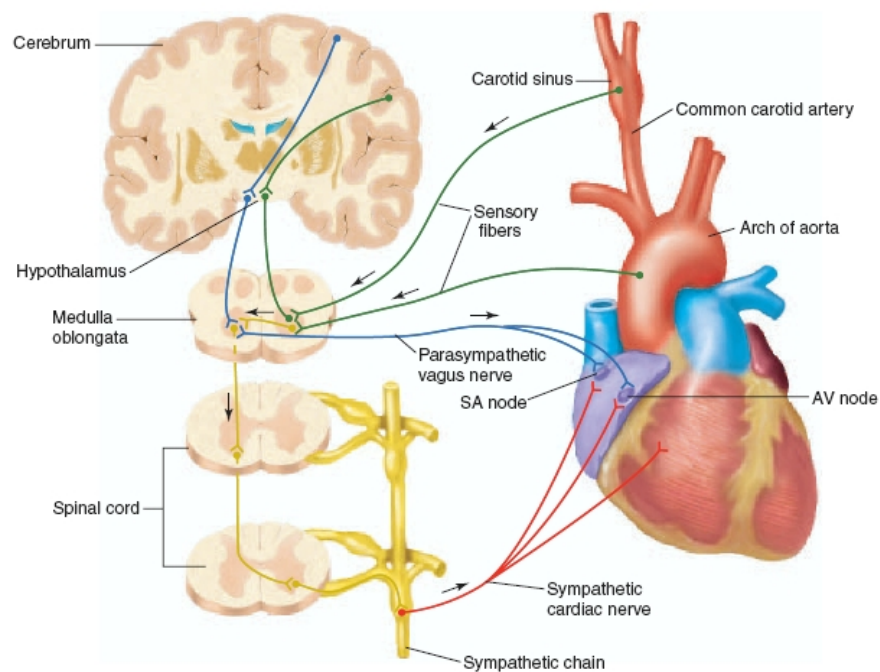
Figure 1.2. Structures involved in the baroreceptor reflex. The cardiac control centers in the medulla regulate the cardiac rate. Acting through the activity of motor fibers within the vagus and sympathetic nerves controlled by these brain centers, the function of baroreceptors is to counteract blood pressure changes for minimizing pressure fluctuations. Reprinted from (Fox, 2006).
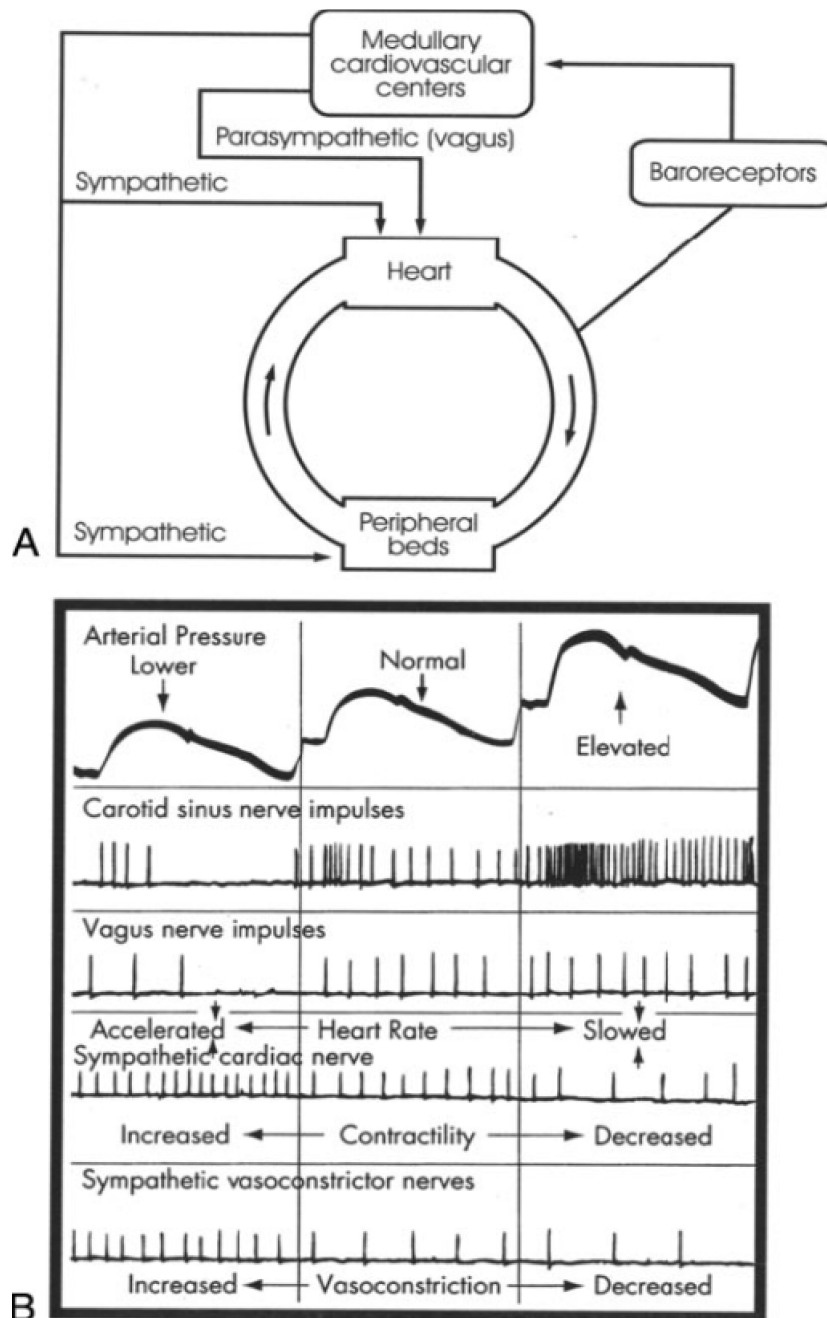
Figure 1.3 Arterial baroreceptor control of the circulation. A, The major components of the baroreceptor reflexes are (1) an afferent limb comprising the arterial baroreceptors in the carotid sinus and aortic arch and their respective sensory nerves, the glossopharyngeal and vagus nerves; (2) the cardiovascular centers in the medulla oblongata that receive and integrate the sensory information; and (3) an efferent limb comprising the sympathetic nerves to the heart and blood vessels and the parasympathetic (vagus) nerves to the heart. The baroreceptors are stimulated by stretch of the vessel wall, which results from an increase in transluminal pressure. B, Impulses originating in the baroreceptors tonically inhibit discharge of the sympathetic nerves to the heart and blood vessels, and tonically facilitate discharge of the vagus nerves to the heart. An increase in ABP increases baroreceptor afferent activity, resulting in further inhibition of the sympathetic nerves and activation of the vagus nerves. This produces vasodilation, venodilation, and reductions in stroke volume, HR, and cardiac output, which tend to normalize ABP. A decrease in ABP has opposite effects. Reprinted from (Cristal et al., 2012).

7

1.1.2 Effectors of Baroreceptors

In terms of control theory, the ABP control system can be seen as a negative feedback control system. A general diagram is showed in figure 1.4.
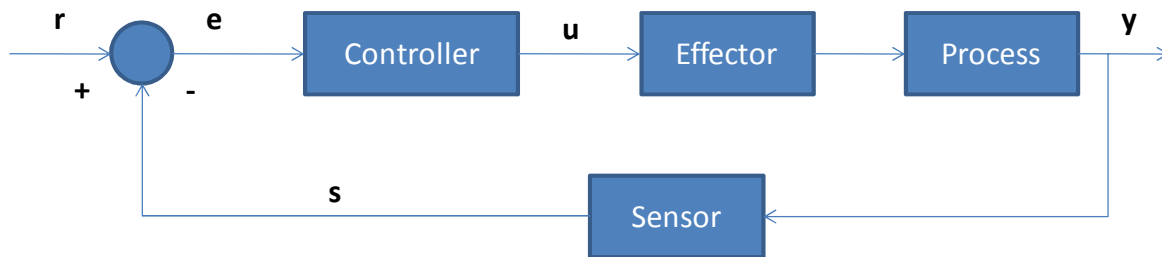
Figure 1.4. General structure of the control system.

The system regulates the output value (y) that is measured by a sensor. Its sensor output (s) is compared with a set-point (r) with the aim to minimize the difference between these two signals, the error signal (e). The output of the process is regulated by the controller by means of its effectors. These effectors are the actuators of the controller process. In circulation control figure 1.4 can be translated as follows:

General system	Circulation
Process	blood vessels + heart
Controller	Central nervous system (CNS)
Effector	e.g. Heart rate, peripheral resistance
Sensor	e.g. baroreceptors
Output value (y)	e.g. arterial pressure
Sensor signal (s)	Afferent nerve activity
Reference input (r)	Set by brain centers
Control signal (u)	Efferent nerve activity

The structure of circulation control can be summarized by figure 1.4. However, the real situation is more complicated. For example, the presented system assumes a single input – single output system, while in circulation control multiple inputs and outputs are present with multiple regulation loops interacting within the system.

As described before, the baroreflex is an important element in short term ABP regulation. Once baroreceptors respond to wall stretching by generating impulses in their

afferent nerves and the impulses are conducted to the central nervous system in the brain, these signals are processed to result in efferent nerve activity, which stimulates the effectors that are used by baroreflex to control blood pressure. For example, in response to an ABP increase, a reflex decrease in sympathetic activity reduces HR, cardiac contractility and peripheral resistance.

Relevant effectors to control blood pressure are: HR, systemic resistance, blood volume and contractility of the heart. These effectors act on different time scales and have different effectiveness. For example, changes in venous volume have the slowest action. Changes in peripheral resistance are faster but less effective, whereas changes in HR are almost immediate but even less effective. Heart contractility is the least effective of these four effectors (Wesseling et al., 1985).

In the next section a brief description of how these effectors can influence ABP control is shown.

Baroreflex on heart rate. An increase of HR will result in an increase in blood flow (q) if SV is constant, considering

$$q=HR \cdot SV \tag{1.1}$$

There are two nervous pathways in the CNS to affect the HR, the sympathetic and the parasympathetic nerves (vagal nerves). Increasing the vagal activity will cause a decrease in HR while an increase of sympathetic activity will cause a HR increase. As vagal responses are much faster than sympathetic responses, the vagal response will have a prompter effect on regulation.

Baroreflex on peripheral resistance. The sympathetic nerves have impact on the arterioles by constriction and dilatation of vessels, causing changes in peripheral resistance and thereby affecting ABP. The influence of peripheral resistance is clear if we take into account the relation between pressure and resistance, this can be showed by Poiseuille's law, with q=blood flow, p=pressure difference between input and output, =blood viscosity, L=length of the vessel, r=radius of the vessel and R=peripheral resistance.

$$q = \frac{\Delta p\, \pi r^4}{L8\eta} = \frac{\Delta p}{R_s} \qquad with \qquad R_s = \frac{L8\eta}{\pi r^4} \tag{1.2}$$

Hence, an increase in peripheral resistance will cause an increase in pressure at equal flow, or decrease flow at equal pressure. Note particularly in this equation that the rate of

blood flow is directly proportional to the fourth power of the radius of the vessel, which demonstrates that the diameter of a blood vessel plays by far the greatest role of all factors in determining the rate of blood flow through a vessel. The fourth power makes it possible for the arterioles, responding with only small changes in diameter to nervous signals or local tissue chemical signals, either to turn off almost completely the blood flow to tissues, or at the other extreme to cause a vast increase in flow. Thus, changes in the radius of a vessel will have a great influence on resistance. In short, peripheral resistance changes depend on changes in vessel radius of small vessels (Guyton et al., 2006).

Baroreflex on volume. Another way to influence ABP is by means of blood volume. The venous side of circulation is also innervated by the sympathetic nervous system. Constriction of the venous blood vessels will decrease the total blood volume. The majority of the blood volume is in the venous part of the circulation under a low pressure. Increasing the blood capacity is a powerful mechanism to decrease the ABP.

The veins contain 75% of total blood volume. Therefore, changing this volume has the greatest influence on arterial pressure. As volume is equal to $r^2 L$ and L is constant for blood vessels, volume depends strongly on vessel radius changes in the venous system.

Baroreflex on contractility. Increasing heart contractility will cause an increase in SV and a decrease in ejection time, thereby facilitating ejection and increasing ABP. As seen before, an increase of SV will result in an increase of blood flow.

The inotropic state of the myocardium is modulated by autonomic and hormonal stimulation. Increased contractility results from sympathetic stimulation, and from circulating norepinephrine, epinephrine. Decreased contractility results from reducing normal sympathetic tone, or from parasympathetic stimulation.

The graph in figure 1.5 demonstrates that at any given right atrial pressure, the cardiac output increases during increased sympathetic stimulation and decreases during increased parasympathetic stimulation. These changes in output, caused by nerve stimulation, result both from changes in HR and from changes in contractile strength of the heart because both change in response to nerve stimulation (Guyton et al., 2006).
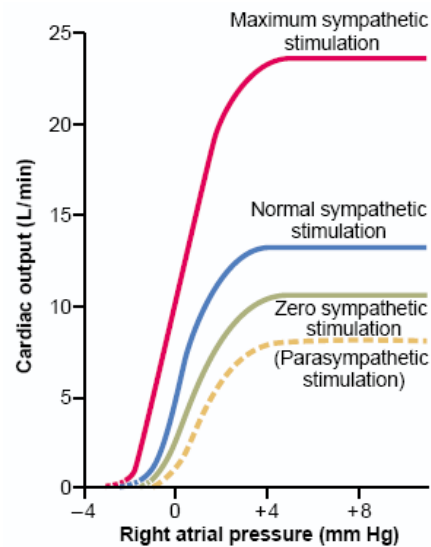
Figure 1.5. Effect on the cardiac output curve of different degrees of sympathetic or parasympathetic stimulation. Reprinted from (Guyton et al., 2006).

1.2 Cardiovascular hemodynamic monitoring

Functional hemodynamic monitoring can be defined as the assessment of the dynamic interactions of hemodynamic variables in response to a defined perturbation (Pinsky et al., 2005). Hemodynamic monitoring plays an important role in the management of acutely ill patients, and its main goal is to provide data that help in the optimization of end organ tissue oxygenation and effectively combat global tissue hypoxia, shock, and multiorgan failure; such paradigm is routinely used in the OR during high-risk surgery and in the intensive care unit (ICU). Monitoring can aid in identifying underlying pathophysiological processes and thus in selecting preemptive actions and appropriate forms of therapy. Hemodynamic assessment of the patient can include both invasive and noninvasive parameters. From direct measurements, cardiac performance can be further evaluated by calculating derived parameters.

Direct measurements that can be provided by cardiovascular monitoring are: HR, that can be obtained from the ECG monitor; systolic and diastolic blood pressures, that can be obtained indirectly with a sphygmomanometer or more accurately with an intra-arterial catheter; pulmonary arterial pressures, that can be obtained with the use of a Swan-Ganz catheter; right atrial pressure, that can be obtained by using the right atrial lumen of the Swan-Ganz catheter; and CO.

Continuous blood pressure, SV and CO measurements are crucial for:

11

- Monitoring therapeutic interventions, with the aim of establishing a patient's initial hemodynamic status and measuring the response to various therapeutic interventions such as fluid transfusion and the use of inotropic and vasoactive drugs for supporting the heart and circulation.

- Fluid management: the continuous monitoring of SV and stroke volume variation (SVV) provide powerful insights into the fluid status of the patient.

- Improving patient outcomes: avoiding low blood flow and low or excessive fluid administration contributes to a better recovery after surgery.

1.2.1 Arterial blood pressure monitoring

Blood pressure is proportional to the force exerted by the blood against any unit area of the vessel wall. ABP is not a single pressure but a range of pressure values from systole and diastole. Mean arterial pressure (MAP) best approximates the organ perfusion pressure in noncardiac tissues, as long as venous or surrounding pressures are not elevated (Pinsky et al., 2005; Guyton et al., 2006).

Non invasive monitoring of blood pressure

The most common method of non invasive measurement of blood pressure is the auscultatory method which is based on the correlation of ABP and Korotkoff sounds (Chung et al., 2013).

The oscillometric method measures the changing amplitude of pulse pressures in the occluding cuff as the cuff is deflated from above systolic blood pressure (SBP) to below diastolic blood pressure (DBP). An electronic transducer detects the pulse pressure (PP) wave, as well as the gauge pressure, in the cuff (Chung et al., 2013).

Another non-invasive method of measuring beat-to-beat ABP is used by Finapres, which exploits infrared light transmission to measure ABP in the finger (Wesseling et al., 1995; Imholz et al., 1998) and offer the benefits of continuous ABP monitoring.

Invasive monitoring of blood pressure

Invasive ABP monitoring is a technique mainly used in the OR and in the ICU and is also commonly used in patients undergoing major surgery. Moreover, it is considered the

gold standard for measurement of ABP. Arterial catheterization will often be performed for high-risk surgical patients undergoing procedures with expected large fluid shifts; this is the only way to visualize the entire ABP waveform, and this also allows easy blood withdrawal for repeated biochemical analyses. The technique involves the insertion of a catheter into a peripheral artery; the most common site is the radial artery due to ease of access, ease of actual cannulation and low rate of complications (Scheer et al. 2002). Although this method of direct measurement offers reliable and accurate measurements, there are disadvantages and risks associated with invasive monitoring. Invasive arterial line waveforms also contain a large host of additional information such as continuous PP values representing arterial stiffness, diastolic pressures representing systemic vascular tone, and respiratory variation of blood pressure reflecting degrees of hypovolemia (Lamia et al., 2005).

1.2.2 Cardiac Output monitoring

CO is the volume of blood pumped per minute by each ventricle, and is the product of HR and SV. The SV of the ventricle is determined by the interactions between its preload, contractility and afterload. The measurement of CO provides an estimate of whole-body perfusion, oxygen delivery, and ventricular function. Systemic vascular resistance cannot be measured directly; however, monitoring CO allows for a better understanding of the causes of ABP variation (Prabhu et al., 2007).

CO monitoring is a useful tool in the assessment of patient's circulation. For instance, if CO falls, this provokes low levels of cellular oxygenation (hypoxia) which can cause tissue and organ failure.

CO can be measured by *thermodilution,* which is one of the most common approaches in use today and is considered as the golden standard approach to CO monitoring. This method uses a special thermistor – tipped catheter (Swan-Ganz catheter) inserted from a central vein into the pulmonary artery. An injection of cold solution into the right atrium causes a decrease in blood temperature, which is measured by a thermistor in the pulmonary artery. The decrease in temperature is inversely proportional to the dilution of the solution (i.e. CO) (Berthelsen et al., 2002; Mathews et al., 2008).

Mathematical models for cardiac output estimation.

In the cardiovascular system, the relationship between ABP and CO is quite complex. Most of the methods proposed to estimate flow from pressure operate at a beat-by-beat time resolution, i.e. one value for SV is computed for each beat.

SV is estimated from aortic pressure waveform using several methods based on systemic circulation models, which include the lumped Windkessel model, model based on systolic area, Liljestrand & Zander model, Wesseling model, among others (Sun et al., 2005). In these methods, SV is estimated from the systolic, diastolic, or both systolic and diastolic portion of the pressure waveform (Mathews et al., 2008).

The technique adopted by the commercial monitor PiCCO^{TM} (Pulsion Medical Systems) is *pulse contour analysis,* which is a modification of the systolic area method. For the continuous calculation of CO, the method uses a calibration factor (cal) determined by thermodilution CO measurement and the HR, as well as the integrated values for the area under the systolic part of the pressure curve (P(t)/SVR), the aortic compliance (C(p)) and the shape of the pressure curve, represented by change of pressure over change of time (dP/dt) (Mathews et al., 2008).

Although PiCCO^{TM} system would allow a real beat-to-beat analysis of SV, CO, and systemic vascular resistance, for reasons of readability, the displayed values consist of a sliding average of the preceding 12 seconds.

Moreover, PiCCO^{TM} system needs to be calibrated initially by an arterial thermodilution measurement to calibrate aortic impedance, which differs from patient to patient. In addition, a continuous determination of the cardiac afterload, in terms of systemic vascular resistance, becomes possible due to beat-to-beat measurements of ABP and HR. This device was used to collect the data recorded during major surgery analyzed in this thesis.

1.3   Cardiovascular models

Several cardiovascular models, have been proposed with the aim of elucidating the baroreflex function and the relationship with other control mechanisms. The proposed models vary in different aspects such as the approach used, for example if they are based on black box models, where minimal a priori hypotheses about the possible interactions of

the measured variables are necessary (Baselli et al., 2001; Aletti et al., 2009), or based on physiological descriptions (Guyton et al. 1972); the level of details by which nonlinearities are modeled (Cavalcanti et al., 1996), or the inclusion of specific features of real cardiovascular dynamics (De Boer et al., 1987), such as respiratory entrainment, the 10 s rhythm (Hyndman et al., 1971) or long term blood pressure fluctuations. Some of the first mathematical models of baroreflex were based on detailed physiological descriptions of the heart and vasculature (Guyton et al. 1972); however, they were unable to reproduce specific features of cardiovascular dynamics, such as the spontaneous variability of HR and ABP (Di Rienzo et al., 2009). Following the same research line, Hyndman et al. (1971) exposed an explanation for spontaneous and repetitive fluctuations of ABP with a typical period of about 10 s by including a nonlinear element followed by a time delay in the baroreflex feedback. Baroreflex modeling using nonlinear system was also showed by Cavalcanti et al. (1996), who simulated the latent period of the baroreceptor regulation through a pure time delay placed in the feedback branch using system nonlinearity model dynamics.

Another beat-to-beat model of the cardiovascular system was developed to study the spontaneous short-term variability in ABP and HR data by De Boer et al. (1987). The model consisted of a set of differential equations representing the control of HR and peripheral resistance by the baroreflex, Windkessel properties of the systemic arterial tree, contractile properties of the myocardium, and mechanical effects of respiration on ABP.

TenVoorde et al. (2000) also explored cardiovascular modeling taking into account a simple beat-to-beat hemodynamic part, considering Starling heart and Windkessel models, linked to a detailed continuous neural control model. The intermediate between continuous and beat-to-beat part is an integral pulse frequency modulator acting as cardiac pacemaker driven by sympathetic and vagal outflows (TenVoorde et al., 2000).

Dynamic properties of a nonlinear model of the human cardio-baroreceptor control loop were estudied by Seidel et al. (1998), they showed that an increase of sympathetic time delays leads via a Hopf bifurcation to sustained HR oscillations, besides, they studied the interaction of heartbeat, respiration, and Mayer waves and the occurrence of more complex rhythms, including entrainment and chaotic dynamics.

Since the cardiovascular system presents several closed-loop interactions between many variables, including RR interval and ABP, other models have been proposed to

investigate this relationship (Baselli et al., 1994; Patton et al., 1996). Baselli et al. (1994) proposed a direct identification procedure using a closed-loop model, taking into account that variability in ABP does cause variability in HR and vice versa, and considering an exogenous input: respiration. Parameters relevant to Starling effect, to Windkessel model, and to the gain of baroreceptor mechanisms are assessed by this model (Baselli et al., 1994). Some approaches use the coherence function as a classical tool to quantify the strength of the linear coupling between ABP and RR interval. However, this analysis is not reliable if ABP and RR interval strongly interact in a closed loop, where feedforward (causality from RR to SBP) and feedback (causality from SBP to RR) pathways are involved. Models taking into account causality have proven to provide informative insights into cardiovascular control (Barbieri et al., 2001; Porta et al., 2002; Nollo et al., 2005; Chen et al., 2011). Figure 1.6 shows a model of cardiovascular short-term regulation and the relationship between ABP, CVP, RR and respiration. The relationship between RR and ABP includes feedback mechanism through the arterial baroreflex and feedforward mechanism that represents the direct influence of RR interval on ABP, which is mediated by a perturbation mechanism based on the Starling law and diastolic runoff. Respiration affects RR by the mechanism known as respiratory sinus arrhythmia (RSA), and respiration affects ABP and CVP through mechanical movements of the thorax. CVP affects RR through the cardiopulmonary reflex and also affects ABP directly through the heart and vasculature (Barbieri et al., 2001).

Regarding cardiopulmonary baroreflex, there are few models aimed to explain the integrated functioning of the arterial and cardiopulmonary baroreflex control. Mukkamala et al. (2006a) proposed a noninvasive technique for estimating the closed-loop gain values of the arterial TPR baroreflex and the cardiopulmonary TPR baroreflex by mathematical analysis of beat-to-beat fluctuations in ABP, CO, and SV. They used chronic arterial baroreceptor denervation in seven conscious dogs instrumented with an aortic catheter and ultrasonic aortic flow probe. The results indicated that the baroreceptor denervation abolished arterial TPR baroreflex functioning, that match with the physiological knowledge, and cardiopulmonary TPR baroreflex functioning was enhanced due to a central compensatory mechanism (Mukkamala et al., 2006a).

A model of diastolic blood pressure (DBP) variability was proposed by Aletti et al. (2012) and showed an interpretation of the proportional effect of arterial baroreflex vs. cardiopulmonary baroreflex components of ABP control during lower body negative

pressure (LBNP) and bed rest experiments, they concluded that during bed rest cardiopulmonary baroreflex was blunted and that ABP maintenance in the presence of an orthostatic stimulus relied mostly on arterial control.

On the other hand, one technique widely applied in the assessment of cardiovascular regulation is the analysis of the power spectrum. The role of parasympathetic and sympathetic activities in determining the variability in HR and ABP can be analyzed for its spectral components: low-frequency interval (0.04 to 0.15 Hz) and high-frequency interval (0.15 to 0.5 Hz). The area under the high-frequency oscillations is considered to represent parasympathetic (vagal) modulation, whereas the area under the low-frequency oscillations or the low-frequency to high-frequency power ratio is considered to reflect sympathetic modulation (Pagani et al., 1986).
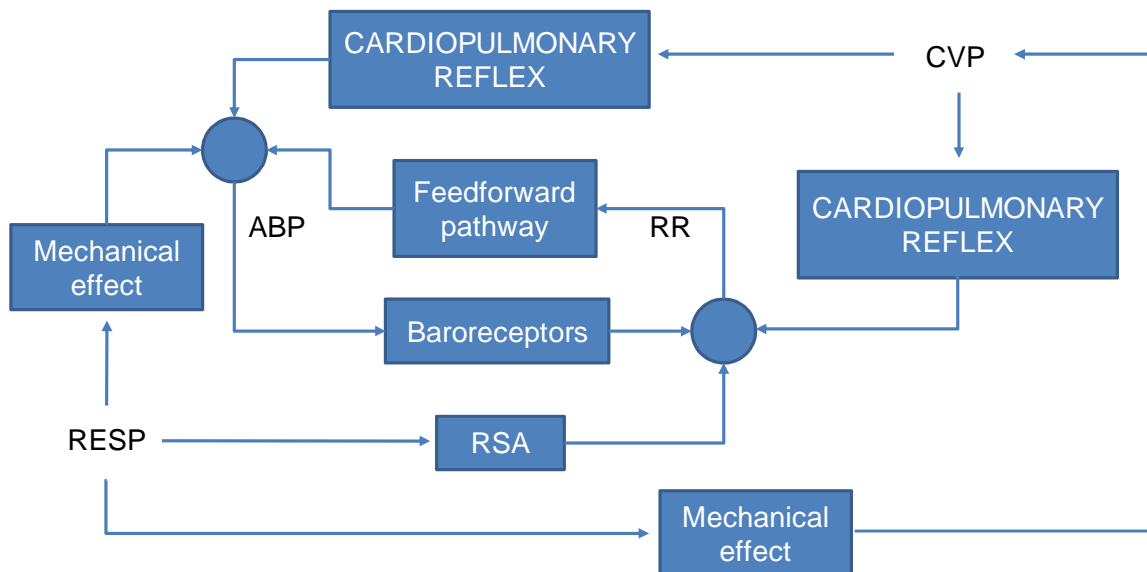
Figure 1.6. Simplified model of cardiovascular short-term regulation. Mechanical effect refers to mechanical influence through muscle activity, RSA (respiratory sinus arrhythmia).

1.4 Maneuvers used to explore arterial and cardiopulmonary baroreflexes

Several experimental maneuvers have been employed by researchers to study the cardiopulmonary baroreflex. Some of these are LBNP, congesting cuffs, elevation of legs and lower body positive pressure, head-out water immersion, upright tilting and respiratory maneuvers (Hughson et al., 2004; Bevegård et al., 1977; Epstein 1976; Mark et al., 1983). There are also several techniques that have been used to measure arterial baroreflex gain,

for example, through the use of vasoactive drugs to measure the change in HR in response to changes in ABP (Smyth et al., 1969), or noninvasive maneuvers which are mainly the Valsalva maneuver and the neck chamber technique (La Rovere et al., 2008).

Hemorrhage is a serious complication during major surgeries and also a cause of death in both civilian and battlefield trauma. Controlled human experimentation may contribute to develop procedures to predict the magnitude of hemorrhage and the likelihood for progression to hemorrhagic shock, but controlled study of severe hemorrhage in humans is not possible. LBNP is a widely used technique for studying the cardiovascular responses to simulated orthostatic stress and hypovolemia (Brown et al., 2003); this maneuver induces fluid shifts by pooling blood in the legs and abdomen, through subatmospheric pressure which is applied to vessels and viscera in the pelvis and abdomen as well as lower extremities and activating a number of cardiovascular adjustments that tend to maintain central blood volume and ABP (Hisdal et al., 2002). In addition, this technique offers several advantages. The suction chamber is simple and inexpensive, the subject and equipment can remain in one position throughout the experiments and the suction can be terminated quickly facilitating studies and allowing exploring the responses to a rapid increase in venous return at the end of suction. LBNP may be a useful model to simulate hemorrhage (table 1.1), and to study many of the physiological compensatory mechanisms in response to acute hemorrhage. Under both conditions of hemorrhage and LBNP, the stimuli for cardiovascular compensation are similar: decrease of venous return and preload, resulting in decreased SV and CO (Cooke et al., 2004).

Table 1.1. Comparison of hemorrhage severity in humans and magnitude of LBNP

LBNP	Hemorrhage
10-20 mmHg 400-550 ml fluid displaced	Mild 400-550 ml ~10% of total blood volume
20-40 mmHg 500-1,000 ml fluid displaced	Moderate 500-1,000 ml ~10-20% of total blood volume
$\geq$ 40 mmHg $\geq$ 1,000 ml fluid displaced	Severe > 1,000 ml > 20% of total blood volume

Data from Cooke et al. (2004)

Levels higher than -20 mmHg of LBNP presumably inhibit both cardiopulmonary and arterial baroreceptors, while low levels (i.e., -20 mmHg) also known as mild LBNP, were hypothesized to be useful for studying the role of cardiopulmonary receptors in humans, as the absence of significant changes in ABP (Fu et al., 2009; Brown et al., 2003).

Passive leg raising is a maneuver that increases right cardiac preload, likely through an increase in the mean circulatory pressure which is the driving pressure for venous return. If the right ventricle is preload responsive, the increase in systemic venous return results in an increase in right CO and hence in the left ventricular filling. Passive leg raising has gained interest as a test for monitoring functional hemodynamic and assessing fluid responsiveness since it is a simple way to transiently increase cardiac preload and it acts as a self-volume challenge which is easy to perform and completely reversible. In addition, passive leg raising helps to detect fluid responsiveness in critically ill patients with spontaneous breathing. As the respiratory variability of cardiovascular signals cannot be used for predicting volume responsiveness in these kind of patients, passive leg raising represents an alternative in OR or ICU. Its optimal use requires a real-time cardiovascular assessment device able to quantify accurately the short-term hemodynamic response. Besides, passive leg raising can be used to study responses to stimulation of cardiopulmonary baroreceptors. (Monnet et al., 2008; Marik et al., 2011)

1.4 Objectives

This thesis is based on the study of arterial and cardiopulmonary baroreflexes, since the study of these two baroreflexes represents a useful tool in the assessment of autonomic control of the cardiovascular system. Taking into account that arterial and cardiopulmonary baroreflexes have a crucial role in ABP control, baroreflex measurement has been shown to be a source of valuable information in the clinical management.

The broad objectives of this thesis are:

1. To quantify the causal interactions between HR and ABP in patients undergoing general anesthesia for major surgery, in particular during anesthesia induction with a bolus of

propofol, and to evaluate the possible effects of propofol and of intubation and onset of mechanical ventilation on ABP autonomic control, before the beginning of surgery, in normotensive and hypertensive patients.

2. To identify arterial and cardiopulmonary baroreflex control of HR and sympathetic mediated heart rate variability (HRV) responses to mild, rapid and short duration LBNP cycles, by black box modeling of HRV, and to shed light on the possible occurrence of the "reverse" Bainbridge Reflex.

3. To explore the response of cardiopulmonary baroreflex control of afterload and ventricular contractility to changes in venous return through fluid infusion maneuvers during major surgery and during orthostatic challenge by LBNP, in spontaneous conditions and under the effects of cardiovascular deconditioning (i.e., during an LBNP experiment before and on day 50 of bed rest).

The data used in this thesis were acquired during major surgery and during an experiment entailing cycles of mild LBNP performed before and during a head down bed rest (HDBR) study.

The cardiovascular response during these maneuvers was assessed by the implementation of mathematical models of arterial and cardiopulmonary baroreflexes control on ABP.

CHAPTER 2

Arterial baroreflex control during anesthesia induction

2.1 Introduction

The baroreflex control of HR can be measured by the baroreflex sensitivity (BRS) index or BRS gain, defined as the reflex-induced change in interbeat interval in milliseconds per mmHg of blood pressure change. BRS has been assessed by means of different mathematical approaches and models, based on the quantification of the relationship between the beat-by-beat variations of ABP (or, more specifically, of SBP), as the input to the baroreceptors, and of HR.

The most commonly used methods for the estimation of BRS are based on open loop systems, considering the RR interval as the output and ABP as the input. Thus, the effects of ABP on HR through the baroreflex are considered, but the effects of RR on ABP are neglected (Barbieri et al., 2001).

Several techniques have been proposed to evaluate the baroreflex gain, such as the infusion of vasoconstrictive drugs to increase ABP and evaluation of the subsequent lengthening of the heart period (Smith et al., 1969); the detection of sequences of SBP and RR interval values characterized by the simultaneous increase or decrease of both variables (Bertinieri et al., 1985); and the calculation of the magnitude of the SBP-RR transfer function. However these methods only consider SBP changes that contribute to RR variations while in the intact circulation, an important contribution to cardiovascular variability is represented by the causal effects of RR interval to SBP, which have been detected in healthy humans (Barbieri et al., 2001; Nollo et al., 2005).

It is assumed that BRS provides insight into the functioning of the cardiac baroreflex, but also about the responsiveness of cardiovascular regulation mediated by the autonomic nervous system (ANS) as a whole. Several physiological and clinical studies have emphasized that BRS can be strongly altered by pathologies as well as therapeutic interventions. For instance, baroreflex gain is altered in hypertension due to the impairment of autonomic cardiac control (Prys-Roberts et al., 1971; Howell et al., 2004; Foëx et al., 2004; Parati et al., 2012; Grassi et al.,2009).

Baroreflex control of heart rhythm under anesthesia has been the object of very few investigations, mainly because of technical difficulties related to data collection during surgery.

Propofol is known to act as a vasodilator and to reduce ABP (Sellgren et al., 1994; Ogawa et al., 2006), and its effects on vascular resistance were found to be more pronounced than the ones caused by other anesthetics (Rouby et al., 1991). However, only a few papers investigated the effects of propofol anesthesia on BRS, and their results often appear contrasting and not conclusive. Central sympatholytic and/or vagotonic mechanisms were suggested to explain the decrease in HR following anesthesia induction, which was observed despite decreased arterial pressures (Cullen et al., 1987). Although an impairment of BRS was not reported, this effect was interpreted as a "resetting" of the baroreflex (Cullen et al., 1987; Samain et al., 1989). In another work, the study of propofol administration before and during microlaryngoscopy showed that BRS, muscle sympathetic nervous activity and ABP were reduced by propofol (Sellgren et al., 1994).

A decrease of BRS under propofol anesthesia was reported by other authors as well (Chen et al., 2011; Sato et al., 2005; Keyl et al., 2000; Ebert et al., 2005). Xu et al. showed,

in an animal model, that BRS was preserved and HR did not change for low doses of propofol (Xu et al., 2000).

As far as human studies are concerned, (Chen et al., 2011) studied baroreflex control of HR during induction of propofol anesthesia in healthy volunteers by adopting a closed loop model, whereas (Bassani et al., 2012) applied the Granger causality approach during craniotomy, and found a significant causality from SBP to HR, suggesting that baroreflex control was still active under anesthesia. Nevertheless, the main limitations of these two papers were that the former dealt with healthy volunteers and not with surgical patients, while the latter did not compare baroreflex control of HR with pre-surgical values or epochs.

Thus, there is a need for a systematic and rigorous methodological approach to the assessment and monitoring of the alterations of BRS due to anesthesia during surgery. The different and sometimes contrasting results reported in the literature may be explained by the large differences in study setups (e.g., animal studies vs. clinical studies, studies of spontaneous variability vs. pharmacological studies, …) by the different mathematical methods used to quantify BRS, and by the lack of a standardized protocol in clinical studies (differences in anesthesia induction procedures, highly heterogeneous patient populations in terms of clinical status, inclusion of minor surgery with ASA I ,…).

Hypertensive subjects are exposed to an increased risk of peri-operative myocardial ischemia (Prys-Roberts et al., 1971; Howell et al., 2004), and uncontrolled hypertensive patients were found to be more prone to intra-operative hypotension (Howell et al., 2004; Foëx et al., 2004) than normotensive subjects.

In view of the above, this study pursues two goals. The first is to compare BRS following anesthesia induction via propofol and after intubation to pre-induction baseline values through a systematic and mathematically robust analysis. This will permit to evaluate the potential blunting of baroreflex control of HR and its residual responsiveness under anesthesia and during mechanical ventilation, prior to the beginning of surgery. For this purpose, four different mathematical methods, which are proposed in literature for the analysis of cardiac BRS were applied to pre-operative and intra-operative data from patients undergoing major surgery, including a sub-population of hypertensive patients. The second goal is to quantify and track the trend in BRS following anesthesia induction

and the switch from spontaneous to mechanical ventilation, and to assess different trends in a hypertensive population when compared to normotensive patients.

2.2 Clinical Protocol

Data from 17 patients undergoing major surgical procedures involving assisted ventilation were analyzed. The patients were divided into 7 chronic hypertensive (CH) patients and 10 non hypertensive (NH) patients. The presence of chronic hypertension was determined from patient clinical history and/or antihypertensive drug prescription in the period immediately preceding surgery. Only patients with the ASA physical status higher than I were included. Patients in treatment with beta-adrenergic blocking agents or suffering from arrhythmias were excluded.

Invasive ABP was measured via an arterial catheter placed in the brachial artery and recorded by a GE S/5 Avance Carestation© monitor at a sample frequency of 100 Hz. The signal was acquired with a custom software (termed "Global Collect", Labview 2011©) developed to collect and visualize data (Toschi et al., 2010). All surgical maneuvers, fluid and drug administered were recorded through an ad-hoc developed interactive user interface, to acquire annotated files.

Surgeries were performed in the University Hospital "Tor Vergata" in Rome, Italy. Patients received 2 mg/kg of Midazolam and 5mcg/kg of Sufentanil as premedication, when they were lying and still conscious, 3 minutes before the starting of anesthetic procedure. General anesthesia was induced through a bolus of propofol (2mg/kg) and maintained by total intravenous anesthesia (TIVA, 6-8 mg / (kg hr)). Patients gradually ceased to spontaneously breath and were mechanically assisted by a facemask operated by anesthesiologist. 0,15 mg/kg of cisatracurium was administered as a muscle relaxant to facilitate endotracheal intubation. After the intubation, the mechanical ventilation was started.

The study was approved by the local Ethics Committee, and the patients gave their written, informed consent to participate.

2.3   Methods

2.3.1 Pre-processing and spectral analysis

The recorded signals were subdivided into three epochs: 1) baseline phase, i.e. the period before induction, when the patient is still conscious; 2) general anesthesia phase, the immediate period after bolus injection and after the transitory phase when patient is deeply sedated; 3) post-intubation period, i.e. the period after intubation and the beginning of mechanical ventilation, before surgical incision and far from other maneuvers like fluid and drug administration.

A robust algorithm was employed for the detection of the onset of each beat in the ABP waveform. The algorithm is based on the slope sum function, which amplifies the rising part of ABP waveform in each beat (Zong et al., 2003). SBP is the local maximum within a time window following each onset and DBP is the local minimum within a window before each onset. Beat-by-beat series of SBP and DBP were then obtained. PP was computed as the difference between SBP of the current cardiac cycle and DBP of the previous cycle beat-by-beat. The duration of each heartbeat is estimated by the time difference between adjacent onsets and it was considered a surrogate of the distance between consecutive R peaks (RR interval). The heart period (HP) estimated in this manner is termed RR in this chapter by virtue of the equivalent physiological meaning. The HR was calculated as 60/RR (bpm).

Two-minute long stationary subseries were selected for each epoch by performing a Dickey-Fuller stationary test. In this way, the transitory phase due to bolus injection and the sympathetic response to the stimuli produced by intubation maneuver were excluded by the analysis. These series were pre-processed with an adaptive filter (Wessel et al., 2000) in order to remove artifacts and/or ectopic beats, and average values were computed for the resulting SBP, DBP and RR series.

Beat-by-beat series were then detrended and resampled at 1 Hz by means of antialiasing filter, to obtain zero-mean time series in order to perform spectral analysis. Power spectral density was computed via autoregressive (AR) estimation and powers in the very low frequency band (VLF, $f < 0.04$ Hz), low frequency (LF) band ($0.04 < f < 0.15$ Hz) and high frequency (HF) band ($0.15 < f < 0.4$ Hz), were calculated. The values of total

power (TP) were computed as well. The AR model order range was between 8 and 12, and the optimal model order was chosen according to the Akaike Information Criterion (AIC).

2.3.2 BRS indices

Baroreflex quantification was obtained by using the spectral method, the transfer function method, the sequence method and the application of a bivariate model.

SBP and RR spectra were calculated for the frequencies in the LF and HF bands associated to spectral coherence higher than 0.5 (Robbe et al., 1987), and the BRS index was estimated as their ratio:

$$\text{LF} = \sqrt{\frac{\text{LF}_{\text{RR}}}{\text{LF}_{\text{SBP}}}}; \quad \text{HF} = \sqrt{\frac{\text{HF}_{\text{RR}}}{\text{HF}_{\text{SBP}}}} \tag{2.1}$$

BRS was also estimated as the average gain of the transfer function between SBP and RR in LF and HF band with high coherence ($\geq$0.5) (Saul et al., 1991):

$$H(f) = \frac{S_{xy}(f)}{S_{xx}(f)} \tag{2.2}$$

where $S_{xx}(f)$ is SBP spectrum and $S_{xy}(f)$ is the cross spectrum between SBP and RR.

In addition, we investigated a time domain approach, i.e. the sequence method, which consists in identifying the sequences where RR and SBP simultaneously increase (up sequence) or decrease (down sequence) over three or more beats. Up or down sequences are identified by variations greater than 1 mmHg in SBP and 4ms for RR (Bertinieri et al., 1985). Both up and down sequences are considered baroreflex sequences if the selected SBP and RR sequences are strongly correlated, i.e. if the correlation coefficient is higher than 0.8. For each baroreflex sequence the regression slope is estimated using a linear regression and the averaged slope value is considered as a BRS index.

The bivariate model approach assesses BRS by considering the causal relationship from SBP to RR, i.e. the feedback mechanism, and RR to SBP, i.e. the feedforward mechanism. The relationship SBP RR represents the cardiac baroreflex, i.e. the actual feedback mechanism, whereas the relationship RR SBP represents the direct influence of RR interval on SBP, which is not mediated by autonomic control, but instead by a

perturbation mechanism based on the Starling law (a longer RR induces an increased left ventricular end-diastolic volume and, in turn, a larger SV) and diastolic runoff (a longer RR induces a larger decay of diastolic pressure and, thus a smaller SBP, keeping constant the other variables like SV) (Barbieri et al., 2001; Wyller et al., 2011; Porta et al., 2002).

An autoregressive bivariate model of order $p=8$ was computed as follows:

$$Y[n] = \sum_{k=1}^{p} A[k]Y[n-k] + W[n] \tag{2.3}$$

where

$$A[k] = \begin{bmatrix} a_{11}[k] & a_{12}[k] \\ a_{21}[k] & a_{22}[k] \end{bmatrix}, Y[n] = \begin{bmatrix} RR[n] \\ SBP[n] \end{bmatrix}, W[n] = \begin{bmatrix} W_{RR}[n] \\ W_{SBP}[n] \end{bmatrix} \tag{2.4}$$

and the coefficients a_{ij} were then used to calculate the gains of the transfer functions:

$$G_{SBP \to RR}(f) = \frac{A_{12}(f)}{1 - A_{11}(f)} \qquad G_{RR \to SBP}(f) = \frac{A_{21}(f)}{1 - A_{22}(f)} \tag{2.5}$$

where $A_{ij}(f) = \sum_{k=1}^{p} a_{ij}[k] e^{-jfk2}$

The maximum value of the coherence between RR and SBP series in LF and HF band was identified. The values of the gains $G_{SBP \; RR}$ and $G_{RR \; SBP}$ associated to these frequencies were calculated, according to the procedure reported in (Barbieri et al., 2001; Wyller et al., 2011).

2.3.3 Granger causality test

A time series $u=\{u(i), i=1,...,N\}$ is said to Granger-cause the series $y=\{y(i), i=1,...,N\}$ ($u \quad y$), if the prediction of the current y based on past values of u and y is significantly more successful than the prediction based only on the past values of y. In this case, the past of u contains information useful for predicting $y(i+1)$ that is not in the past of y (Soderstrom et al., 1988; Bassani et al., 2012).

Assuming that variables u and y are stochastic and stationary, Granger causality can be assessed by the F-test (Bassani et al., 2012). The output y is modeled by an autoregression on its past values plus an exogenous input u, i.e. by an ARX model. The ARX model is compared to a simple AR model of y defined as:

$$y(n) = \sum_{i=1}^{n_a} a_{yy,i} y(n-i) + w_y(n) \tag{2.6}$$

where n_a is the AR model order and w_y is a zero mean white Gaussian noise (WGN) with variance σ^2_{AR}. Considering u as the exogenous input, the ARX model for y is defined as

$$y(n) = \sum_{i=1}^{n_a} a_{yy,i} y(n-i) + \sum_{i=0}^{n_b} b_{yu,i} u(n-i) + v_y(n) \tag{2.7}$$

where n_b is the ARX model order and v_y is a zero mean WGN with variance σ^2_{ARX}.

For both AR and ARX models, the mean squared prediction error (MSPE) is assessed as

$$\sigma^2 = \frac{1}{N} \sum_{i=1}^{N} e^2(i) \tag{2.8}$$

where $e(i)$ is the prediction error, i.e. the difference between the estimated series and the actual values $e(i) = \hat{y}(i) - y(i)$.

The null hypothesis is that the ARX model does not reduce the MSPE with respect to the AR model and this is tested by an F distribution:

$$F = \frac{\sigma^2_{AR} - \sigma^2_{ARX}}{\sigma^2_{ARX}} \frac{N - n_a - n_b - 1}{n_b + 1} \tag{2.9}$$

where n_a is the AR model order, n_b is the model order of the exogenous part and N is the signal length.

Both feedback and feedforward pathways were tested. In the first case the y series was RR and the exogenous input u was SBP, in the latter case the y series was SBP and the exogenous input u was RR. Both the AR and ARX model orders were limited to range between 8 and 12, and the optimal number of the coefficients was chosen according to the AIC. The coefficients were estimated via least square method.

The obtained F values were compared to the critical values of the F distribution, which were calculated from an F distribution with (n_b+1, $N-n_a-n_b-1$) degrees of freedom at p equal to 0.01, which is the probability to reject the null hypothesis. If the F value is larger than this critical value, the null hypothesis is to be rejected and the alternative hypothesis, i.e. a significant causal relationship from u to y, can be accepted with an error probability equal to p.

2.3.4 Statistical Analysis

A one-way repeated measures ANOVA was performed for each index, with surgery epochs being the repeated factor. Post-hoc comparisons were performed using the paired Student's t-test with Bonferroni correction in order to verify significant differences between the general anesthesia induction and post intubation epochs with respect to the baseline condition. Unpaired two-sample Student's T-test was used to compare results from NH and CH patients for each epoch (baseline, general anesthesia and post intubation) in order to verify the effects of altered ABP control on the response to propofol induction. Continuous variables are expressed as mean ± standard deviation. A p-value < 0.05, 2-tailed, was considered statistically significant.

2.4 Results

The main characteristics of the enrolled patients as well as the types of surgery are summarized in table 2.1. NH and CH patient groups did not differ significantly in any of the characteristics listed. Figure 2.1 shows an illustrative example of SBP and RR time series analyzed in this work.

Table 2.1. Demographic and anamnestic data of patient population

	non hypertensive patients	chronic hypertensive patients
N	10	7
Gender (male/female)	7/3	6/1
Age(yr)	63.6±10.6	67.9±10.6
Weight (kg)	77.5±13	78.7±7.3
Height (cm)	170±8.3	168±3.9
Organ object to surgery:		
Liver	6	3
Kidney	1	1
Pancreas	3	2
Carotid	0	1
ASA classification	2.5 ±0.5	2.6±0.5
Smoke (yes/no)	3/7	1/6
Drugs (Diuretics/ACE I /Ca^{++}antagonist)	2/0/1	0/4/1
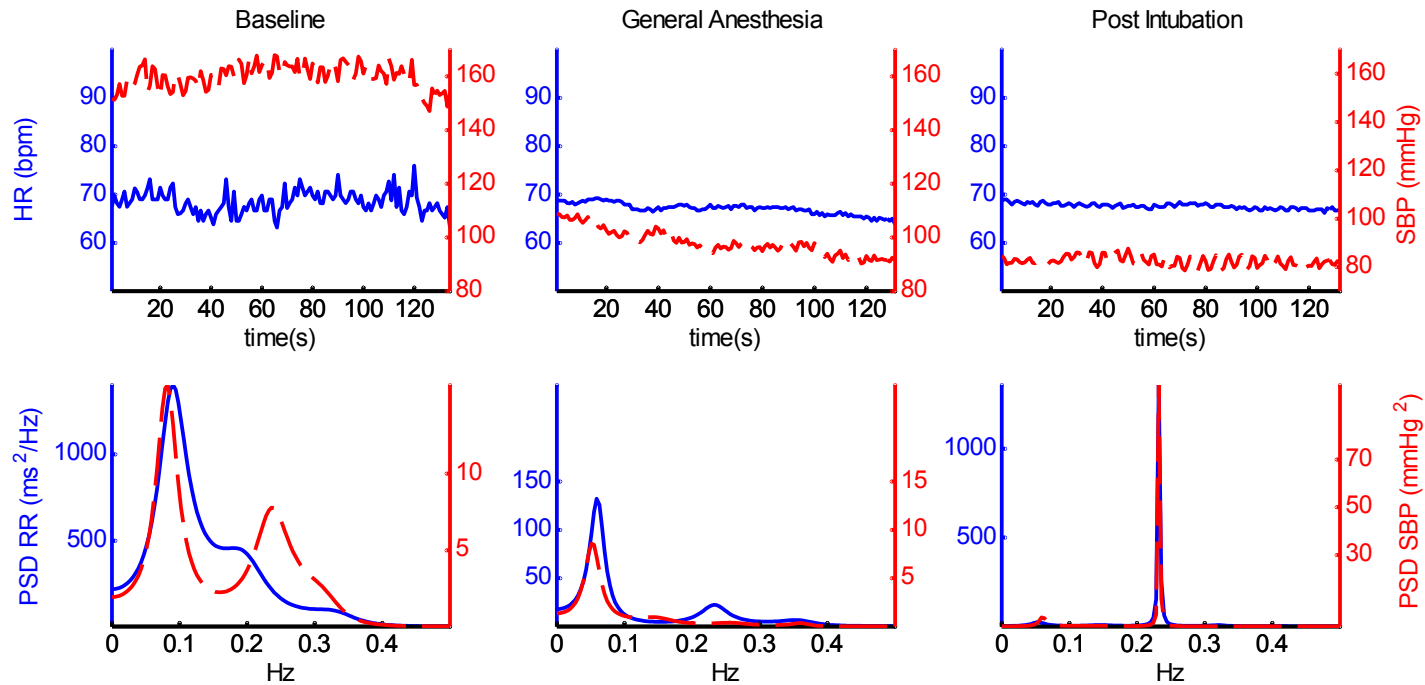
Figure 2.1 Upper panels: HR and SBP time series of a patient during baseline, general anesthesia induction and post-intubation epochs. Lower panels: corresponding power spectra. Solid lines and left axes refer to RR signal, shaded lines and right axes to SBP signal, respectively. Notice that after intubation most of the power is centered on the respiratory frequency, which is a clear effect of mechanical ventilation.

2.4.1 Time domain results

No significant changes in HR between surgery epochs were seen in the NH group or in the CH group, and no significant differences in HR were found when comparing the two groups (table 2.2).

In NH and CH patients, mean values of SBP, MAP and PP significantly decreased after anesthetic procedures and after intubation in comparison with baseline condition (table 2.2). DBP significantly decreased after intubation in both groups, whereas a significant decrease of DBP after induction was found in NH patients only.

SBP and DBP values of NH and CH patients did not differ significantly at baseline, but resulted significantly lower after intubation in hypertensive patients with respect to normotensive patients. MAP and PP values did not show significant differences between NH and CH patients. The variation of SBP and DBP estimated as the difference between post intubation values minus baseline values resulted significantly larger in the CH group (table 2.5). Accordingly, after intubation CH patients showed lower ABP values than NH group.

2.4.2 Spectral Analysis

RR and SBP fluctuations were significantly reduced in general anesthesia and post intubation epochs with respect to the baseline condition. After intubation, mechanical ventilation resulted in a strong entrainment of respiratory frequency around 0.2 Hz in the ABP and RR series as shown in figure 2.1. For this reason, the HF spectral components were not estimated after intubation. HF spectral components did not show any significant difference between groups in baseline and during induction and no significant differences were reported between the baseline and general anesthesia conditions.

LF spectral components significantly decreased in RR, SBP, DBP and MAP series from baseline to general anesthesia and post-intubation epochs in both patient groups. LF power of PP changed significantly from baseline to post-intubation only in NH patients. LF power of SBP in CH patients was significantly higher than in NH patients at baseline (table 2.3).

Table 2.2 Mean values of HR and ABP signals estimated in each epoch for each group of patients. Values are presented as mean±std.

		BASELINE	GENERAL ANESTHESIA	POST-INTUBATION
HR (bpm)				
	NH	70.1±12.1	66.1±11.8	65.7±9.2
	CH	73.4±13.2	73.1±21.5	70.1±17.8
SBP (mmHg)				
	NH*	144±18.8	108±25.2†	110±24.6†§
	CH*	156±24.1	116±20.1†	82.8±12.8†‡
DBP (mmHg)				
	NH*	68.8±10	56.6±10.9†	57.5±7.6†§
	CH*	72±9	59.6±9.2	44.3±6.1†‡
MAP (mmHg)				
	NH*	95.9±10.5	73.9±14.2†	76.3±13.3†§
	CH*	102.9±12.1	80.4±12.5†	57.6±7.9†‡
PP (mmHg)				
	NH*	75.2±18.2	51±19†	52.2±20.7†
	CH*	84.4±23.3	56.9±17.5†	38.5±10.5†‡

NH: non hypertensive patients; CH: chronic hypertensive patients
*ANOVA for repeated measures p-value <0.05 †post-hoc comparison vs baseline p-value<0.05
‡ post-hoc comparison vs general anesthesia
§ Unpaired Student's t-test p-value <0.05 NH vs CH

Total RR power decreased significantly after propofol induction and post-intubation epochs with respect to baseline in NH and CH patients. No significant differences were seen between groups in any of the epochs.

Total power of SBP and DBP in CH patients was significantly lower in the general anesthesia induction epoch when compared to the baseline epoch, while total power of MAP in CH patients was significantly higher in baseline than general anesthesia and post-intubation epochs, and total power of SBP and PP were significantly lower in NH when compared to CH patients in the post-intubation epoch (table 2.3).

2.4.3 Causality test and BRS indices

All NH and CH patients passed Granger causality test for both feedback (SBP → RR) and feedforward (RR → SBP) pathways and in each epoch.

BRS gain values estimated in the LF band with the transfer function method, the spectral method (α_{LF}) and through the bivariate model (SBP → RR) were found to be significantly lower in CH patients than in NH patients at baseline (table 2.4).

Only NH patients showed a significant variation in BRS values: α_{LF} and the gain of SBP → RR in LF band were significantly reduced after propofol induction and post intubation epochs.

No significant differences were found in feedforward gains both between groups and within each group.

The variation of BRS, estimated as the difference between post intubation values minus baseline values resulted significantly different between the two groups: NH patients showed a larger variation than CH patients (table 2.5, figure 2.2).

BRS gain values estimated in the HF band were excluded from the statistical analysis due the strong entrainment produced by mechanical ventilation at those frequencies.

Table 2.3 Power spectral components of HR and ABP signals estimated in each epoch for each group of patients. Values are presented as mean±std.

		BASELINE	GENERAL ANESTHESIA	POST-INTUBATION
LF RR (ms^2)	NH [*]	36069±29684	11279±22675[†]	5089±5243[†]
	CH [*]	21536±10338	6226±2959[†]	5481±10036[†]
LF SBP (mmHg^2)	NH [*]	444±320[§]	295±426	119±172[†]
	CH [*]	838±319	359±193[†]	199±359[†]
LF DBP (mmHg^2)	NH [*]	251±186	89.8±134[†]	45.6±62[†]
	CH [*]	347±233	75.0±33.5[†]	53.5±83[†]
LF MAP (mmHg^2)	NH[*]	329±285	134±187[†]	63.8±101[†]
	CH	508±280	164±66[†]	106±202[†]
LF PP (mmHg^2)	NH[*]	171±87.2	146±204	29.6±30.3[†‡]
	CH	404±533	195±133	137±252
TP RR (ms^2)	NH [*]	61562±46235	22021±38281[†]	11380±10650[†]
	CH [*]	33916±15682	12460±5495[†]	10828±14913[†]
TP SBP (mmHg^2)	NH	961±1068	632±1069	305±230[§]
	CH	1269±603	558±272[†]	986±919
TP DBP (mmHg^2)	NH [*]	572±744	237±481	84.4±74[†]
	CH [*]	511±396	127±62.4[†]	178±218
TP MAP (mmHg^2)	NH	774±1051	381±826	134±111
	CH [*]	758±405	262±89[†]	326±319[†]
TP PP (mmHg^2)	NH	283±149	255±350	121±65.6[§]
	CH	627±761	309±209	469±420

NH: non hypertensive patients; CH: chronic hypertensive patients. [*]ANOVA for repeated measures p-value <0.05 [†]post-hoc comparison vs baseline p-value<0.05. [‡] post-hoc comparison vs general anesthesia. [§] Unpaired Student's t-test p-value <0.05 NH vs CH

Table 2.4. BRS and bivariate model gain values estimated with different methods (transfer function (TF), method, sequence method and bivariate model) in LF and HF spectral bands in each epoch for each group of patients. Values are presented as mean±std

		BASELINE	GENERAL ANESTHESIA	POST-INTUBATION
TF LF (ms/mmHg)				
	NH [*]	9.8±3.5[§]	6.1±4.6	6.5±2.5
	CH	5.2±2.0	4.5±1.5	5.8±3.2
TF HF (ms/mmHg)				
	NH	8.9±4.3	11.4±9.8	
	CH	7.6±3.1	10.8±5.3	
LF (ms/mmHg)				
	NH [*]	9.1±3.5[§]	6.2±3.9[†]	6.9±3.0
	CH	5.2±1.6	4.5±1.6	6.0±3.8
HF (ms/mmHg)				
	NH	8.4±4.7	9.3±6.0	
	CH	6.1±2.3	6.9±3.4	
Seq. Met. (ms/mmHg)				
	NH	11.1±6.4	11.7±6.6	8.0±5.3
	CH	7.9±1.7	10.5±4.1	6.3±3.4
SBP RR (LF) (ms/mmHg)				
	NH [*]	7.8±4.9[§]	3.7±2.9[†]	3.3±2.5[†]
	CH	3.3±1.7	3.4±2.3	4.2±3.4
SBP RR (HF) (ms/mmHg)				
	NH	4.9±3.6	5.1±4.7	3.9±2.8
	CH	2.5±1.8	3.9±2.7	2.9±2.3
RR SBP (LF) (mmHg/ms)				
	NH	0.08±0.07	0.11±0.06	0.09±0.07
	CH	0.11±0.08	0.36±0.72	0.07±0.05
RR SBP (HF) (mmHg/ms)				
	NH	0.08±0.04	0.09±0.09	0.19±0.24
	CH	0.06±0.04	0.08±0.03	0.03±0.02

NH: non hypertensive patients; CH: chronic hypertensive patients. [*]ANOVA for repeated measures p-value <0.05 [†]post-hoc comparison vs baseline p-value<0.05. [‡] post-hoc comparison vs general anesthesia epoch. [§] Unpaired Student's t-test p-value <0.05 NH vs CH

Table 2.5. Variation values of HR, ABP and BRS indices estimated as the difference between general anesthesia induction and baseline epoch, and between post intubation and baseline epoch for each group of patients. Values are represented as mean±std

		General anesthesia - Baseline	Post Intubation - Baseline
HR (bpm)			
	NH	-4.0±8.3	-4.4±6.7
	CH	-0.29±9.7	-3.3±8.9
SBP (mmHg)			
	NH	-36.6±15.4	-34.5±21.8[§]
	CH	-40.0±25.3	-73.6±25.0
DBP (mmHg)			
	NH	-12.2±9.4	-11.4±10.4[§]
	CH	-12.4±6.4	-27.6±13.8
LF (ms/mmHg)			
	NH	-2.8±1.6[§]	-2.2±4.0
	CH	-0.69±2.5	0.85±3.9
TF LF (ms/mmHg)			
	NH	-3.7±4.3	-3.3±4.2[§]
	CH	-0.62±2.8	0.6±3.5
SBP RR (LF) (ms/mmHg)			
	NH	-4.1±5.6	-4.5±4.2[§]
	CH	0.04±2.8	0.89±3.5

NH: non hypertensive patients; CH: chronic hypertensive patients
[§] Unpaired Student's t-test NH vs CH p-value <0.05

2.5 Discussion

2.5.1 Effects of propofol anesthesia on BRS

The closed-loop interaction between HR and ABP is the effect of baroreflex regulation (feedback from ABP to HR) as well as of mechanical coupling between CO and ABP (feedforward from HR to ABP). A typical tool to quantify the strength of the linear coupling between two signals is the computation of the coherence function; however this approach is not reliable when the signals are related in a closed-loop system. In order to be thorough, we need to mention some methods, based on multivariate autoregressive modeling, that quantify causality also in the frequency domain (Baccala et al., 1998; Faes et al., 2010). Among them, the directed coherence is a method that decomposes the

ordinary coherence function and elicits causality from the spectral representation of the multivariate autoregressive parameters.

In this thesis we employed a causality analysis based on the Granger causality test to robustly estimate the causal relationship between HR and SBP. The quantitative and objective assessment of the causality of the feedback regulation from SBP to HR enables to follow the variations in the strength of the physiological coupling between HR and ABP through different epochs of the clinical protocol: from baseline conditions preceding propofol administration, to the period following induction and preceding intubation, to the onset of mechanical ventilation.

The results obtained employing the various BRS indices considered in this study produced similar results except for the ones obtained through the sequence method. The lower values of BRS gain obtained using the causality approach in comparison with the results obtained using the other methods could be due to the fact that the closed loop model takes into account the baroreflex buffering action on ABP and RR oscillations. Closed loop analysis showed that the feedforward pathway was unaffected by propofol induction, as expected given the purely mechanical nature of this coupling relationship.

Although the causality approach is the most appropriate from a mathematical point of view as it separates the oscillatory contributions of baroreflex from the mechanical effects of runoff on ABP, also the transfer function method and the ratio of power spectra were able to track the change in the BRS.

The main advantage of these methods with respect to the sequence method is the possibility to disentangle the contribution of slow oscillations relating to the sympathetic nervous system, from the oscillations at higher frequencies mainly related to the vagal and respiratory activity. The main limitation of the sequence method is that no mathematical model is assumed for the relationship between SBP and RR, so that this technique is unable to separate the SBP and RR oscillations from different origin and not baroreflex mediated. As reported in (Vallais et al., 2009; La Rovere et al., 2011) the use of different BRS estimators can be useful to investigate the relationships between ABP fluctuations and RR oscillations.
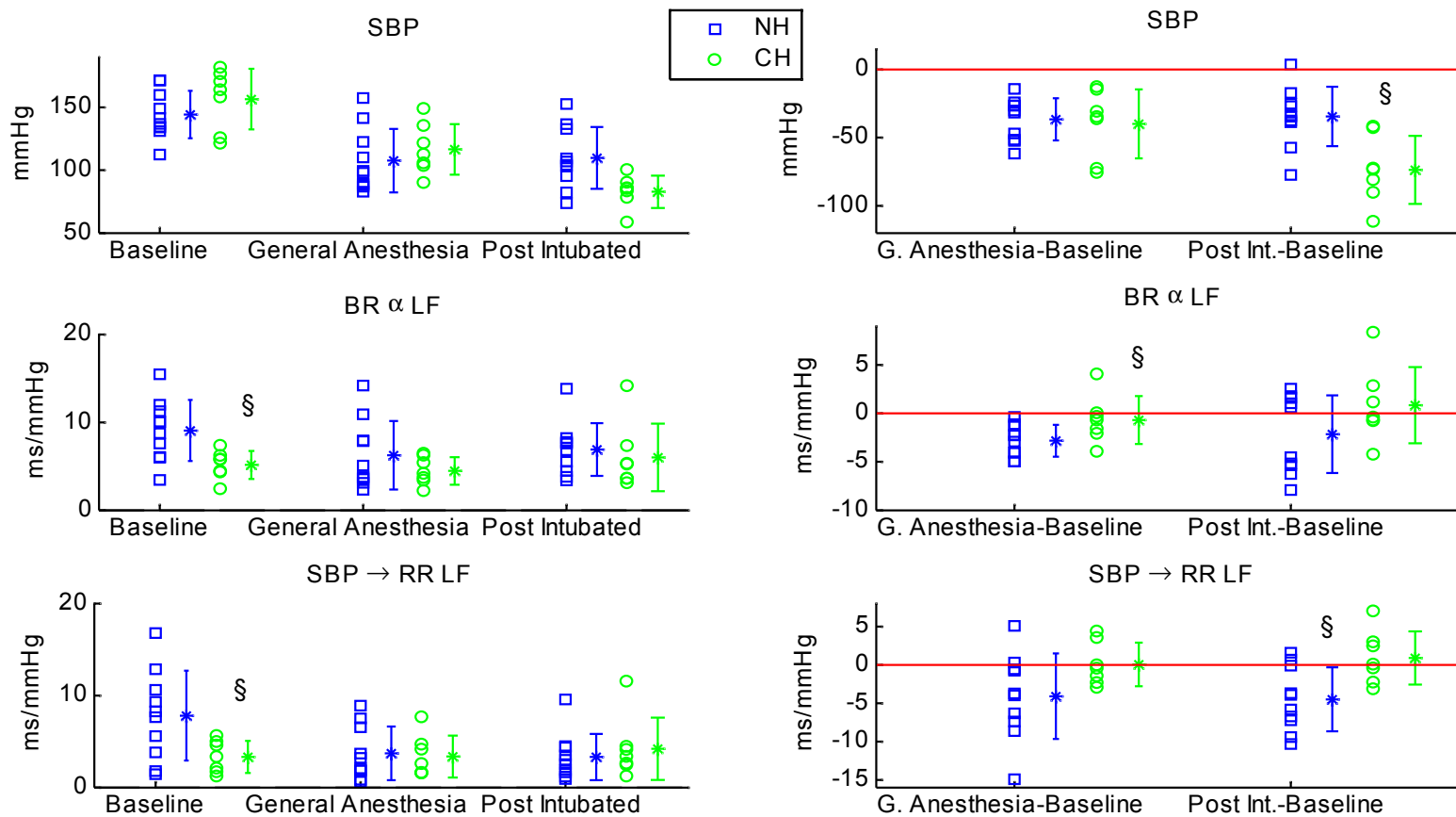
Figure 2.2 Left panels: values of SBP and BRS indices estimated for each epoch and for each NH patient (squares) and CH patient (circles). Boxplot are reported as well. Right panels: values of the differences between the indices estimated during general anesthesia induction and during the post intubation epoch with respect to the baseline epoch. Mean values and standard deviations of deltas are reported for each group of patients. Notice the significant decrease of BRS in NH patients whereas CH showed lower BRS values during baseline without significant changes; and a larger decrease of SBP after intubation in CH group. The symbol § marks the significant differences between NH and CH (p-value <0.05).

2.5.2 BRS in hypertensive vs. normotensive patients

Chronic hypertensive patients and non hypertensive patients both showed a decrease of ABP after propofol infusion, possibly because of the vasodilator effect of propofol (Cullen et al., 1987; Samain et al., 1989). In the work of (Robinson B et al., 1997), the peripheral vascular actions of propofol appeared to be due primarily to an inhibition of sympathetic vasoconstrictor nerve activity. The reduction of sympathetic outflow following propofol administration was also reported by direct measurements of muscle sympathetic nervous activity (Sellgren et al., 1994). Our results showed a decrease of the LF power of both SBP and DBP, which was consistent with a reduced sympathetic vasoconstrictive activity.

SBP was not significantly different between CH and NH patients at baseline. This may be due to the pre-medication administered preceding the onset of anesthesia, which induces a modulation of adrenergic inputs (Weisenberg et al., 2010; Varon et al., 2008). Blood pressure can be elevated in patients who, following pre-medication, are affected by respiratory depression and the ensuing carbon dioxide retention (Greene et al., 1963).

The decrease of SBP and DBP values was more pronounced in the CH group when compared to NH. In particular, in CH patients ABP values decreased further after intubation, and the drop from baseline values was on average 46% vs 24% in NH patients.

Except for the sequence method, all BRS indices yielded lower values of BRS in CH patients vs NH patients at baseline. It is well known that hypertensive patients are characterized by an altered cardiac baroreflex control (Sevre et al., 2001; Matsukawa et al., 1991) and this was confirmed by our pre-induction calculations of BRS. The endotracheal intubation is known to be a sympathetic stimulus, so it should be expected an increase of BRS and ABP values, CH patients showed an opposite trend: a further decrease of ABP values. The larger drop in ABP associated with a lower BRS in the CH group is consistent with this pathological condition, which is known to be affected by an altered sympathetic outflow to vasculature in hypertensive subjects. In addition, chronic hypertension is often associated to a hypersympathetic activity and this condition may affect the centrally mediated baroreflex control (Foëx et al., 2004; Abboud et al., 1982).

Only NH patients showed a drop of BRS values estimated in the LF band in the epochs after general anesthesia from baseline. In NH patients, the reduced LF power in

SBP and DBP as well as the decrease in BRS occurring after anesthesia induction is consistent with a reduction of sympathetic autonomic outflow (Sellgren et al., 1994; Robinson B et al., 1997). Still, the blunting of baroreflex control of HR may not entail a complete impairment of the control system, and it could be hypothesized that the ability to respond to pressure variations under anesthesia is partially preserved.

Finally, the absence of significant changes in average HR values was found to be accompanied by a significant decrease of the LF component and total power in the HRV spectra. The decrease of RR variance may be explained by the aforementioned diminished sympathetic outflow, and the maintenance of HR could be explained by the counterbalance of the positive chronotropic effects of propofol to the change in sympathetic nervous activity, which is expected to cause a deceleration of the heart rhythm. Specifically, ligand-gated ion channels are likely to be one of the major sites of action of anesthetic agents, and the GABA and ionotropic glutamate (NMDA) receptors are known to be affected by anesthetic drugs (Krasowski 1999). In particular, propofol was shown to potentiate $GABA_A$ currents and to augment the GABAergic input to the cardiac vagal neurons by increasing both phasic and tonic $GABA_A$ receptor currents (Bentzen et al., 2011), with an inhibiting effect on vagal control of HR.

CHAPTER 3

Arterial and cardiopulmonary baroreflex control on heart rate

3.1   Introduction

Mild LBNP is an experimental model of reduction of the heart preload, which is not as severe as moderate hemorrhage, but which can be useful to investigate the response to a diminished venous return of both cardiopulmonary and arterial baroreflexes to the maintenance of arterial blood pressure in humans. Low levels of LBNP are supposed to selectively unload cardiopulmonary baroreceptors (Berdeaux et al, 1992; Robinson T. et al., 1997; Thompson et al., 1991), resulting in reflex peripheral vasoconstriction without changes in HR. This assumption is based on the observations of decreased CVP, which leads a reduction of neural firing from cardiopulmonary baroreceptors, and unchanged MAP, that evidence the absence of changes of neural firing from arterial baroreceptors.

Hence, the resulted reflex responses during mild LBNP have been explained by cardiopulmonary baroreflex effects (Wolthius et al., 1974; Kimmerly et al., 2002; Thompson et al., 1990).

However, transient reductions in MAP during rapid onset and release of mild LBNP may be detected as was reported by (Hisdal et al., 2001, 2002) suggesting that cardiopulmonary baroreceptors are unloaded and the arterial baroreflex is engaged during mild LBNP.

A transient reduction in SBP and DBP which were restored presumably through the arterial baroreflex feedback mechanism, after ~15 heartbeats, was founded by Fu et al. (2009), also considering an unloading of arterial baroreflex at the onset and during mild LBNP. Other work that provides evidence of engagement of arterial baroreceptor was carried out by Taylor et al. (1995) where aortic pulse area was reduced during non hypotensive hypovolemia induced by mild LBNP in a study using magnetic resonance imaging.

Interaction between arterial and cardiopulmonary baroreflexes was showed as well by Pawelczyk et al. (1989) suggesting that reductions in central blood volume augment both HR and blood pressure carotid baroreflex responses in man by reducing an inhibitory influence from cardiopulmonary receptors. However, the quantification of the relative dynamic contribution of arterial and cardiopulmonary baroreflex is not totally elucidated yet.

However, the work of Aletti et al. (2012) proved that arterial baroreflex is the main player in the mediation of total peripheral resistance (estimated by means of DBP variability) during incremental levels of LBNP before and after bed rest. In order to complete these investigations about the relative contribution of arterial and cardiopulmonary baroreflex, the analysis of the HRV in maintaining cardiac output in the same conditions is fundamental and this study represents a completion of the previous work (Aletti et al., 2012).

Moreover, the LBNP protocol permits to investigate the short term control induced by a decrease of venous return, so the "reverse" Bainbridge reflex was investigated as well. In fact, the "reverse" Bainbridge reflex implies that, following a reduction in venous return that causes an unloading of cardiopulmonary baroreceptors, a reflex-induced decrease in HR would occur (Cristal et al., 2012). In other words, a "reverse" Bainbridge reflex would

decelerate the HR in conditions of poor diastolic filling. This reverse reflex may be elicited by non hypotensive hypovolemia induced by mild LBNP.

Reflex tachycardia was demonstrated with volume loading and reflex bradycardia was observed with volume reduction in dogs (Bainbridge et al., 1915; Vatner et al., 1975). These findings are opposite to expected responses elicited by arterial baroreflex.

On the other hand, Triedman et al. (1993) found that mild hypovolemia induced by hemorrhage through a standard blood donation of 450 ml did not produce significant changes in mean HR, while decrease in vagal modulation of HR was seen in HF band and a reduction of arterial baroreflex gain in HF band also was found (Triedman et al., 1993), suggesting that arterial baroreflex is also engaged during mild hypovolemia. Floras et al. (2001) also suggested that arterial baroreflex are perturbed during low levels of LBNP, where muscle sympathetic nerve activity was recorded, reporting that reductions in CVP with -5mmHg LBNP had no effect on ABP, SV, CO (determinants of arterial baroreceptor discharge), or HR but elicited a significant reflex rise in sympathetic discharge to skeletal muscle, and a significant reduction of parasympathetic modulation of HR was found, response that cannot be attributed to unloading of inhibitory reflexes arising from low-pressure mechanoreceptors.

In order to explain short term control mechanisms of HR and ABP, black box models have been proposed (Baselli et al., 1988; Aletti et al., 2009; Barbieri et al., 2001, 2002; Mukkamala et al., 2006a). In addition, the utility of inclusion of CVP in the analysis of changes in circulation control during manipulations of central volume has been shown by Barbieri et al. (2002), that applied a bivariate AR model to estimate the relationship between respiration and CVP. The results of Barbieri et al. (2002) identified the presence of a Bainbridge reflex in humans during a maneuver of volume expansion, based on baroreflex and respiratory sinus arrhythmia gains. However the model of Barbieri et al. (2002) did not involve CVP measurements in the RR variability estimation.

In this work, hemodynamic measurements collected during an LBNP experiment, repeated before and on day 50 of a long-duration, head-down bed rest (HDBR) study, were analyzed by a black box, multi-input–single-output model for the prediction of short-term, beat-by-beat RR fluctuations.

Exposure to actual or simulated microgravity by head down bed rest (HDBR) leads to cardiovascular deconditioning with the associated reductions in blood pressure regulation

during orthostatic stress. To maintain adequate blood pressure and cerebral perfusion during orthostatic stress, reflex adjustments occur to increase HR and peripheral vasoconstriction to compensate for a decreased venous return and SV. Several factors contribute to the diminished ability to maintain blood pressure in bed rest: reductions in plasma volume (Convertino et al., 1996; Buckey et al., 1996), diminished baroreflex control of HR (Sigaudo-Roussel et al., 2002), and/or vascular resistance (Moffitt et al., 1998).

The response of ABP to LBNP may be affected by cardiovascular deconditioning evoked by exposure to long duration bed rest. In this context, a reset of baroreflex system may take place and adaptation responses of arterial and cardiopulmonary baroreflex may occur. For instance, Pawelczyk et al. (1989) reported that the gain of the carotid baroreflexes was linearly and inversely related to decreases in CVP during LBNP procedure, whereas Cooper et al. (2001) showed that vascular resistance responses were enhanced during LBNP. This evidence of enhancement of arterial baroreflex can be affected by the addition of prolonged bed rest condition.

A black box model of HRV from multiple inputs was proposed with the aims of 1) to identify arterial and cardiopulmonary baroreflex control of HR and sympathetic and respiratory sinus arrhythmia mediated HRV responses to mild, rapid onset and short duration LBNP cycles and 2) to assess the effects of long duration bed rest induced cardiovascular deconditioning.

Since the Bainbridge reflex was eventually described as full cardiopulmonary reflex, encompassing both increases in HR during hypervolemia and decreases in HR during hypovolemia (Mark et al., 1983; Barbieri et al., 2002), this study search for a possible "reverse" Bainbridge reflex, i.e. an effect on short term control of HR in response to a decrease in cardiac preload.

3.2   Experimental protocol

A subset of data from Women's International Space Simulation for Exploration (WISE-2005) study was analyzed. During this protocol no nicotine, alcoholic beverages or caffeine were permitted. Baseline testing was conducted 7 days prior to the start of head down bed rest (pre-HDBR), and post-intervention testing was conducted following 60 days

of HDBR. Further details on protocol are reported in (Arbeille et al., 2008; Guinet et al., 2009; Hodges et al., 2010). Experiments were carried out at the Institute for Space Physiology and Medicine Clinical Research Facility in Toulouse, France. All procedures were approved by Ethics Committee from University of Waterloo, Canada, and the French Committee for Health, in agreement with the Helsinki convention, and all participants gave their prior informed consent.

The subset of data consists of seven healthy women (age 33 ± 1yr, height 165 ± 4cm, weight 59 ± 3Kg) from control group; the data selection was based on data quality, because the model applied required high-quality signals with no unfilterable artifacts or noise and more than 2 min of recordings in each level of suction. The same data set was used also in the work of Aletti et al. (2012).

The continuous LBNP experiment was a subset of the battery of cardiophysiology tests completed during a 60-day-long, 6° HDBR. Subjects were placed in a custom-made LBNP chamber and sealed at the iliac crest with a neoprene "skirt". They were then outfitted with a 3-lead ECG (Colin, St. Antonio, TX, USA), respiration belt (PowerLab), finger blood pressure cuff (reconstructed to brachial and height-corrected, Finometer, FMS, Amsterdam, The Netherlands) and a 2.5 cm, 22-gauge catheter was inserted in the right antecubital vein. The catheter was connected to a pressure transducer held at the level of the heart to estimate CVP, according to the dependent right arm technique (Gauer et al., 1956). Signals were collected at 1,000 Hz on a PowerLab Data Acquisition System running Chart software (PowerLab, Sydney, Australia).

Incremental levels of lower body suction (0, -10, -20, -30 mmHg) were progressively applied to subjects, at least 2 min per level, and with transition time between each level <5 s. The experiment was completed once before entry into bed rest and then repeated again on day 50 of HDBR.

3.3   Methods

3.3.1 Signal pre-processing

RR series were extracted from ECG waveforms by identification of QRS complexes and of R peaks. Beat-by-beat series of DBP and SBP were extracted from ABP waveforms, considering values between consecutive R peaks. DBP (i) was considered as the onset of

the current beat on the ABP waveform following R(i); thus, SBP(i) follows DBP(i), while RR(i-1) indicates the difference between R(i), that is the occurrence of the R peak in the current beat, and R(i-1), that is the occurrence of the R peak in the previous beat.

Beat-by-beat series of CVP were obtained as the mean value of continuously recorded CVP over each cardiac cycle, i.e., between two consecutive R peaks. Stationary segments of two minutes were selected for each LBNP phase. Beat-by-beat series were detrended, divided by mean values and resampled in the time domain at 1 Hz. Figure 3.1 shows an example of the time series from one subject during the LBNP experiment before bed rest.
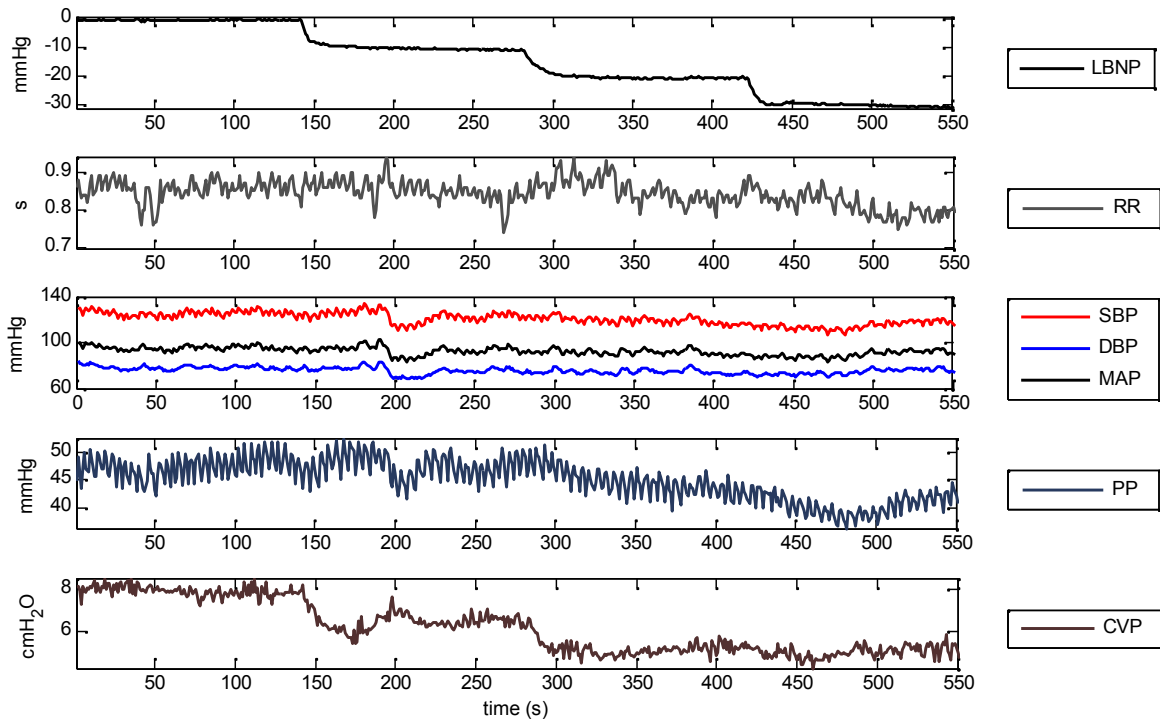
Figure 3.1 Beat by beat hemodynamic series from one subject during lower body negative pressure (LBNP) experiment before bed rest. SBP, systolic blood pressure; DBP, diastolic blood pressure; MAP, mean arterial pressure; PP, pulse pressure; CVP, central venous pressure.

3.3.2 System identification of RR variability

The model of RR prediction previously proposed (Baselli et al., 1994) was improved by including the relationship between CVP and RR with the aim to elucidate the cardiopulmonary baroreflex modulation of RR variability and to investigate the presence of a "reverse" Bainbridge.

$$RR(i) = \sum_{j=1}^{p} h_{ABR} \cdot SBP(i-j) + \sum_{j=1}^{q} h_{RSA} \cdot RESP(i-j) + \sum_{j=1}^{r} h_{CP} \cdot CVP(i-j) + w(i) =$$

$$RR_{/SBP} + RR_{/RESP} + RR_{/CVP} + W \tag{3.1}$$

The model is composed of three deterministic components and a stochastic noise (W) that represents the residual predictions error. Equation 3.1 models the prediction of beat-by-beat oscillations of the RR interval from SBP, CVP and respiration (RESP) time series. The model is therefore meant to describe the black box identification of arterial baroreflex modulation of RR variability ($RR_{/SBP}$), the black box identification of cardiopulmonary baroreflex modulation of RR variability which encompasses the "reverse" Bainbridge reflex ($RR_{/CVP}$), the black box identification of respiratory sinus arrhythmia ($RR/_{RESP}$) and noise on the prediction which represents very slow oscillations relating to nonlinear HR control, humoral and thermoregulatory effects, etc.

The model orders *p,q,r* were determined by AIC and they were set in the range between 8 and 12. Model coefficients were identified by least-squares minimization algorithm. Furthermore, spectral decomposition of RR variability and analysis of impulse responses of the transfer functions obtained from the model were performed.

Complete characterizations of dynamics of all three model components are given by their respective (unknown) impulse responses: h_{ABR}, h_{RSA} and h_{CP}. In linear systems theory, the impulse response provides a complete characterization of the dynamic properties of the system, since the response of this system to any arbitrary input can be predicted mathematically by convolving the input with the impulse response (Khoo et al., 2000). h_{ABR}, for instance, quantifies the time-course of the change in RR resulting from an instantaneous unitary increase in SBP, whereas h_{CP} quantifies the time-course of the fluctuation in RR associated with an instantaneous increase in CVP.

Impulse responses of the model components (Eq. 3.1) were constructed using Laguerre expansion according to the method proposed by Marmarelis et al. (1993), and the least square error method.

For example, arterial baroreflex (ABR) impulse response is expanded to be the sum of weighted Laguerre basis functions:

$$h_{ABR}(\ ) = \sum_{j=0}^{p-1} c_j^{ABR} L_j(\ ) \tag{3.2}$$

where $L_j(\ )$ represents the j-th order discrete-time orthonormal Laguerre function, and c_j^{ABR} are the corresponding unknown weights that are assigned to $L_j(\ )$ in the arterial baroreflex impulse response. The impulse responses of the other model components (h_{RSA}, h_{CP}) are similarly expanded as weighted sums of Laguerre functions.

Some advantages of projecting the signals on the Laguerre basis are that the method provides a significant reduction of the number of parameters that need to be estimated, the estimated impulse responses are smoothed, accurate kernel estimates can be obtained from short experimental data records, the technique is robust in the presence of data-contaminating noise and does not require long computing time (Blassi et al., 2006; Marmarelis et al., 1993).

3.3.3 Spectral analysis

Power spectral density was computed via AR estimation for each variability series obtained from measurements and from model prediction, before and during bed rest. Spectral analysis was performed in the frequency bands and with optimal order as was explained in chapter 2.

The proportional contribution of the arterial baroreflex related component vs. the cardiopulmonary baroreflex-related component to the variability of RR interval was assessed through the following ratios: LF power of $RR_{/SBP}$ over LF power of RR (LF $RR_{/SBP}$/LF RR) to quantify the amount of RR variability explained by SBP; LF power of $RR_{/CVP}$ over LF power of RR (LF $RR_{/CVP}$/LF RR) to quantify the amount of RR variability explained by CVP.

3.3.4 Baroreflex sensitivity

The baroreflex functioning is described by BRS index or BRS gain, that was assessed by means of the bivariate model. The bivariate model approach assesses BRS by considering concurrently the causal relationship from SBP to RR, i.e. the feedback mechanism modeling baroreflex control of HR, and RR to SBP, i.e. the feedforward mechanism. This method was described and compared to other methods in chapter 2.

3.3.5 Statistical analysis

A two-way repeated-measures ANOVA test was performed, with LBNP epochs being the repeated factor and pre-HDBR and HDBR conditions the second factor. One-way repeated-measures ANOVA was applied to spectral indices obtained both in pre-HDBR and HDBR. Post hoc comparisons were performed by Fisher's least significant difference test to verify significant differences between a specific level of LBNP and baseline (BL). Paired two-sample Student's t-test was used to compare pre-HDBR and HDBR for each LBNP epoch (e.g., BL pre-HDBR vs. BL HDBR), to verify the effects of cardiovascular deconditioning on the response to LBNP. Significance to reject the null hypothesis that variations between the mean values of spectral indices before and during bed rest were not significant was set at $P < 0.05$.

3.4   Results

3.4.1 Time domain analysis

HR significantly increased during HDBR from BL to -20 mmHg and -30 mmHg of LBNP, while PP and SBP decrease from BL to -30 mmHg LBNP in HDBR and pre-HDBR respectively. CVP significantly decreased from baseline, progressively with increasing intensities of LBNP, before and during HDBR. Only PP and HR showed significant changes between pre-HDBR and HDBR, HR was significantly lower in each of the four experimental epochs in pre-HDBR, and PP resulted significantly smaller during HDBR at baseline and -10mmHg of LBNP. These results are shown in table 3.1 (see also Aletti et al. (2012)).

3.4.2 Frequency domain analysis

Values of LF, LF%, total power, LF/HF for the main hemodynamic variables before and during bed rest in each epoch of LBNP are reported in table 3.2. These are the most meaningful indices, since the LF band is related to sympathetic control of vascular tone, which causes blood pressure to fluctuate (Akselrod et al., 1981). Regarding the indices of HR variability, which are traditionally interpreted as representative of the impact of sympathovagal balance on HR, total RR power tended to decrease at the onset of LBNP in

pre-HDBR and to increase again for larger levels of LBNP. A significant increase in LF% of RR was found on day 50 of HDBR at -30mmHg, possibly as a reflection of the reduced variability of HR and respiration, which can also reduce the power of RR in the respiratory band. A significant increase in total power of SBP was reported at -10 mmHg with respect to baseline in pre-HDBR, while this was not the case in HDBR. Total power of SBP at baseline and at -20mmHg was significantly smaller before bed rest than during HDBR. A significant higher value of SBP LF% at -20 mmHg on day 50 HDBR with respect to pre-HDBR condition was found. LF power of SBP showed a significant smaller value in pre-HDBR in comparison with HDBR, in baseline and during LBNP.

CVP LF% resulted significantly lower at -20mmHg in HDBR condition with respect to baseline, besides at the same LBNP level CVP LF% was higher in pre-HDBR than in HDBR. CVP total power showed only a significant increase at -30 mmHg from baseline, in pre-HDBR condition.

RR LF/HF ratio was higher during bed rest, with respect to pre-HDBR; further, post hoc comparisons showed a significant increase of LF/HF of RR during bed rest passing from BL to -30 mmHg LBNP.

Table 3.1. Time domain indices before (PRE) and during bed rest (HDBR), in each of the four experimental epochs of the continuous LBNP maneuver

		BL	-10	-20	-30
HR, bpm[a,b]	**PRE**[‡]	$64.0\pm 6.8^{\#}$	$62.4\pm 6.2^{\#}$	$65.4\pm4.7^{\#}$	$69.6\pm 3.2^{\#}$
	HDBR[‡]	70.9 ± 4.7	75.0 ± 6.9	$81.0\pm8.4^{\S}$	$88.7\pm11.1^{\S}$
SBP, mmHg[a]	**PRE**[‡]	127.0 ± 7.2	123.7 ± 7.7	119.4 ± 8.0	$116.8\pm 7.9^{\S}$
	HDBR[‡]	118.0 ± 13.2	117.3 ± 11.1	113.9 ± 9.6	110.3 ± 12.4
DBP, mmHg	**PRE**[‡]	73.7 ± 6.7	71.7 ± 6.1	70.8 ± 5.4	71.2 ± 5.3
	HDBR	73.5 ± 8.9	73.4 ± 8.6	73.6 ± 7.9	73.4 ± 9.6
MAP, mmHg	**PRE**[‡]	93.5 ± 6.3	90.8 ± 6.0	88.3 ± 5.5	87.7 ± 5.0
	HDBR[‡]	91.3 ± 10.0	90.2 ± 9.0	88.8 ± 8.1	87.1 ± 10.0
PP, mmHg[a,b]	**PRE**[‡]	$53.3\pm 7.3^{\#}$	$52.0\pm 7.7^{\#}$	48.6 ± 8.7	45.6 ± 9.5
	HDBR[‡]	44.5 ± 7.0	43.9 ± 6.7	40.4 ± 6.5	$36.9\pm 7.0^{\S}$
CVP, mmHg[a,b]	**PRE**[‡]	7.3 ± 0.9	$4.8\pm 0.9^{\S}$	$3.3\pm1.5^{\S}$	$2.2\pm 2.6^{\S}$
	HDBR[‡]	6.7 ± 1.3	5.5 ± 1.5	$5.1\pm1.4^{\S}$	$4.4\pm 1.3^{\S}$

Values are expressed as mean $\pm$ SD. [a]Two-way ANOVA row factor (effect of bed rest), p-value < 0.05. [b]Two-way ANOVA column factor (effect of LBNP), p-value <0.05. [‡]One-way ANOVA, p-value < 0.05. [§]significant post-hoc comparison between each LBNP level and BL (in PRE and HDBR condition). [#]Paired t-test between the same LBNP phase (PRE vs HDBR) p-value < 0.05.

Table 3.2. Main frequency domain indices of hemodynamic variability before (PRE) and during bed rest (HDBR) in each epoch of LBNP.

LF		BL	-10	-20	-30
RR[a]	**PRE**	0.086±0.043	0.081±0.081	0.079±0.045	0.082±0.056[#]
	HDBR	0.184±0.148	0.089±0.067	0.139±0.070	0.315±0.289
SBP[a]	**PRE**	0.026±0.016[#]	0.034±0.019[#]	0.028±0.019[#]	0.035±0.019[#]
	HDBR	0.131±0.072	0.091±0.058	0.131±0.085	0.243±0.195
DBP[a]	**PRE**	0.113±0.064	0.098±0.061	0.124±0.074	0.124±0.067
	HDBR	0.189±0.110	0.135±0.080	0.202±0.098	0.341±0.238
CVP[b]	**PRE**	0.050±0.038	0.076±0.084	0.276±0.498	0.820±1.174[§]
	HDBR	0.072±0.082	0.043±0.033	0.144±0.176	0.482±1.005
LF %					
RR[a, c]	**PRE**	72.8±10.1	73.9± 8.9	74.2±10.1	65.0±11.1[#]
	HDBR	77.0± 9.8	76.7±11.2	84.1± 6.9	87.5± 6.1[§]
SBP[a]	**PRE**	72.3±12.4	68.1± 8.4	71.3±10.7[#]	74.3±15.3
	HDBR	73.7±14.7	79.4±16.4	87.3± 6.8	83.3±18.4
DBP	**PRE**	87.3± 9.1	85.6± 7.3	90.5± 5.8	85.5± 9.4
	HDBR	82.0± 6.8	85.8± 4.7	88.9± 7.7	88.1± 8.5
CVP	**PRE**	48.8±15.3	50.1±22.7	58.2±12.4[#]	54.5±17.4
	HDBR	51.6±19.4	46.1± 7.1	36.0± 8.4[§]	49.8±14.1
LF/HF					
RR[a]	**PRE**	4.8± 2.9	4.2± 3.0	5.5± 3.9	6.8± 8.0[#]
	HDBR	6.4± 3.9	6.4± 4.9	8.7± 4.5	15.5±14.5[§]
SBP[a]	**PRE**	5.3± 3.1[#]	7.2± 5.3[#]	7.9± 7.4[#]	9.3± 9.0
	HDBR	15.2±11.0	11.7± 4.0	15.3± 7.8	22.5±25.8
DBP	**PRE**	29.3±22.4	19.4±11.0	26.4±14.3	27.6±15.0
	HDBR	19.6±15.5	12.1± 4.2	17.8± 9.7	21.5±25.2
CVP	**PRE**	2.3± 1.7	2.9± 1.6[#]	2.7± 1.4	3.3± 2.5
	HDBR	3.5± 6.8	1.2± 0.5	2.4± 4.0	2.3± 2.8
TOTAL POWER					
RR[a]	**PRE**	0.197±0.126	0.138±0.134	0.152±0.087	0.213±0.156
	HDBR	0.319±0.207	0.157±0.120	0.217±0.120	0.442±0.383
SBP[a]	**PRE**	0.051±0.024[#]	0.109±0.087[§]	0.058±0.033[#]	0.071±0.039
	HDBR	0.398±0.282	0.203±0.187	0.206±0.106	0.437±0.392
DBP	**PRE**	0.188±0.116	0.216±0.160	0.167±0.074[#]	0.212±0.120
	HDBR	0.399±0.239	0.239±0.189	0.291±0.110	0.501±0.342
CVP[b]	**PRE‡**	0.250±0.231	0.594±0.889	1.068±1.689	3.470±4.309[§]
	HDBR	0.181±0.144	0.134±0.093	1.050±1.981	1.026±1.796

Values are expressed as means ± SD. [a] Two-way ANOVA row factor (effect of bed rest), *p*-value <0.05. [b]Two-way ANOVA column factor (effect of LBNP), *p*-value < 0.05. [c] Two-way ANOVA interaction, *p*-value < 0.05. ‡One-way ANOVA, *p*-value < 0.05.[§]Significant post hoc comparison between each LBNP level and BL. [#]Paired t-test between the same LBNP phase, PRE vs HDBR *p*-value < 0.05.

3.4.3 Spectral decomposition of RR variability

Figure 3.2 shows both the results of the identification of the components of RR variability (left), and of the computation of the relevant spectra (right), before (top) and on day 50 of HDBR (bottom). Because of signals were detrended and divided by mean value, signals are unitless, spectral densities are in $[Hz^{-1}]$, and power of spectral components is unitless. RR_{PRED} is the prediction of RR from the model, i.e., the sum of $RR_{/SBP}$, $RR_{/CVP}$, and $RR_{/RESP}$. Moreover, figure 3.3 and table 3.3 show results of spectral decomposition of RR variability and the relative contribution of its model components in the LF band.

The contribution of SBP variability to the prediction of RR variability ($RR_{/SBP}$) was largely predominant in all experimental conditions both before and during bed rest (figure 3.3). The contribution of $RR_{/SBP}$ assessed by (LF $RR_{/SBP}$/LF RR) was significantly larger on day 50 of HDBR at -20mmHg with respect to pre-HDBR condition.

CVP contributed little to the identification of RR variability and to its spectral decomposition. However, the contribution of $RR_{/CVP}$ in the LF band in pre-HDBR is completely different with respect to the values obtained on day 50 of HDBR. In pre-HDBR, the contribution of $RR_{/CVP}$ significantly increased at -20 mmHg with respect to baseline, whereas on day 50 of HDBR it is significantly decreased at -30 mmHg (table 3.3), as a result, its contribution resulted significantly lower than in pre-HDBR condition at -30mmHg of LBNP (figure 3.4).

3.4.4 Analysis of impulse responses

The average impulse response is shown in figure 3.5, which describes RR oscillations in function of a unitary decrease of CVP (negative impulse). A "reverse" Bainbridge would cause a transitory increase of RR (decrease of HR). Therefore the found initial transitory, which takes few seconds, fits with the hypothesis of "reverse" Bainbridge reflex. This phenomenon is more evident at -30 mmHg in pre-HDBR condition, where the undershooting is also limited, and at -10 mmHg on day 50 of HDBR. At -30mmHg on day 50 this transitory increasing of RR disappears. Notice that HR was significantly higher on day 50 of HDBR than pre-HDBR during all the LBNP epochs.

Figure 3.6 shows the average impulse response that represents RR fluctuations in function of a unitary increase of SBP. A transitory increase of RR was observed during the

first seconds, this increase was more evident at -30mmHg during pre-HDBR and after HDBR, suggesting an activation of the arterial baroreflex.
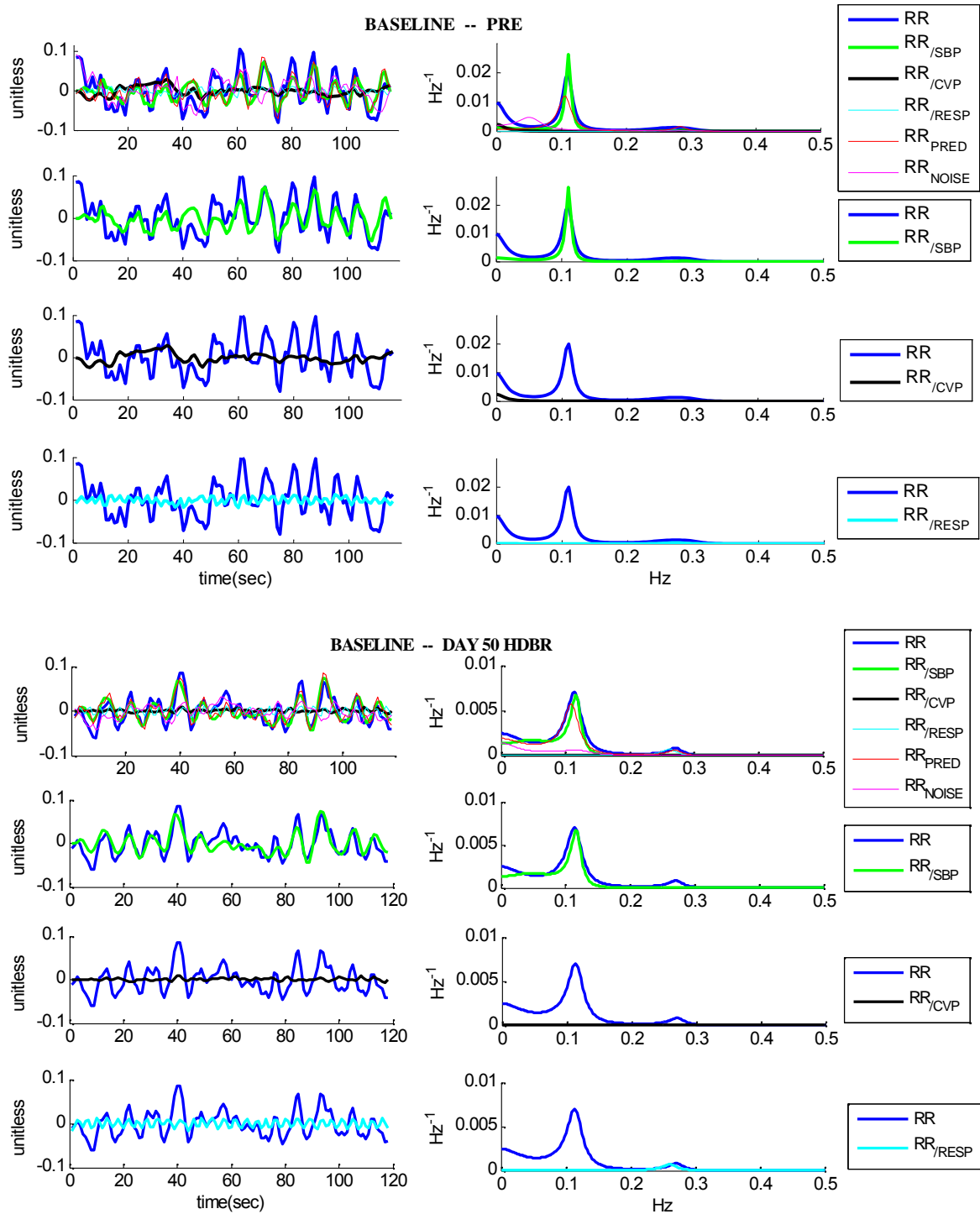

Figure 3.2. Time series (left) and spectra (right) of RR, and of the predicted model components: $RR_{/SBP}$, $RR_{/CVP}$, $RR_{/RESP}$, RR_{PRED} (model prediction) and RR_{NOISE} of one subject at baseline (BL), before bed rest (top) and on day 50 of HDBR (bottom).

3.4.5 Baroreflex sensitivity gain

BRS gain (SBP RR) estimated in the LF band decreased with increasing levels of LBNP, in pre-HDBR a significant decrease was found at -30mmHg, while on day 50 of HDBR significant lower values were found at -20mmHg and -30mmHg in comparison with baseline. Furthermore, at -20mmHg BRS gain resulted significantly lower on day 50 of HDBR with respect to pre-HDBR condition (table 3.4). During HDBR, a significant reduction of the BRS gain (SBP RR) in the HF band was observed at different levels of LBNP. Regarding the feedforward pathway, no changes were reported.

Table 3.3. Ratio between LF absolute power of each predicted component and LF absolute power of RR, during LBNP maneuver before and after HDBR.

		BL	-10	-20	-30
LF RR$_{/SBP}$/LF RR %[a]	**PRE**	22.3±23.7	30.6±31.1	26.0±13.0[#]	27.9±19.6
	HDBR	35.9±28.1	32.7± 6.8	49.0±15.9	39.8±25.4
LF RR$_{/CVP}$/LF RR %[a,b]	**PRE** [‡]	3.0± 1.0	4.7± 3.2	8.6± 4.9[§]	6.8± 4.9[#]
	HDBR	5.6± 4.3	4.8± 4.9	3.1± 2.4	1.4± 1.0[§]
LF RR$_{/RESP}$/LF RR %	**PRE**	0.9± 1.6	1.9± 2.5	0.8± 1.0	2.1± 2.1
	HDBR	1.8± 2.5	1.4± 2.7	0.4± 0.5	0.7± 0.7

Values are expressed as means ± SD. [a]Two-way ANOVA row factor (effect of bed rest), *p*-value <0.05. [b]Two-way ANOVA interaction, *p*-value < 0.05. [‡]One-way ANOVA, *p*-value < 0.05. [§]Significant post hoc comparison between each LBNP level and BL. [#]Paired t-test between the same LBNP phase, PRE vs HDBR *p*-value < 0.05.
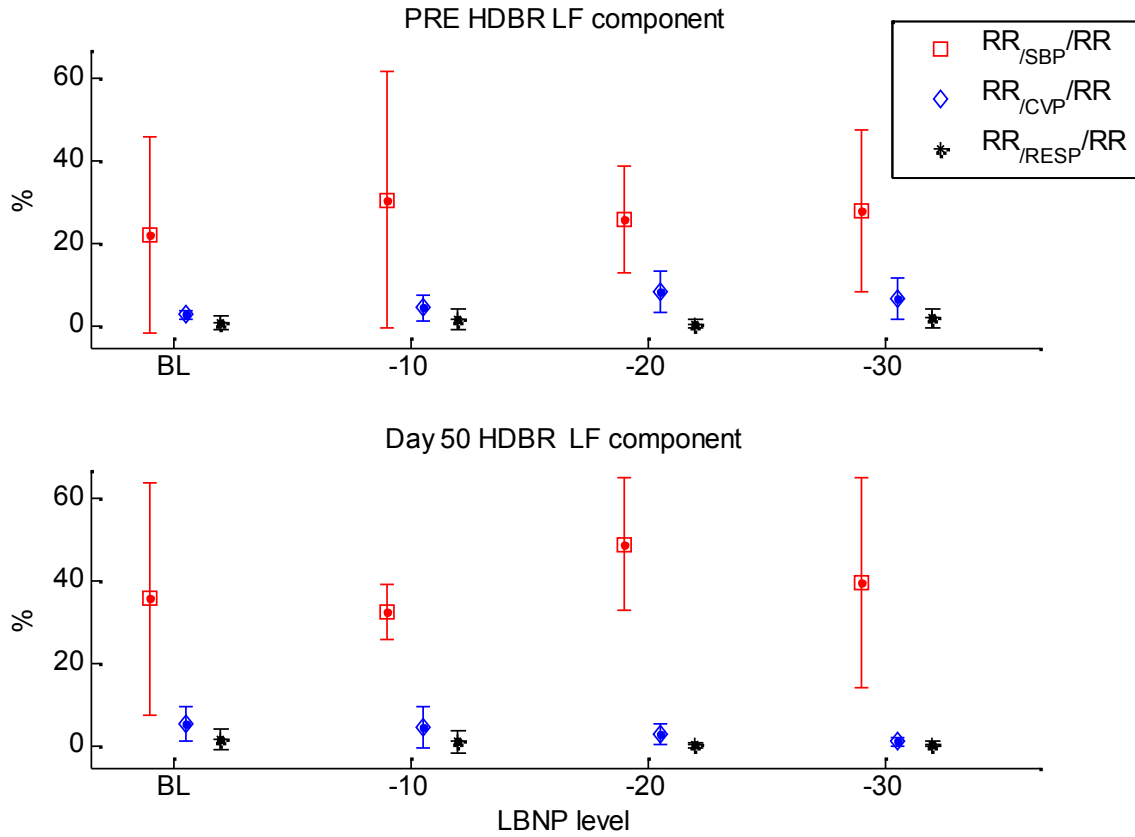
Figure 3.3. Mean and standard deviation of ratio between LF absolute power of each component and LF absolute power of RR before and on day 50 of bed rest, during LBNP maneuver.
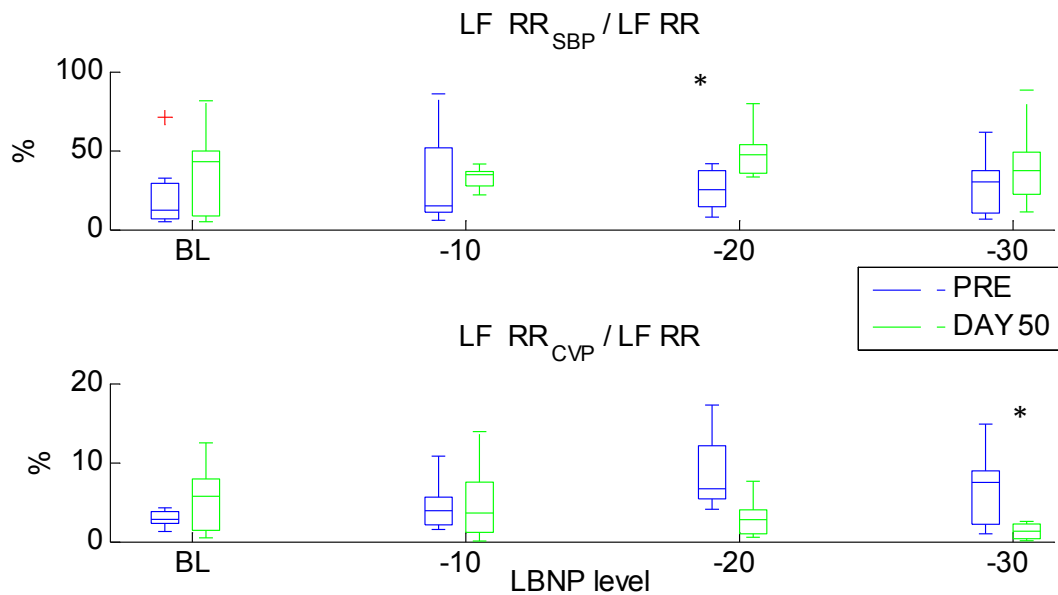

Figure 3.4. Ratio between LF absolute power of $RR_{/SBP}$ and $RR_{/CVP}$ components and LF absolute power of RR before and on day 50 of bed rest, in each LBNP epoch. The symbol * marks the significant differences between pre-HDBR (PRE) and day 50 of HDBR (DAY 50).
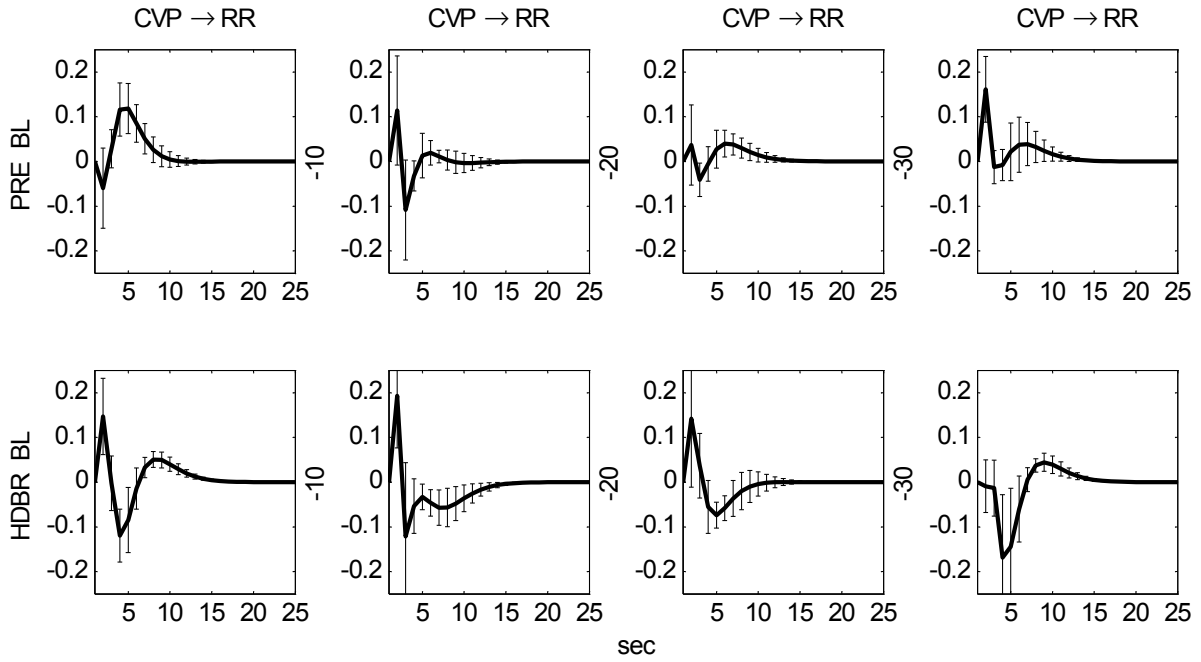
55

Figure 3.5. Average impulse response for the CVP to RR filter of the proposed model, (mean±SE). Before and after 50 days of bed rest, during LBNP maneuver.
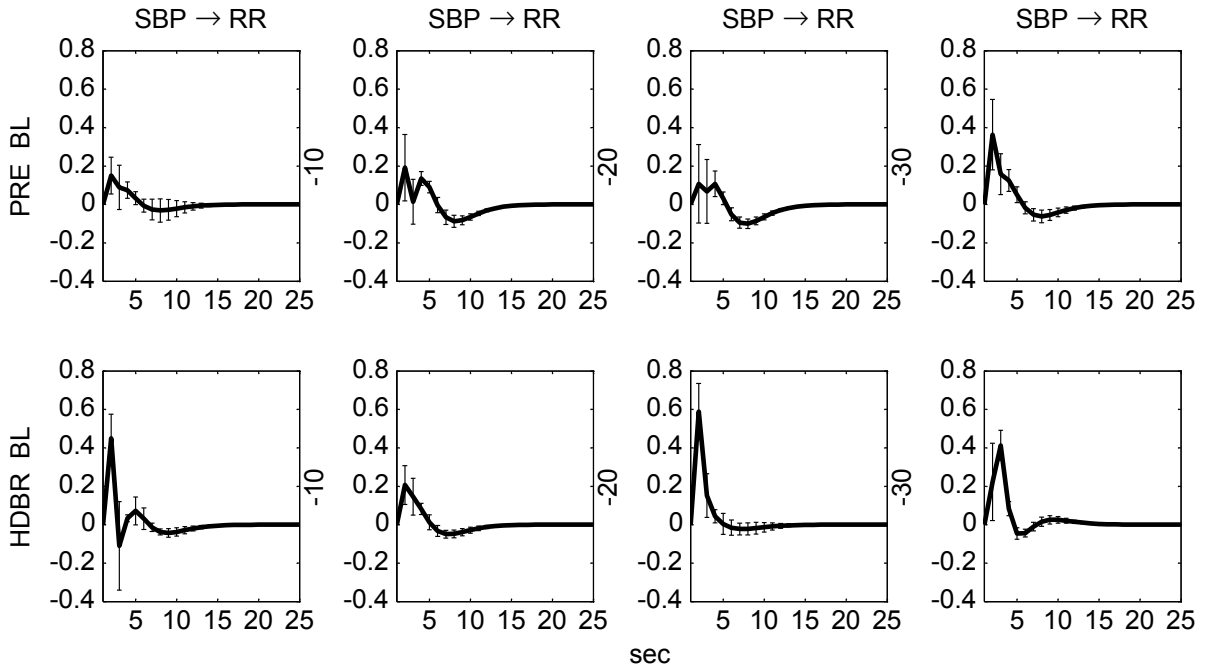

Figure 3.6. Average impulse response for the SBP to RR filter of the proposed model, (mean±SE). Before and after 50 days of bed rest, during LBNP maneuver.

56

Table 3.4. Bivariate model gain values estimated in LF and HF bands in each LBNP epoch before and after bed rest.

		BL	-10	-20	-30
SBP RR LF [a,b]	**PRE**	13.9± 8.6	9.8±2.4	8.8± 4.3[#]	6.8± 3.7[§]
(ms/mmHg)	**HDBR‡**	8.8± 4.4	7.1±2.0	5.1± 1.5[§]	4.8± 1.9[§]
SBP RR HF[b,c]	**PRE**	11.0±4.1	8.7± 5.5	13.7±7.0[#]	8.2±2.5
(ms/mmHg)	**HDBR‡**	13.2±4.8	8.7± 3.3[§]	6.6±3.1[§]	6.0±3.2[§]
RR SBP LF	**PRE**	0.037± 0.015	0.052±0.028	0.061± 0.057	0.069± 0.036
(mmHg/ms)	**HDBR**	0.063± 0.066	0.074±0.030	0.085± 0.036	0.081± 0.032
RR SBP HF [a]	**PRE**	0.053±0.034	0.040± 0.017	0.059±0.034	0.058±0.036
(mmHg/ms)	**HDBR**	0.069±0.038	0.098± 0.081	0.091±0.045	0.139±0.156

Values are expressed as mean ± SD. [a] Two-way ANOVA row factor (effect of bed rest), *p*-value < 0.05. [b] Two-way ANOVA column factor (effect of LBNP), *p*-value < 0.05. [c] Two-way ANOVA interaction, *p*-value < 0.05. ‡One-way ANOVA, *p*-value < 0.05. [§]Significant post hoc comparison between each LBNP level and BL. [#]Paired t-test between the same LBNP phases, PRE vs HDBR *p*-value < 0.05

3.5   Discussion

The model proposed in this work contributes to elucidate complex input-output dynamic relationships between cardiovascular variables. In particular, the additional input of CVP in the model of HR control evidenced the role of cardiopulmonary baroreflex. Thus, through the proposed model we can understand the relationship between both arterial and cardiopulmonary baroreflexes, during the experimental challenges of venous return decrease.

The result of unchanged HR and arterial pressure (SBP, DBP, MAP) at low levels of LBNP (table 3.1) is in accordance with other investigations (Johnson et al., 1974; Victor et al., 1987; Jacobsen et al., 1993; Robinson T et al., 1997; Brown et al., 2003).

The inability to selectively and unambiguously deactivate the cardiopulmonary receptors during mild LBNP makes it difficult to draw definitive conclusions concerning the interaction between arterial and cardiopulmonary baroreflexes and the importance and strength of a "reverse" Bainbridge reflex. If the presence of a "reverse" Bainbridge reflex is hypothesized, a decrease of HR should be expected in response to increasing levels of LBNP, i.e. lowering of CVP, but the average values of the time series seems not to support this hypothesis (table 3.1) neither during pre-HDBR condition nor on day 50 of HDBR.

The existence of a "reverse" Bainbridge reflex would imply that the cardiopulmonary receptors are active under baseline conditions and that they impose a tonic stimulatory influence on the sinoatrial node firing rate. The deactivation of these receptors by means of a venous return reduced would initiate a decrease in HR (Cristal et al., 2012).

A study performed by Boettcher et al. (1982) concluded that the Bainbridge reflex, i.e., the tachycardia that occurs with volume loading, appears to exist in primates including man. However, the extent of utilization of this reflex decreases significantly from nonprimate mammals (dogs) to subhuman primates (baboons) to man, hinting a weak Bainbridge reflex in humans.

The analysis of average impulse response, which described RR oscillations in function of CVP fluctuations, showed that a mechanism consistent with the "reverse" Bainbridge effect was elicited during mild LBNP cycles, but its limited relevance tended to disappear in the presence of cardiovascular deconditioning due to prolonged bed rest (Figure 3.5). Cristal et al., (2012) explained that the lack of change in HR during moderate LBNP suggests that if a "reverse" Bainbridge reflex is present in humans, it is not very powerful because it can be completely nullified by what is likely a moderate arterial baroreceptor-mediated tachycardic effect.

The proposed black box model showed a predominant contribution of SBP variability to the prediction of RR variability (table 3.3, LF RR$_{/SBP}$/LF RR), which suggests that control of HR appeared to be predominantly due to arterial baroreflex. This predominant contribution had a much larger effect on HR control during bed rest than in pre-HDBR. A previous study (Aletti et al., 2012) on the regulation of afterload by means of a model of DBP variability found similarly the predominant role of the arterial baroreflex. Furthermore the contribution of RR$_{/CVP}$ that represents the cardiopulmonary baroreflex, showed a limited role in the prediction of RR variability and the trend values of LF RR$_{/CVP}$/LF RR were different in pre-HDBR with respect to on day 50 of HDBR. This result suggests that the small contribution of cardiopulmonary baroreflex-mediated regulation of HR was more important at high levels of LBNP in pre-HDBR, while on day 50 of HDBR the role of cardiopulmonary baroreflex at the same levels tends to become even smaller. The further reduction of cardiopulmonary baroreflex contribution on vasomotor tone in simulated weightlessness conditions was also observed by Aletti et al. (2012).

During bed rest the results showed a reduction in PP mean value with increasing levels of LBNP, accompanied by an increase in HR, similar results are reported in previous works (Hughson et al., 1994; Iwasaki et al., 2000). According to the literature, cardiovascular deconditioning is induced by prolonged exposure to actual or simulated microgravity (Butler et al., 1991; Buckey et al., 1996), which in this case was achieved by means of prolonged bed rest. Responses that reflex the orthostatic intolerance have been reported as decreased SV (Buckey et al. 1996), myocardial atrophy (Levine et al. 1997), reduced BRS (Sigaudo-Roussel et al. 2002; Convertino et al., 1990) and increased distensibility of lower extremity blood vessels (Moffitt et al., 1998). In this study, evidence of cardiovascular deconditioning can be supported by the finding of reduced BRS during high levels of LBNP with prolonged bed rest.

One of the mechanisms that diminish the orthostatic tolerance during bed rest is the reduced vasoconstrictor response (Buckey et al., 1996). Our results on day 50 of HDBR showed that DBP and LF% power of DBP did not show differences at the same levels of LBNP before bed rest (table 3.2). This can be explained by an effective maintenance of vasoconstrictive responses to LBNP during bed rest.

An important aspect to consider is that tachycardia induced by long duration bed rest is the main player in the compensation of the reduced circulating volumes, and this may be one of the reasons why the cardiopulmonary branch of the baroreflex is less effective, and of the predominance of the mechanisms that pertain to the arterial side of the circulation. In this framework, it should also be noted the reduced variability of respiration; therefore, our findings suggest that the role of the cardiopulmonary and respiratory mediated mechanisms is limited.

The results of BRS gain obtained by means of a bivariate model showed reduced values during high levels of LBNP before and on day 50 of HDBR in the LF band (table 3.4). This result suggests a progressive impairment of arterial baroreflex with high levels of LBNP, which is more relevant with the combined effect of bed rest. According to the literature there have been several experiments that reported a reduction of BRS during bed rest and during LBNP maneuver (Eckberg et al., 1992; Ferretti et al., 2009; Barbieri et al., 2002; Iwasaki et al., 2000). In a similar study, baroreflex response was assessed after 28 days of continuous HDBR in a control group and in a countermeasure group with strenuous short-term exercise. Results showed a significant reduction in baroreflex slope (Hughson et al., 1994).

A greater decrease of BRS on day 50 of HDBR in comparison with values before bed rest could be an effect of the cardiovascular deconditioning. Regarding the effects of RR to SBP i.e. the feedforward mechanism, no changes were reported in this pathway. This may be expected, as the mechanical coupling between HR (i.e., CO) and ABP should not be altered by bed rest, while the main changes are known to affect neural regulation of cardiovascular function.

Despite that HRV modeling has been extensively studied, in this study was proposed a model with the aim to disentangle the role of both arterial and cardiopulmonary baroreflex control of HR, considering the interaction between RR and SBP that describes the feedback pathway of baroreceptive mechanism; respiration as an exogenous input which affect RR by respiratory sinus arrhythmia, and the interaction between RR and CVP, which represents the cardiopulmonary baroreflex modulation of RR variability. The role of Bainbridge reflex in humans has been controversial, but the results of this study showed a "reverse" Bainbridge possibly limited by a tachycardic effect elicited by arterial baroreflex. For this reason, the net effect could be a negligible change in HR, but the impulse response analysis permitted to highlight a transitory response and disentangle both mechanisms. In other words, "reverse" Bainbridge in humans might be overshadowed by an opposing reflex, besides the fact that the entire Bainbridge reflex has been shown poorly developed or less sensitive in humans.

CHAPTER 4

Cardiopulmonary baroreflex control of afterload and heart contractility

4.1 Introduction

Beat-by-beat values of HR and of ABP are the most accessible variables providing information about complex interactions between cardiac and vascular regulation, in addition to the effect of respiratory activity. However, the analysis of ABP series still bears some unexplored aspects besides the well documented and investigated baroreflex regulation of ABP. There are relatively few studies focused on discriminate the contribution of DBP and PP on cardiovascular regulatory mechanisms, although they suggest the clinical relevance of their analysis (Haider, et al., 2003; Sesso et al., 2000; Aletti et al., 2009). Analysis of beat-to-beat variability of ABP and of the features of the ABP wave can provide with a powerful insight of autonomic nervous system control of circulation. The relationship between ABP and HR variability has been amply studied,

mainly by the baroreflex responses considering the closed loop regulation (Barbieri et al., 2001; Porta et al., 2002; Chen et al., 2011). An extension of SBP-HR closed loop identification model (Baselli et al., 2001) was proposed by (Aletti et al., 2009) by means of a more detailed analysis of ABP, and expanding SBP forecast into the sum of separate DBP and PP predictions. We followed the approach of the black box model system identification proposed by (Aletti et al., 2009), including the relationship between CVP and PP and the relationship between CVP and SV to model the control of ABP by cardiopulmonary baroreflex.

In this chapter an explorative study was carried out, with the aim of disentangling the contribution of cardiopulmonary baroreflex control of afterload and heart contractility, in two different protocols oriented to study the effects of a fluid removal and the fluid loading, i.e. decrease and increase of venous return. In the first protocol, LBNP procedure was applied to volunteer subjects before and on day 50 of bed rest; since LBNP maneuver redistributes fluid from the upper body to the lower extremities, cardiopulmonary baroreflex responses to hypovolemia can be assessed by this maneuver. In the second protocol, data from patients undergoing major surgical procedures were analyzed; this analysis was focused on the maneuver of fluid administration, taking into account a segment before and after of fluid infusion.

Regarding LBNP experiment, preload and afterload changed with graded LBNP, HR increased, and SV and CO decreased. Thus, the working point on the left ventricular function curve is shifted to the left and downward, similar to hypovolemia (Lollgen et al., 1992). The hypothesis about the response of cardiopulmonary baroreflex to fluid removal by LBNP is that ventricular contractility controlled by this baroreflex will be reduced to regulate cardiac filling volume in response to a decrease in SV and preload. Regarding the second protocol, fluid infusion causes an increase in CVP which leads to increase SV and thus ventricular contractility controlled by cardiopulmonary baroreflex is expected to increase reflecting the heart response of pumping excess volume.

On the other hand, securing hemodynamic stability in order to prevent hypotension and organ perfusion deficiencies is one of the main challenges faced by the anesthesiologist or intensivist during major surgery as well as in the ICU. In this context, one of the most commonly practiced maneuvers is intravenous administration of colloids or crystalloids, where increasing circulating volume will aid in maintaining ABP through modulation of arterial resistances and ventricular contractility mediated by the

cardiopulmonary baroreflex; thus, the goal is to estimate the variation in cardiopulmonary baroreflex gain, before and after fluid infusion.

Hemodynamic management and appropriate fluid therapy remains a challenge in critically ill patients (Michard et al., 2002; Goepfert et al., 2007). Inadequate CO and reduced organ perfusion may lead to impaired microcirculation and multiorgan dysfunction. In addition, the strategy of fluid management involves several variables such as the type of fluid, the volume quantity and the rate of infusion. The choice of these variables, however, remains a controversial topic (Grocott et al., 2005). Measurements of CVP or pulmonary artery occlusion pressure (PAOP) have been used as indices of intravascular volume status, and variations in SBP and PP with positive pressure ventilation are a useful method of predicting circulatory responses to a fluid challenge.

The study of the baroreflex responses evoked by fluid infusion may contribute to better understand the physiological mechanism and also can be useful in the guidance of volume therapy.

The goals of this chapter are 1) to quantify the relative contribution of cardiopulmonary baroreflex control of ventricular contractility and afterload modulation of cardiac ejection during mild LBNP; and to investigate its alterations due to long duration bed rest, 2) to assess the response of cardiopulmonary baroreflex to fluid infusion during major surgeries.

4.2   Experimental and clinical protocols

In this chapter, two protocols were considered. The first one was described in chapter 3 and consisted in the LBNP and long duration bed rest experiments.

For the second protocol, hemodynamic signals from 7 patients undergoing major surgical procedures were used. These patients are different from the study illustrated in chapter 2, but the acquisition system and the collected signals are the same.

10 fluid infusion maneuvers were analyzed, each maneuver was considered independently as the condition of the patients can vary during the surgical intervention. The anamnestic characteristics of patients are listed in table 4.1.

Table 4.1. Characteristics of patients' population

n	7
Fluid infusion maneuvers	10
Gender (male/female)	6/1
Age(yr)	53±7.2
Weight (kg)	77.7±19
Type of surgery:	
Liver transplantation	5
Liver resection	1
Hepatectomy	1
ASA classification	2.7±0.6

In this clinical protocol, patients were sedated with propofol and/ or sufentanil (2mg/kg) and sedation was maintained by a total intravenous anesthesia (TIVA, 6-8 mg /(kg hr)); patients were mechanically ventilated with pressure-controlled ventilation. Fluid infusions were carried out with the Belmont FMS 2000™ infuser, which allows fluid infusion at rates from 2.5 up to 750 ml/min. Volume expansion was performed with solutions composed mainly by a mixture of blood recovered from the patient, crystalloids and colloids (reservoir). In this study rapid infusions only were analyzed, and they consisted in boluses of 100 ml or 500 ml administered within 30 sec and 1 minute respectively.

4.3   Methods

4.3.1 Signal pre-processing

Data from LBNP and bed rest procedures were preprocessed as was described in chapter 3.

Signal preprocessing of the second protocol consisted in the selection of artifact free ECG, ABP, CVP, and respiration (Airway flow) signals. Standard and robust algorithms based on ECG and ABP analysis were used to extract beat-by-beat series. R peaks indicative of each cardiac cycle were extracted through ECG processing, hence constructing RR intervals series; CVP was calculated as the mean value of continuously recorded CVP over each cardiac cycle, defined as the interval between two consecutive R

peaks; the value of respiration for each cycle was defined as the mean value of the respiration within an heart cycle.

Segments of three minutes were selected before and after fluid infusion. Fluid infusion maneuvers were analyzed individually and at least 5 min were considered between maneuvers. Zero-mean time series representative of short term hemodynamic variability were obtained by detrending and resampling beat-by-beat series in the time domain through an anti-aliasing low-pass filter (sampling frequency 1 Hz). ECG signal was acquired at a sampling frequency of 300 Hz, ABP and CVP at a sampling frequency of 100 Hz, airway flow at a sampling frequency of 25Hz and SV was acquired with PiCCO™ monitor at a sampling frequency of 2.5Hz.

4.3.2 Mathematical model of cardiopulmonary baroreflex

Two models were implemented for the prediction and spectral decomposition of beat-by-beat fluctuations of SV and PP as an extension of a previously proposed model (Aletti et al., 2009):

$$SV(i) = \sum_{j=1}^{p} h_{DER} \cdot RESP(i-j) + \sum_{j=1}^{q} h_{VC} \cdot CVP(i-j) + \sum_{j=1}^{r} h_{DBP} \cdot DBP(i-j) + w(i) =$$
$$SV_{/RESP} + SV_{/CVP} + SV_{/DBP} + W \tag{4.1}$$

$$PP(i) = \sum_{j=1}^{p} h_{DER} \cdot RESP(i-j) + \sum_{j=1}^{q} h_{VC} \cdot CVP(i-j) + \sum_{j=1}^{r} h_{DBP} \cdot DBP(i-j) + w(i) =$$
$$PP_{/RESP} + PP_{/CVP} + PP_{/DBP} + W \tag{4.2}$$

Equation 4.1 models the prediction of beat-by-beat oscillations of SV from RESP, CVP and DBP series including the effects of cardiopulmonary baroreflex control of ventricular contractility ($SV/_{CVP}$). Since PP has been considered as a surrogate of SV (Blasi et al., 2006; Aletti et al., 2009), the proposed model was also explored by substituting SV values with PP value. The components of SV model and of the PP model represent the following physiological mechanisms:

- $PP_{/RESP}$, $SV_{/RESP}$: mechanical modulation of venous return by respiration.
- $PP_{/CVP}$, $SV_{/CVP}$: effects of preload on SV or PP and cardiopulmonary baroreflex control of ventricular contractility.
- $PP_{/DBP}$, $SV_{/DBP}$: afterload modulation of cardiac ejection.

SV or PP is decomposed into the sum of three components and a residual error. SV or PP depends on the interplay between the modulation of venous return, ventricular filling and ventricular contractility because of respiration and CVP and by afterload effects, considering the previous diastolic value, which represents the opposing pressure at the outlet of the aortic valve during systole. Figure 4.1 shows a diagram of the closed-loop control of circulation, where the cardiopulmonary baroreflex control of afterload and heart contractility are highlighted.

The ability of the sympathetic nervous system to increase heart contractility is counterbalanced by the Frank-Starling mechanism. Stroke volume of the heart increases in response to an increase in the volume of blood filling the heart, i.e. end diastolic volume, when all other factors remain constant, as the increased volume of blood stretches the ventricular wall, causing cardiac muscle to contract more forcefully. SV is related to ventricular contractility through CVP, which is sensed by cardiopulmonary baroreceptors and directly affected by changes in blood volume.

Two major factors affect the PP: 1) the SV of the heart and 2) the compliance (total distensibility) of the arterial tree. A third, less important factor is the ejection from the heart during systole. In this context, translation of SV into PP strictly depends on arterial hemodynamics; nonetheless, as far as beat-to-beat variability is concerned, a hypothesis of constant arterial parameters, principally arterial compliance (Chen et al., 2008), results into a parallel PP and heart ejection dynamics. The approximate parallelism of SV and PP was exploited by Blasi et al., (2006) to draw a surrogate of CO dividing PP by the heart period.

The model orders *p,q,r* determined by AIC were set in the range between 6 and 12. Model coefficients were identified by least-squares minimization algorithm. Furthermore, spectral decomposition of SV and PP variability was performed.
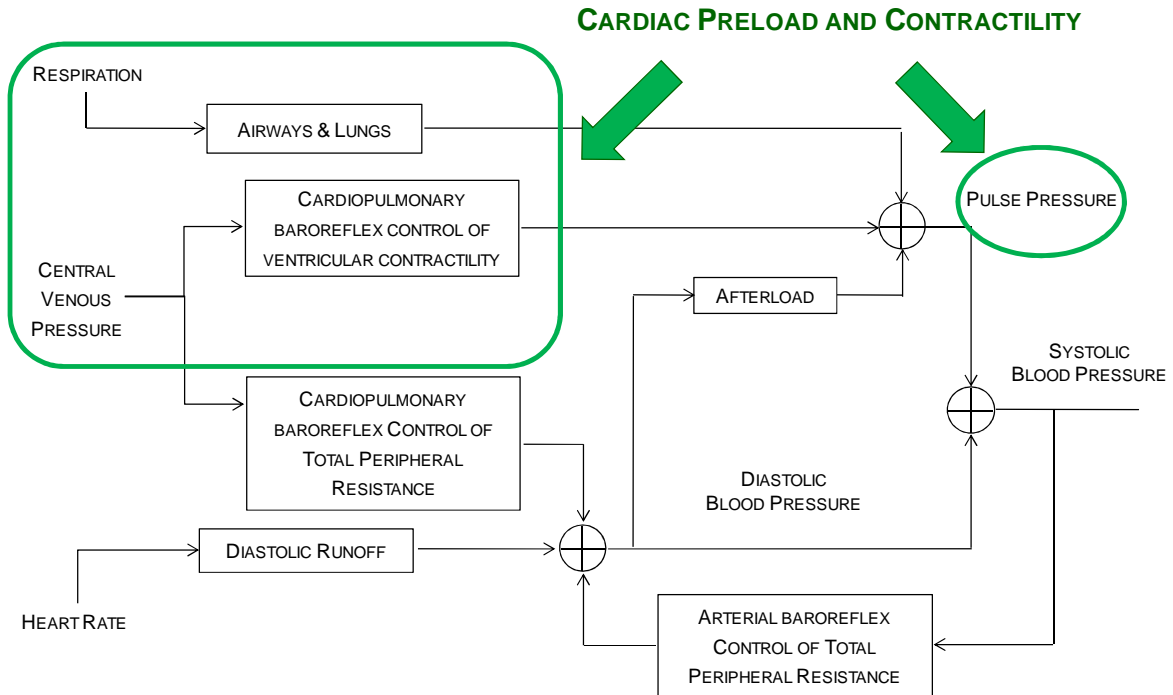
Figure 4.1. Closed-loop control of circulation. Cardiopulmonary baroreflex control of ventricular contractility is exhibited by the relationship between CVP and PP, whereas the cardiopulmonary baroreflex control of afterload resulted of the relationship between DBP and PP.

The contribution of arterial baroreflex and cardiopulmonary baroreflex on SV and PP variability was assessed through ratios between LF powers, e.g. LF power of $PP_{/CVP}$ over LF power of PP (LF $PP_{/CVP}$/LF PP) or LF power of $SV_{/CVP}$ over LF power of SV (LF $SV_{/CVP}$/LF SV).

Impulse responses and step responses of the filter ($PP_{/CVP}$ or $SV_{/CVP}$) are assumed to be representative of cardiopulmonary baroreflex control of ventricular contractility, while the final value of the step response is assumed to quantify the gain of this mechanism.

4.3.3 Statistical analysis

For the first protocol the statistical analysis described in chapter 3 was performed.

For the second protocol, Student's paired t-test or Wilcoxon signed-rank test according to data distribution were performed to compare values before and after fluid infusion. Statistical significance was considered for 2-tailed p-value<0.05.

4.4 Results

4.4.1 LBNP and HDBR protocol

This section is focused on the results of PP and SV prediction models and their spectral decomposition in the first protocol. Results of time and frequency domains were already showed in chapter 3. Table 4.2 shows the frequency domain indices of PP, a significant increase of LF and LF/HF was observed on day 50 of bed rest with respect to pre-HDBR in baseline and in the LBNP levels, whereas LF% resulted in higher values with HDBR at -20mmHg and -30mmHg with respect to pre-HDBR condition. Total power significantly increased at baseline and -20mmHg after bed rest condition in comparison with pre-HDBR values.

Spectral decomposition and gain estimation of PP variability

Figure 4.2 shows an example of the identification of PP variability components (left), and the relevant spectra (right), before (top) and on day 50 of HDBR (bottom).

The contribution of DBP variability to the prediction of PP variability ($PP_{/DBP}$) was predominant in all experimental conditions both before and during bed rest (table 4.3, figure 4.3). The contribution of $PP_{/DBP}$ assessed by the ratio LF $PP_{/DBP}$/LF PP was significantly larger on day 50 of HDBR at baseline and at -10mmHg with respect to pre-HDBR condition. The same contribution was significantly higher at -20mmHg and -30mmHg LBNP level in comparison with baseline in pre-HDBR condition.

The contribution of CVP in the identification of PP variability and to its spectral decomposition was small as shown in the example of figure 4.2. The ratio LF $PP_{/CVP}$/LF PP was significantly decreased at -10mmHg of LBNP on day 50 of HDBR with respect to pre-HDBR condition (table 4.3).

Table 4.2. Main frequency domain indices of PP before and during bed rest in each epoch of LBNP.

LF		BL	-10	-20	-30
PP[a]	**PRE**	0.018±0.019[#]	0.015±0.015[#]	0.027±0.024[#]	0.023±0.017[#]
	HDBR	0.190±0.126	0.141±0.074	0.142±0.066	0.315±0.246
LF %					
PP[a]	**PRE**	61.5± 6.9	47.0±18.7	55.1±11.7[#]	58.6±20.3[#]
	HDBR	69.5±12.7	73.1±19.2	74.6± 9.0	73.6±16.0
LF/HF					
PP[a]	**PRE**	2.0± 0.5[#]	1.7± 1.0[#]	2.7± 2.0[#]	3.0± 2.4[#]
	HDBR	8.3± 5.6	10.8± 7.0	6.6± 3.6	9.1± 7.5
TOTAL POWER					
PP[a]	**PRE**	0.056±0.075[#]	0.128±0.185	0.106±0.094[#]	0.074±0.034
	HDBR	0.739±0.564	0.400±0.362	0.333±0.122	1.024±1.458

Values are expressed as means ± SD. [a] Two-way ANOVA row factor (effect of bed rest), p-value <0.05. [#]Paired t-test between the same LBNP phase, PRE vs HDBR p-value < 0.05.

Figure 4.5 shows an example of the step response of cardiopulmonary baroreflex control of ventricular contractility (G $PP_{/CVP}$) in one subject in pre-HDBR and on day 50 of bed rest. The final value, assumed to represent baroreflex gain, decreases with increasing LBNP levels, at pre-HDBR and on day 50 of bed rest.

LBNP and prolonged bed rest are maneuvers that cause a decrease of venous return which is directly affected by blood volume. If PP is supposed to be a surrogate of SV, then the filter which encompasses PP oscillations in function of CVP fluctuations represents the cardiopulmonary baroreflex control of ventricular contractility. In case of decreased venous return, the gain of this filter is expected to decrease due to the decreased preload, i.e. the end-diastolic pressure when the ventricle has become filled, causing a reduction in ventricular contractility.

Table 4.4 shows the estimated gains for each predicted component of PP variability, $PP_{/DBP}$ gain at -20mmHg and -30mmHg of LBNP significantly decreased with respect to the values at -10mmHg in pre-HDBR. Gain of $PP_{/DBP}$ at baseline was significantly smaller in pre-HDBR condition in comparison with day 50 of bed rest condition. No significant differences were obtained for $PP_{/CVP}$.

Table 4.3. Ratio between LF absolute power of each predicted component and LF absolute power of PP, before and during bed rest in each epoch of LBNP.

		BL	-10	-20	-30
LF PP$_{/CVP}$/LF PP %	**PRE**	3.7± 2.6	7.6± 5.6 [#]	5.7± 4.1	8.9± 6.5
	HDBR	10.3±14.3	2.6± 1.9	5.4± 7.1	9.0±13.6
LF PP$_{/DBP}$/LF PP %[a,c]	**PRE** [‡]	9.9± 4.9 [#]	12.0± 4.8 [#]	25.6±17.3[§]	34.0±20.1[§]
	HDBR	33.3± 9.9	32.6±18.5	28.9±23.6	21.4±16.0
LF PP$_{/RESP}$/LF PP %[b]	**PRE**	0.72± 0.84	0.97± 1.83	0.41± 0.44	1.61± 1.99
	HDBR[‡]	0.21± 0.20	0.33± 0.43	0.19± 0.30	1.74± 2.10[§]

Values are expressed as means ± SD. [a]Two-way ANOVA row factor (effect of bed rest), *p*-value <0.05. [b]Two-way ANOVA column factor (effect of LBNP), *p*-value < 0.05. [c]Two-way ANOVA interaction, *p*-value < 0.05. [‡]One-way ANOVA, *p*-value < 0.05. [§] Significant post hoc comparison between each LBNP level and BL. [#]Paired t-test between the same LBNP phase, PRE vs HDBR *p*-value < 0.05.

Table 4.4. Gain of each predicted component of PP variability, during LBNP maneuver before HDBR and on day 50 of bed rest condition.

		BL	-10	-20	-30
G PP$_{/CVP}$	**PRE**	-0.08 (-0.09,-0.01)	0.03 (-0.17,0.04)	-0.02 (-0.19, 0.02)	-0.001(-0.12, 0.05)
	HDBR	0.17 (-0.63, 0.83)	-0.03 (-0.24,0.23)	-0.13 (-0.45, 0.28)	0.19 (-0.06, 0.41)
G PP$_{/DBP}$[a]	**PRE**[‡]	-0.08 (-0.21,-0.02)[#]	0.01 (-0.02,0.08)	-0.13 (-0.31,-0.06)[§]	-0.28 (-0.32,-0.08)[§]
	HDBR	0.44 (-0.20, 0.55)	0.02 (-0.04,0.51)	0.25 (-0.14, 0.37)	0.11 (-0.004, 0.43)
G PP$_{/RESP}$	**PRE**	0.001 (-0.01, 0.08)	-0.01 (-0.08,0.01)	0.02 (0.01, 0.07)	0.06 (-0.001, 0.26)
	HDBR	0.11 (0.02, 0.11)	0.09 (-0.05,0.15)	0.10 (0.03, 0.49)	0.22 (-0.10, 1.32)

Values are expressed as median (25th percentile, 75th percentile). [a] Friedman test row factor (effect of bed rest), *p*-value<0.05. [‡] Kruskal-Wallis test, *p*-value<0.05. [§] Significant post hoc comparison between -20mmHg and -30mmHg with respect to -10mmHg of LBNP. [#]Wilcoxon signed-rank test between the same LBNP phase, PRE vs HDBR *p*-value=0.08.
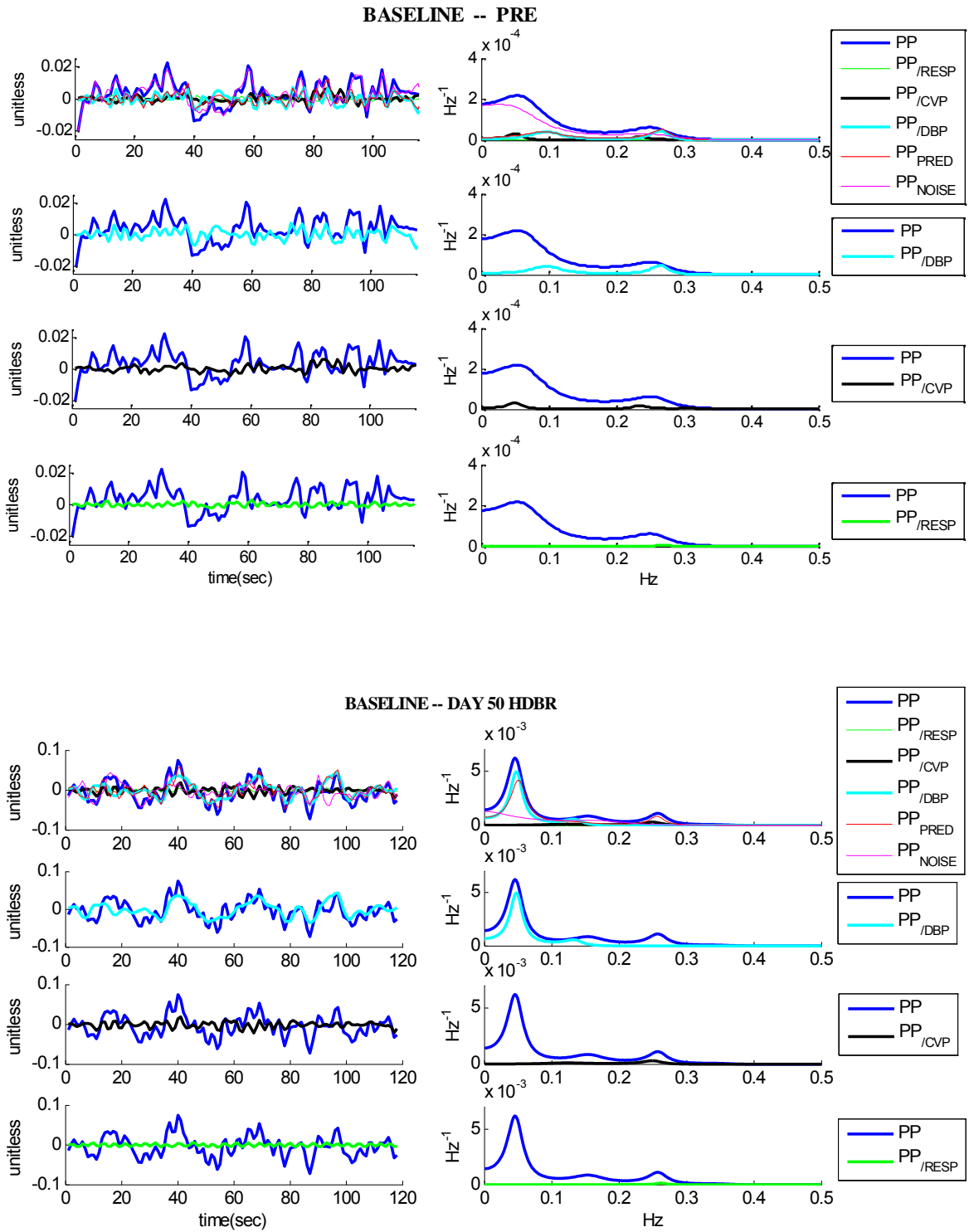
Figure 4.2. Time series (left) and spectra (right) of PP, and of the predicted model components: $PP_{/DBP}$, $PP_{/CVP}$, $PP_{/RESP}$, PP_{PRED} (model prediction) and PP_{NOISE} of one subject at baseline (BL), before bed rest (top) and on day 50 of HDBR (bottom).
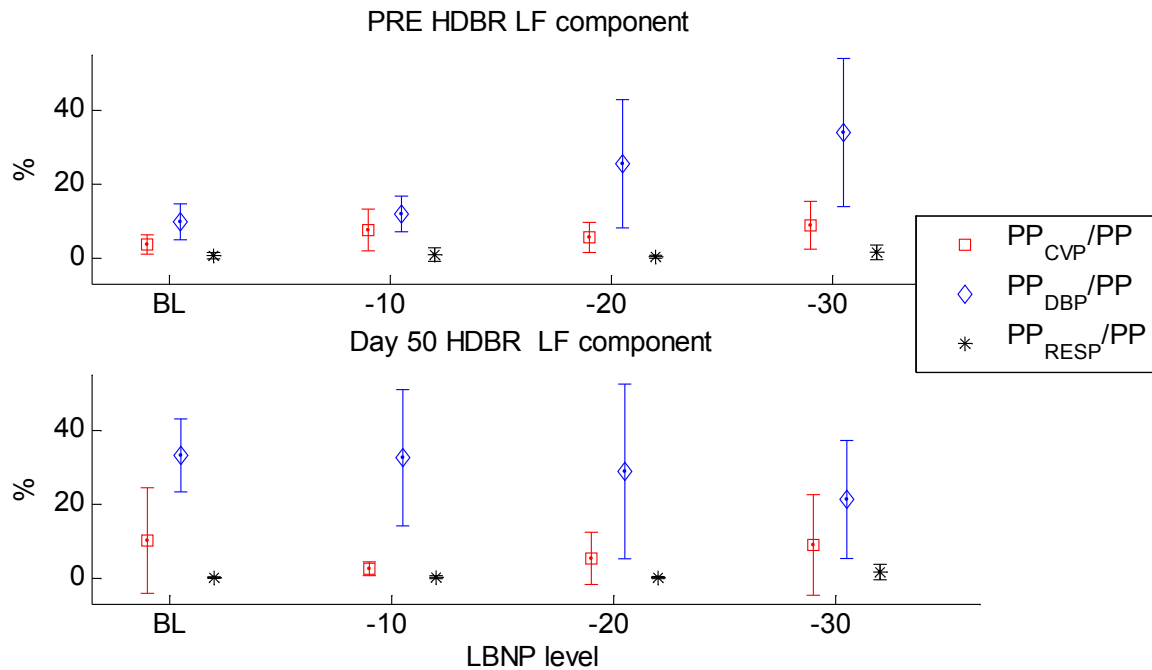
Figure 4.3. Mean and standard deviation of contribution of CVP, DBP and respiration (RESP) in the identification of PP variability represented by the ratio between LF absolute power of each component and LF absolute power of PP before and on day 50 of bed rest.
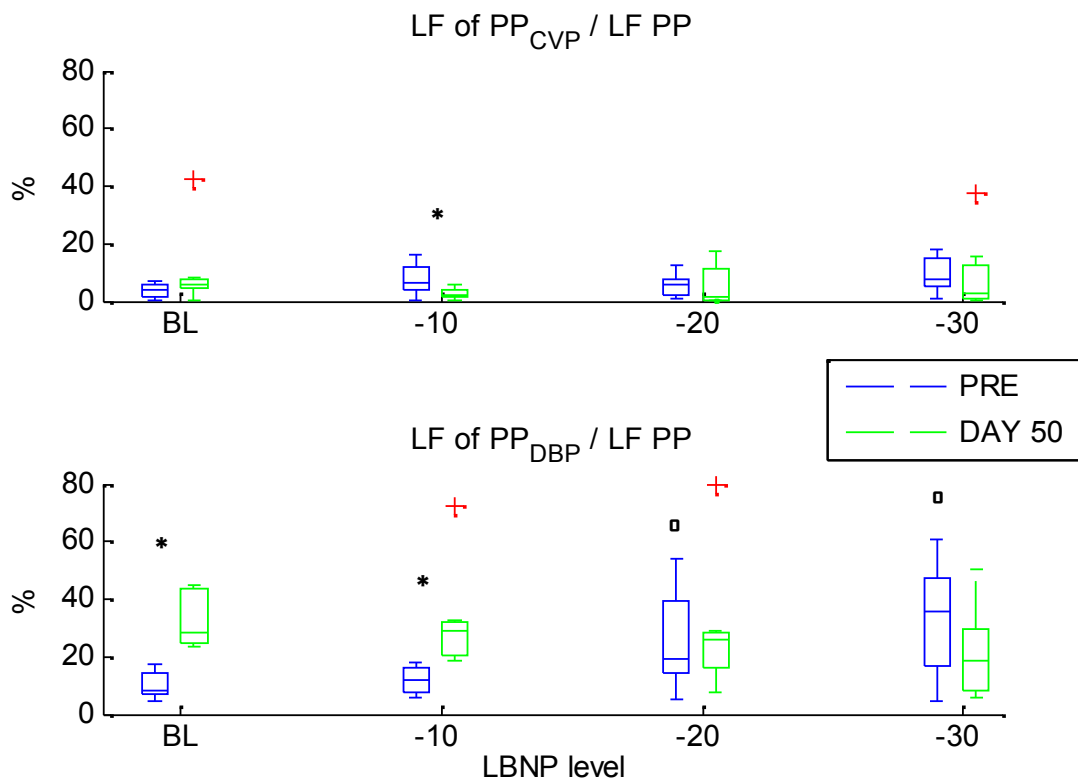

Figure 4.4. Ratio between LF absolute power of $PP_{/CVP}$ and $PP_{/DBP}$ components and LF absolute power of PP before and on day 50 of bed rest. The symbol $*$ marks the significant differences between pre-HDBR (PRE) and day 50 of HDBR (DAY 50). $°$ marks the significant differences between a LBNP level and BL, p-value < 0.05.
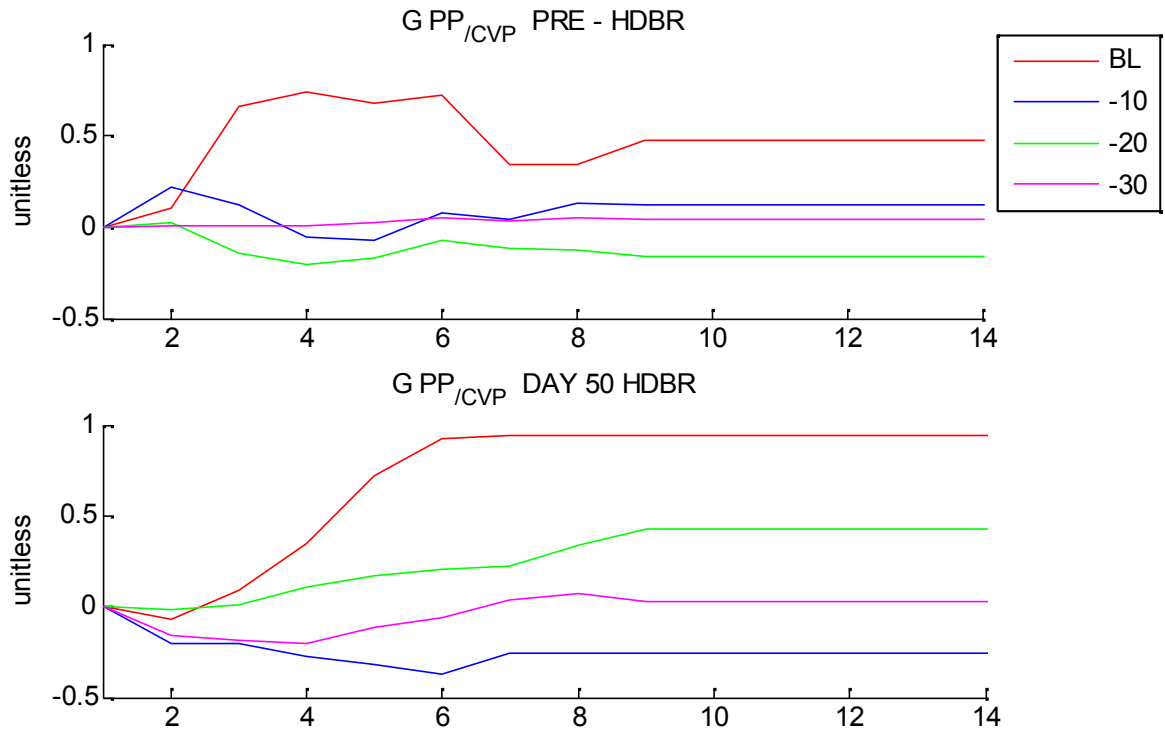
Figure 4.5. Step response of cardiopulmonary baroreflex control of ventricular contractility from one subject during LBNP maneuver in pre-HDBR and on day 50 of bed rest condition.
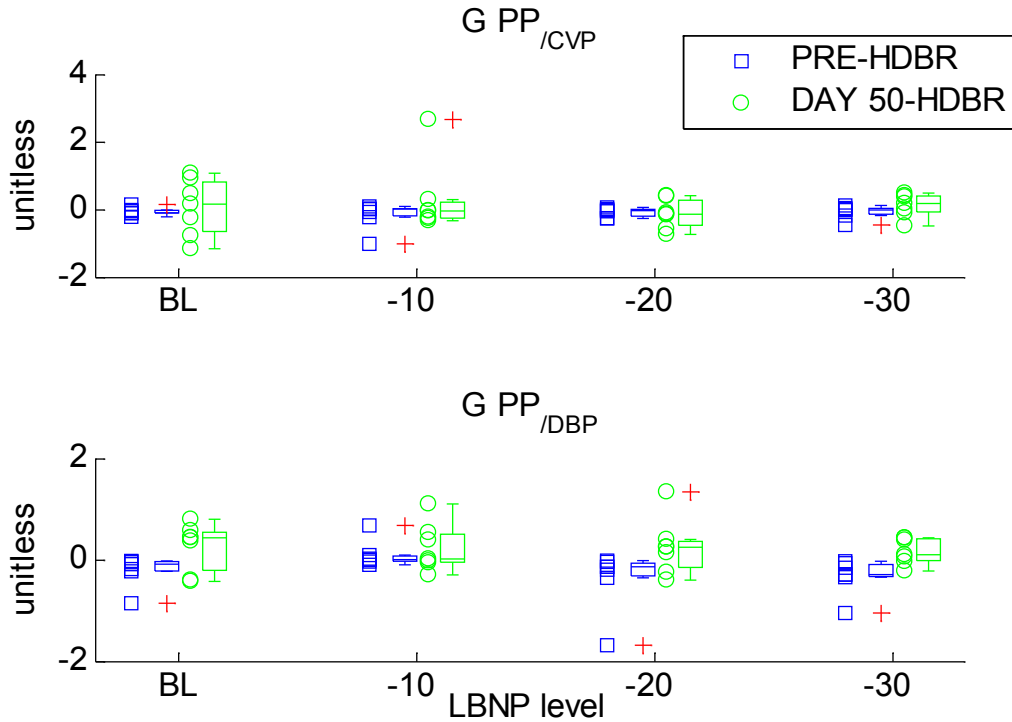

Figure 4.6. Gain of cardiopulmonary baroreflex control of ventricular contractility (G PP$_{/CVP}$) and G PP$_{/DBP}$ (afterload modulation of cardiac ejection) during LBNP maneuver before and after day 50 of bed rest.

Spectral decomposition and estimated gains of SV variability

Figure 4.7 shows an example of the identification of SV variability component, in this example the contribution of DBP variability to the prediction of SV variability ($SV_{/DBP}$) was predominant, which is consistent with the higher values of the ratio LF $SV_{/DBP}$/LF SV reported in table 4.5. During -20mmHg and -30mmHg of LBNP the contribution $SV_{/DBP}$ resulted significantly increased in comparison with baseline at pre-HDBR condition (figure 4.8).

Figure 4.9 shows an example of the step response of cardiopulmonary baroreflex control of ventricular contractility (G $SV_{/CVP}$) from one subject in pre-HDBR and on day 50 of bed rest conditions. In both conditions pre-HDBR and on day 50 of HDBR the gain decreases with incremental LBNP levels. Table 4.6 shows the gain values founded during LBNP maneuvers before and during bed rest. Gain of the predicted component $SV_{/CVP}$ significantly decreased at -20mmH and -30mmHg with respect to baseline before bed rest. Gain of $SV_{/DBP}$ and $SV_{/RESP}$ did not showed any significant changes.

Table 4.5. Ratio between LF absolute power of each predicted component and LF absolute power of SV, during LBNP maneuver before and after day 50 of bed rest.

		BL	-10	-20	-30
LF $SV_{/CVP}$/LF SV %	**PRE**	4.2(2.8, 7.5)	5.4(4.0, 7.3)	3.8(3.5,10.6)	7.6(2.3,16.9)
	HDBR	4.4 (3.4, 5.3)	3.4 (1.9, 4.6)	7.21(3.0,11.8)	16.2 (4.1,20.9)
LF $SV_{/DBP}$/LF SV %[a]	**PRE[‡]**	22.9(4.2,27.0)	25.5 (20.9,31.5)	37.5(29.2,46.7)[§]	33.2(28.1,50.8)[§]
	HDBR	44.6 (22.8,53.2)	40.3 (24.4,66.9)	50.3 (44.1,78.3)	28.5(14.5,44.6)
LF $SV_{/RESP}$/LF SV %	**PRE**	0.19(0.03, 5.37)	0.3(0.12, 5.97)	0.59(0.03, 1.64)	1.20(0.42, 2.87)
	HDBR	0.26 (0.16, 1.85)	0.48(0.18, 3.16)	0.14(0.07, 0.69)	0.05(0.01, 0.14)

Values are expressed as median (25th percentile, 75th percentile). [a] Friedman test row factor (effect of bed rest), *p*-value<0.05. [‡] Kruskal-Wallis test, *p*-value=0.07. [§] Significant post hoc comparison between each LBNP level and BL.
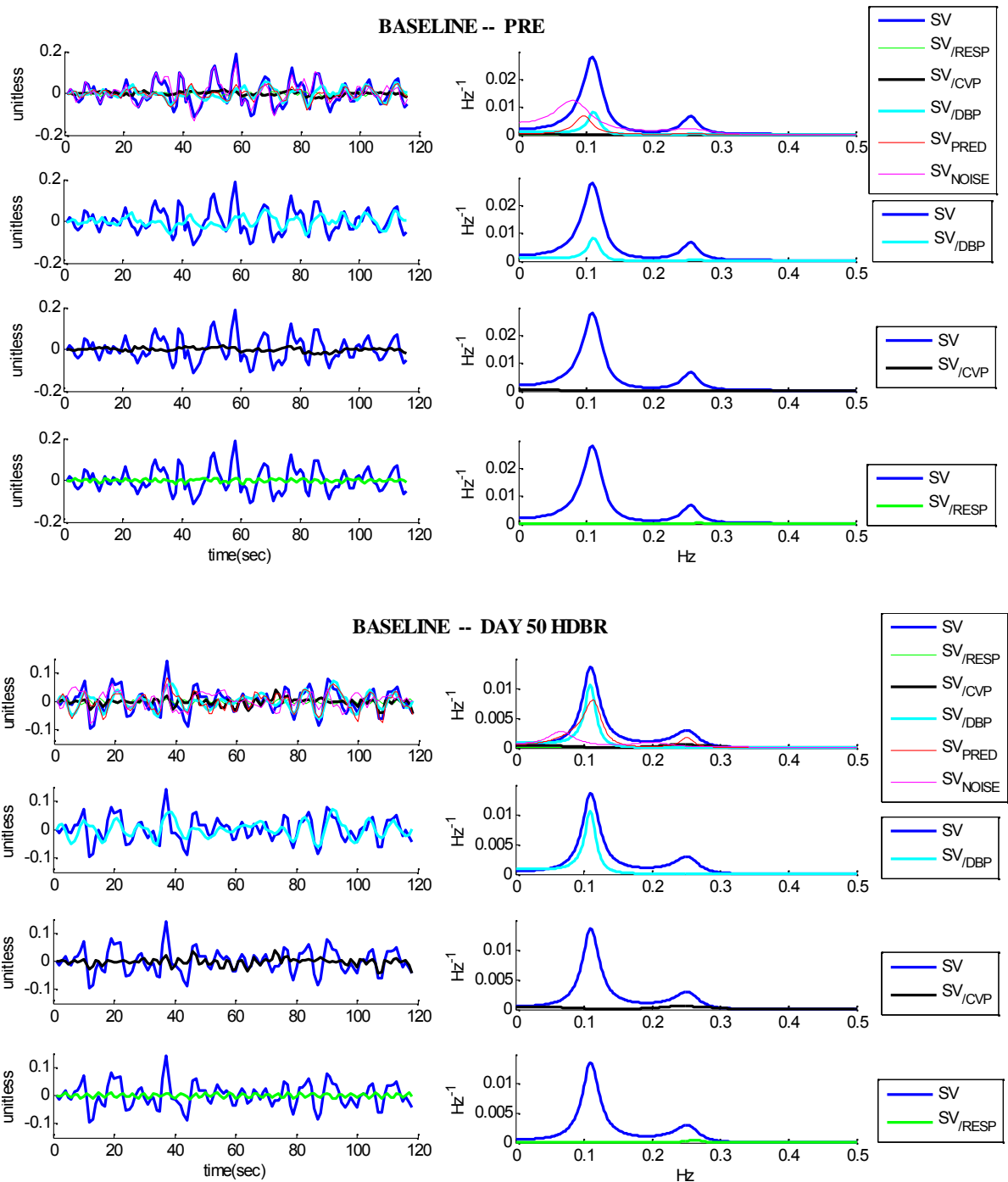
Figure 4.7. Time series (left) and spectra (right) of SV, and of the predicted model components: $SV_{/DBP}$, $SV_{/CVP}$, $SV_{/RESP}$, SV_{PRED} (model prediction) and SV_{NOISE} of one subject at baseline (BL), before bed rest (top) and on day 50 of HDBR (bottom).

Table 4.6. Gain of each predicted component of SV variability, during LBNP maneuver before and after day 50 of bed rest.

		BL	-10	-20	-30
G SV/CVP	**PRE[‡]**	0.11 (0.02,0.35)	0.18 (0.11,0.26)	-0.07 (-0.28, 0.01) [§]	-0.03 (-0.14, 0.03) [§]
	HDBR	0.11 (-0.10,0.17)	-0.04 (-0.24,0.53)	-0.08 (-0.35, 0.05)	0.11 (-0.02, 0.44)
G SV/DBP	**PRE**	-0.05 (-0.11,0.31)	0.23 (0.02,0.75)	0.41 (-0.21, 0.82)	-0.37 (-0.66, 0.39)
	HDBR	0.05 (-0.33,0.65)	0.08 (-0.11,0.64)	0.30 (0.02, 0.50)	0.03 (-0.31, 0.37)
G SV/RESP	**PRE**	-0.05 (-0.08,0.42)	-0.05 (-0.19,0.25)	-0.11 (-0.43,-0.01)	-0.14 (-0.33, 0.13)
	HDBR	-0.06 (-0.16,0.06)	0.09 (-0.42,0.17)	-0.11 (-0.31,-0.01)	-0.08 (-0.41,-0.00)

Values are expressed as median (25th percentile, 75th percentile). [‡] Kruskal-Wallis test, p-value<0.05. [§] Significant post hoc comparison between each LBNP level and BL.
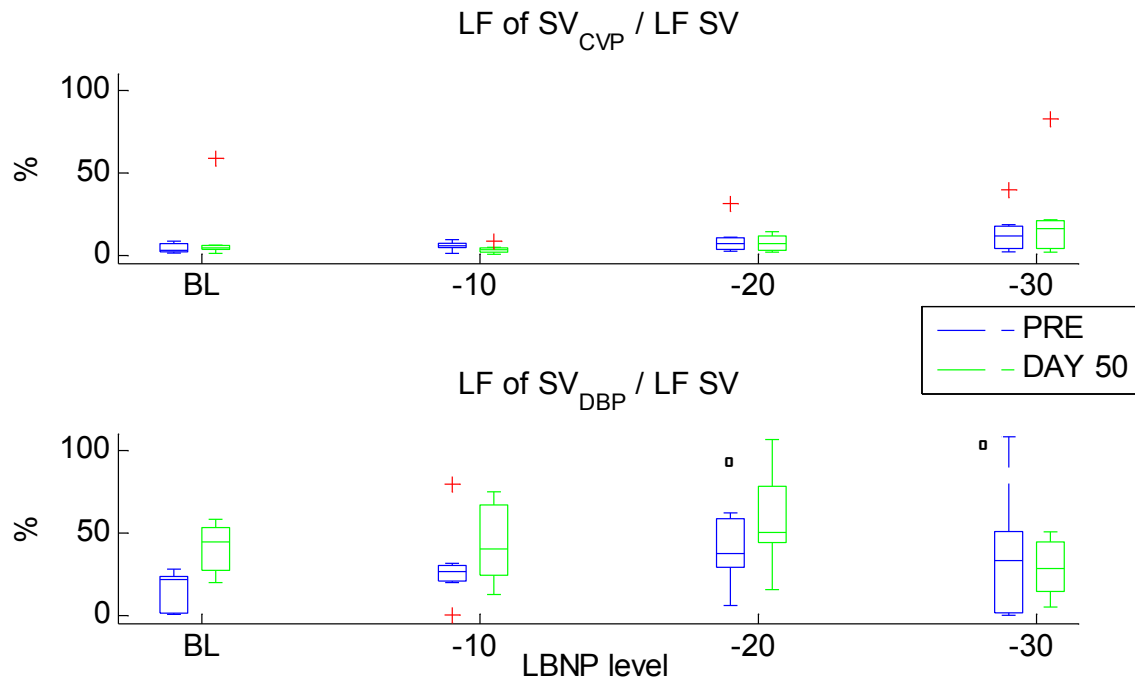

Figure 4.8. Contribution of CVP and DBP in the identification of SV variability represented by the ratio between LF absolute power of each component and LF absolute power of SV before and on day 50 of bed rest. The symbol ° marks the significant differences between each LBNP level and BL, p-value < 0.05.
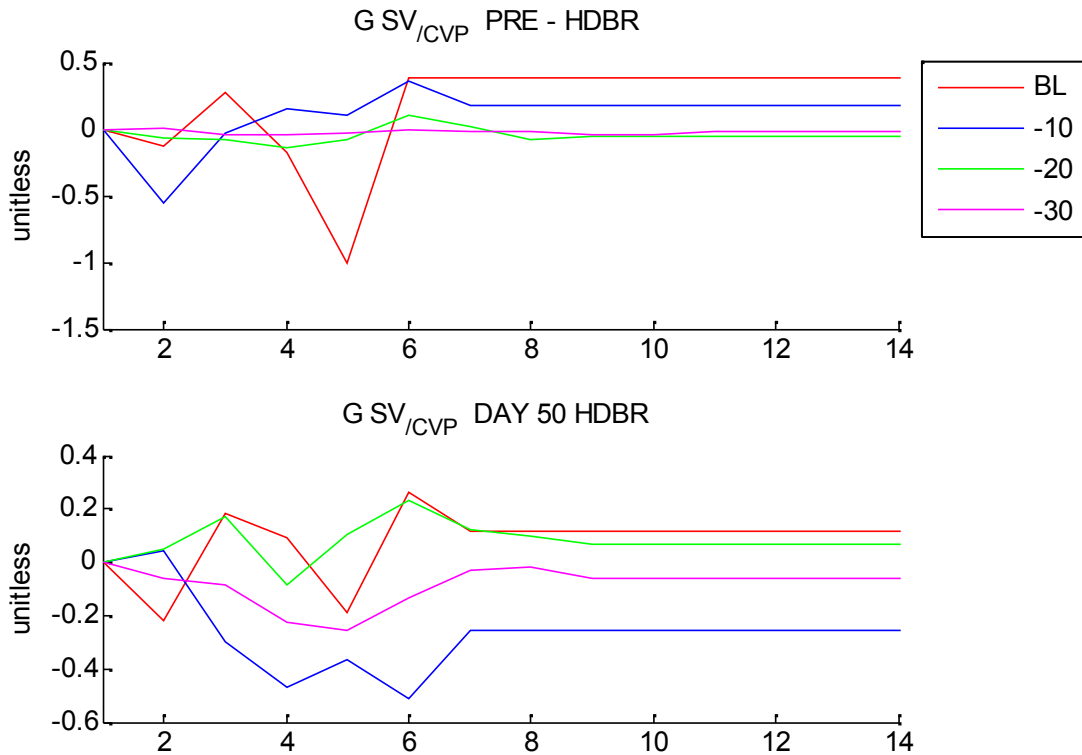
Figure 4.9. Step response of cardiopulmonary baroreflex control of ventricular contractility (G SV$_{/CVP}$) from one subject in pre-HDBR and on day 50 of bed rest conditions.
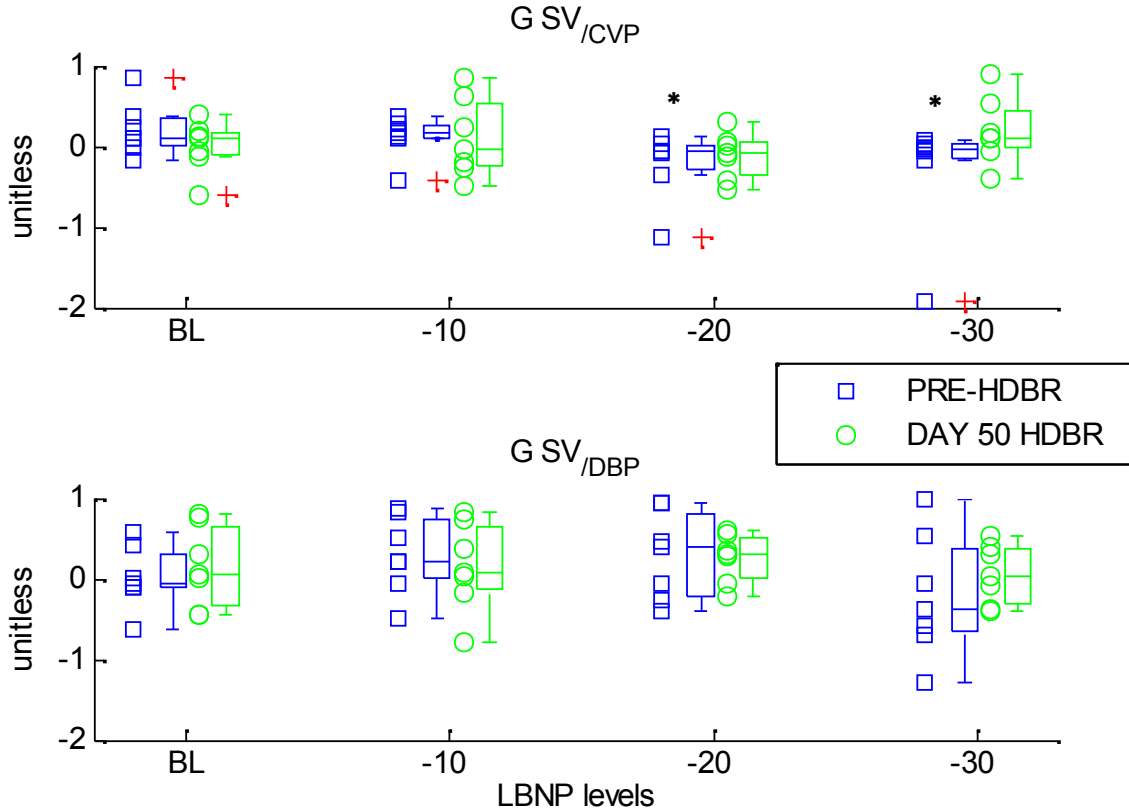

Figure 4.10. Gains of predicted components: SV$_{/CVP}$ and SV$_{/DBP}$ during LBNP maneuver before and after day 50 of bed rest. The symbol * marks the significant differences between each LBNP level and BL, p-value < 0.05.

4.4.2 Rapid fluid infusion during surgery

A significant decrease in RR interval was found after fluid infusion procedure. No significant changes were found in ABP before and after fluid infusion (table 4.7). Power spectral components of HR and ABP signals estimated before and after fluid infusion were not significantly different.

For fluid infusion protocol only the PP variability model was applied, due to the fact that SV measurement from PICCO™ monitor is a resampled signal and it is not a beat-to-beat series.

The ratio LF $PP_{/CVP}$/LF PP increased from pre to post fluid infusion maneuver, while the ratio LF $PP_{/DBP}$/LF PP decreased with the infusion of fluids (table 4.8, figure 4.11). In figure 4.12 two examples of step responses of cardiopulmonary baroreflex control of ventricular contractility (G $PP_{/CVP}$) and afterload modulation of cardiac ejection (G $PP_{/DBP}$) are shown. In figure 4.12 both patients showed an increase of the gain of cardiopulmonary baroreflex control of ventricular contractility after fluid infusion, while G $PP_{/DBP}$ decreased. However, the estimated gains from 10 maneuvers showed no significant differences after fluid infusion with respect to pre infusion values. Figure 4.13, illustrates the values of G $PP_{/DBP}$ which resulted smaller both before and after fluid infusion, in comparison with gain values of G $PP_{/CVP}$.
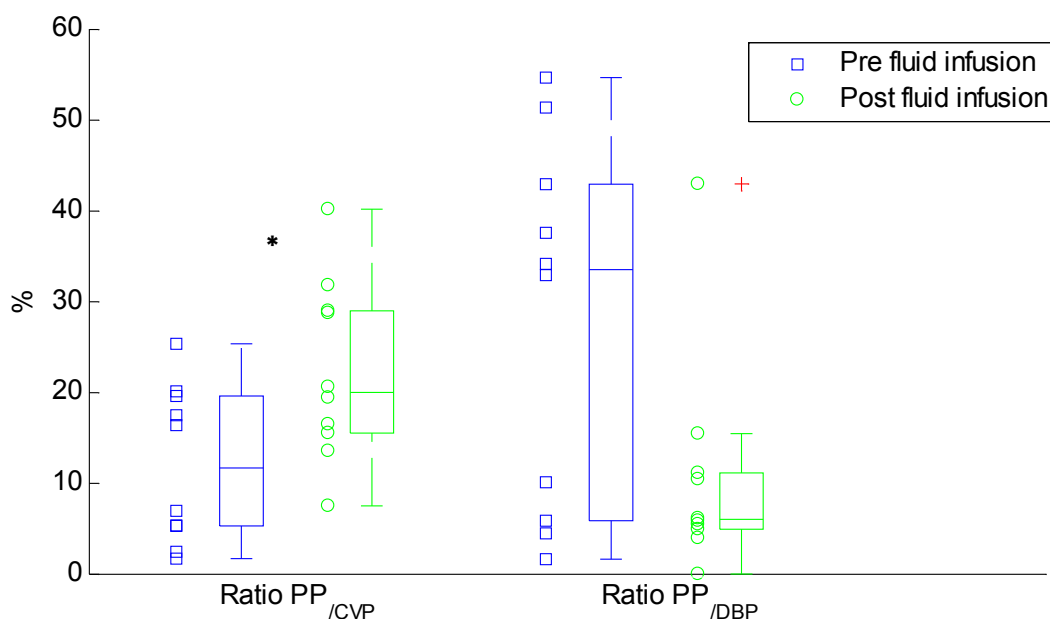

Figure 4.11. Ratio between LF absolute power of $PP_{/CVP}$ and $PP_{/DBP}$ components and LF absolute power of PP, before and after fluid infusion maneuver. Ratio $PP_{/CVP}$: LF $PP_{/CVP}$/LF PP %, Ratio $PP_{/DBP}$: LF $PP_{/DBP}$/LF PP %. The symbol * marks significant differences between pre and post fluid infusion maneuver, *p*-value < 0.05.

Table 4.7. Mean values and power spectral components of HR and ABP signals estimated before and after fluid infusion maneuver. Values are presented as mean±std.

Mean	PRE	POST	HF	PRE	POST
RR, ms*	687.3±126.9	678.6±128.7	RR, ms^2	1240.0±1126.9	1413.9±1716.4
SBP, mmHg	101.0±13.0	101.1±15.4	SBP, mmHg^2	2753.1±3365.6	2132.8±4447.1
DBP, mmHg	50.3±8.3	50.9±8.4	DBP, mmHg^2	1480.7±3795.4	1139.3±2526.5
MAP, mmHg	67.5±9.6	68.3±10.4	MAP, mmHg^2	702.5±1255.6	568.9±870.4
PP, mmHg	50.6±14.7	50.3±15.2	PP, mmHg^2	318.0±365.3	312.2±297.6
CVP, mmHg	9.9±2.8	10.2±2.9	CVP, mmHg^2	1240.0±1126.9	1413.9±1716.4
LF			**HF %**		
RR, ms^2	2163.0±3534.8	1770.1±4056.4	RR	50.2±25.5	54.3±18.5
SBP, mmHg^2	257.0±380.4	181.4±155.4	SBP	83.3±22.4	78.6±14.9
DBP, mmHg^2	76.2±81.6	77.8±64.7	DBP	70.6±25.9	68.0±21.5
MAP, mmHg^2	113.1±196.3	82.4±79.7	MAP	79.9±19.9	77.3±13.2
PP, mmHg^2	15.5±19.9	18.7±28.7	PP	92.5±5.9	91.8±6.8
CVP, mmHg^2	2163.0±3534.8	1770.1±4056.4	CVP	50.2±25.5	54.3±18.5
LF %			**Total Power**		
RR	47.4±25.6	43.3±17.8	RR, ms^2	4690.8±5926.6	4371.9±7862.9
SBP	16.4±22.2	20.5±14.5	SBP, mmHg^2	3155.1±3502.1	2458.5±4575.9
DBP	28.8±25.4	30.9±21.3	DBP, mmHg^2	1591.0±3806.0	1264.3±2510.6
MAP	19.7±19.6	21.8±12.7	MAP, mmHg^2	867.8±1269.3	707.2±932.0
PP	7.3±5.9	7.9±6.6	PP, mmHg^2	336.7±373.5	336.5±314.8
CVP	47.4±25.6	43.3±17.8	CVP, mmHg^2	4690.8±5926.6	4371.9±7862.9

Values are expressed as means ± SD. *Paired t-test between PRE and POST fluid infusion procedure, *p*-value < 0.05.

Table 4.8. Ratio between LF absolute power of PP$_{/CVP}$ and PP$_{/DBP}$ and LF absolute power of PP before (PRE) and after (POST) fluid infusion maneuver.

|	PRE	POST	p-value
LF PP$_{/CVP}$/LF PP %	11.69 (5.30,19.61)	20.02 (15.54,28.99)	0.01
LF PP$_{/DBP}$/LF PP %	33.55 (5.87,42.94)	6.03 (4.95,11.14)	0.06

Values are expressed as median (25th percentile, 75th percentile). Wilcoxon signed-rank test was performed between pre and post fluid infusion phases

Table 4.9. Gain of PP$_{/CVP}$ and PP$_{/DBP}$ before (PRE) and after (POST) fluid infusion maneuver.

	PRE	POST
G PP$_{/CVP}$	0.57 (-0.44, 1.86)	0.42 (-0.22, 2.07)
G PP$_{/DBP}$	0.22 (0.07, 0.60)	0.34 (-0.02, 0.47)
G PP$_{/RESP}$	-0.34 (-0.54, 1.75)	-0.41 (-1.28, 0.89)

Values are expressed as median (25th percentile, 75th percentile). Without significant differences.

a)
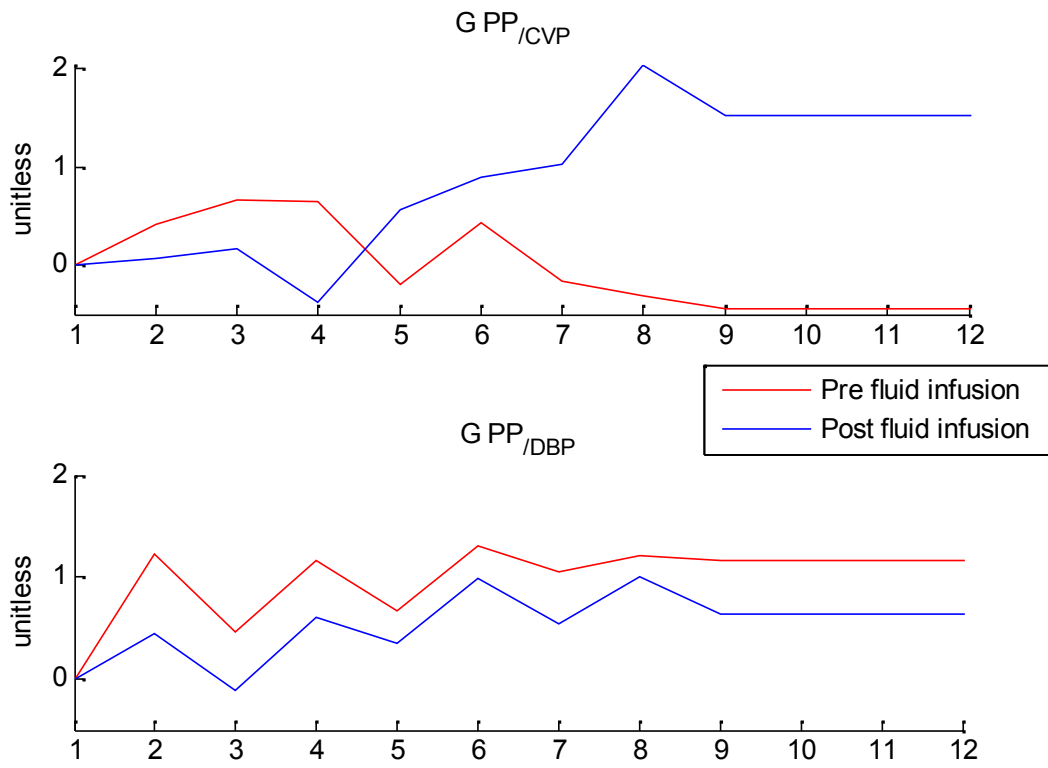
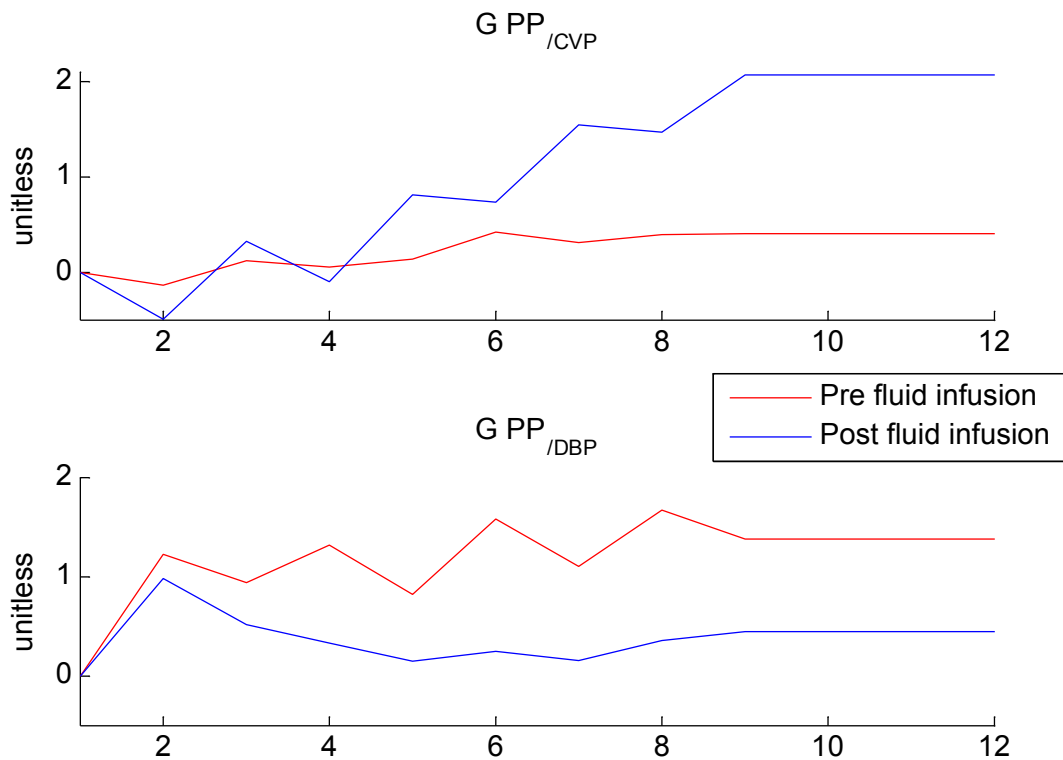

b)

Figure 4.12. Step responses of cardiopulmonary baroreflex control of ventricular contractility (G PP$_{/CVP}$) and afterload modulation of cardiac ejection (G PP$_{/DBP}$) from two subjects (a,b) before and after fluid infusion maneuver.
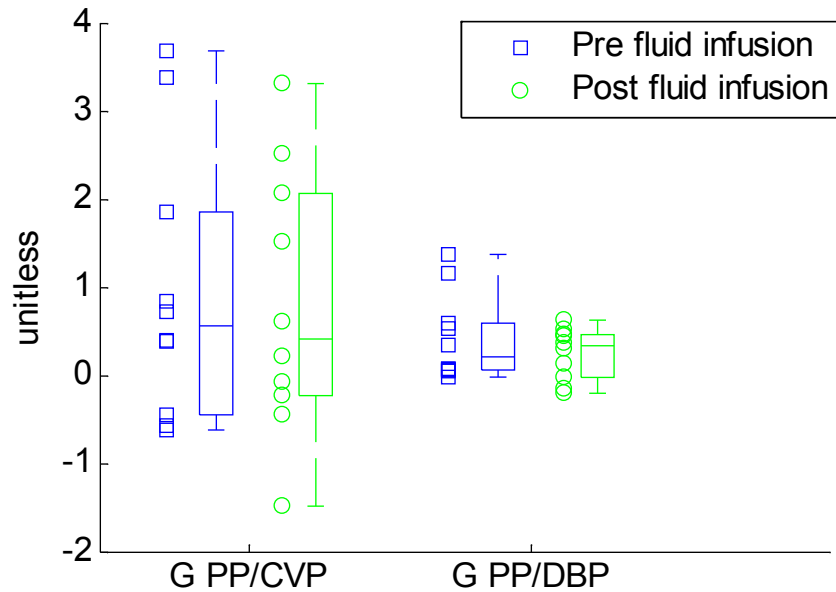
Figure 4.13. Gains of predicted components: $PP_{/CVP}$ and $PP_{/DBP}$ before and after fluid infusion maneuver. No significant differences were found between the values of pre and post fluid infusion.

4.5   Discussion

Responses of cardiopulmonary baroreflex control of afterload and heart contractility to central volume changes were explored in two different protocols, where venous return was changed. In the first one, data from an LBNP protocol were analyzed. LBNP is a maneuver that reduces venous return. In the second protocol, data collected before and after rapid fluid infusion during surgery were analyzed. Fluid infusion is instead a procedure that increases venous return.

In the first protocol, the adaptation to simulated weightlessness and the response to abrupt changes induced by LBNP were studied by system identification of circulation control, applied to non invasive recordings of hemodynamic variables. In particular, a black box model, to assess the influence of LF oscillations of components of PP and SV variability, was applied.

One assumption used in this study was that PP can be used as surrogate of SV. In the first protocol (LBNP and bed rest) black box models were used for PP and SV variability prediction, the results were comparable in average; however, it is important to take into account that SV is an estimated measure from finapres device, thus the results may be affected by a less reliability of measurement.

The gain of cardiopulmonary baroreflex control of ventricular contractility is represented by the filter gain wich encompasses the relationship between PP and CVP. A decrease of this gain is an expected result since the maneuvers analyzed evoke a reduction of venous return reflected by CVP, which is a major determinant of the filling pressure and therefore of the right ventricle preload, which regulates SV through the Frank-Starling mechanism.

A decrease in the gain of cardiopulmonary baroreflex control of ventricular contractility (G $PP_{/CVP}$) was reported in some subjects like in the one illustrated by figure 4.4, with increasing LBNP levels in both conditions, before and on day 50 of bed rest. However, no significant differences were found by considering the entire population. The gain $PP_{/DBP}$ at -20mmHg and -30mmHg was significantly smaller than -10mmHg in pre-HDBR condition.

The results of spectral decomposition of PP variability in the first protocol showed a higher contribution of DBP to PP variability, which suggests a relevant role of the afterload modulation of cardiac ejection, mainly at higher LBNP levels in comparison with baseline during pre-HDBR.

The small contribution of CVP in the identification of PP variability ($PP_{/CVP}$) did not show any significant differences induced by bed rest or LBNP protocol. Only at -10mmHg of LBNP a significant decrease was observed on day 50 of bed rest with respect to pre-HDBR. This decrease in cardiopulmonary baroreflex control of ventricular contractility may be result of the adaptation to long duration bed rest. In addition, the relatively limited contribution of CVP to PP variability through the cardiopulmonary baroreflex pathway when LBNP was applied, was consistent with the results reported by Jacobsen et al. (1993), where evidence that ventricular mechanoreceptors play a small role and sinoaortic baroreceptors a large role in the reflex control of the human skeletal muscle circulation during orthostatic stress was shown. Small contribution of cardiopulmonary branch of baroreflex in non hypotensive LBNP and long-duration simulated microgravity was also reported by Aletti et al. (2012).

Mechanical modulations of venous return and ABP by respiration ($PP_{/RESP}$) were very low both before and on day 50 of bed rest and no clear trends in the response to LBNP were shown.

Moreover, SV prediction variability model showed that the contribution of DBP to the identification of SV significantly increased at higher LBNP levels before bed rest, this result agrees with the results of PP prediction variability model. DBP showed a higher contribution to SV variability prediction with respect to CVP, as in the case of the PP model. In addition, the contribution of SV_{DBP} at baseline and -10mmHg of LBNP showed higher values after bed rest with respect to pre-HDBR, as in the case of PP_{DBP} but without significant differences.

A decrease in the gain of cardiopulmonary baroreflex control of ventricular contractility with incremental levels of LBNP before and after bed rest resulted for some subjects.

Both models provided similar trends, however the use of PP as surrogate of SV must be further investigated.

Regarding fluid infusion protocol, a decrease of RR interval was found during fluid infusion. This result may be consistent with the existence of the Bainbridge reflex in humans also reported by Barbieri et al. (2002), where unloading and loading of cardiopulmonary receptors was employed to assess the influence of central volume on short-term control of HR and ABP. They reported the presence of the Bainbridge reflex (hypervolemia-induced tachycardia) at moderately increased levels of central volume and that short-term cardiovascular control (RSA and baroreflex feedback) appeared to be optimized at mild hypervolemia. A significant decrease of HF power was also reported during 60° leg raising and maximum volume loading. However, Barbieri et al. (2002) used 500 ml of saline infusion and the protocol described in the present thesis analyzed fluid infusions of 100 ml and 500 ml but rapidly infused.

An increase of venous return, induced by fluid infusion procedure, elicited a response of the cardiopulmonary baroreflex control of ventricular contractility, which makes that increased volume stretches the walls of the heart chambers and as a result of the stretch, the cardiac muscle contracts with increased force, and this empties the extra blood that has entered from the systemic circulation. Therefore, the blood that flows into the heart is pumped into the aorta and flows again through the circulation. The examples reported in figure 4.11 showed that the gain of this baroreflex became positive after the fluid infusion maneuver, thus suggesting that the cardiopulmonary baroreflex enhanced ventricular contractility to improve cardiac performance when the circulating volume increased.

However, this trend was observed only in some patients and no significant changes in estimated gains were found.

The contribution of CVP to PP variability (LF PP$_{/CVP}$ / LF PP) increased after fluid infusion, which suggests that the role of cardiopulmonary baroreflex control of ventricular contractility increased with fluid infusion maneuver, while the role of afterload modulation of cardiac ejection seems to decrease, even the trend was not statistically significant.

The limitation of these protocols is that they were not specifically designed for this kind of analysis. In this sense, one of the main issues was the limited length of time series, since the model will be better identified with more than 2 minutes of recording.

For example, during major surgery, the design of a specific protocol to study infusion maneuvers is challenging since fluid infusion does not always occur at the same time or at the same condition during surgery. Also, quantity and rate of fluids can be different and data come from patients, which differ from many factors, such as surgical procedure, severity of the condition and respective medical treatment or prescribed medicines.

CHAPTER 5

Discussion and conclusion

This thesis was focused on the study of the responses of the arterial and cardiopulmonary baroreflexes to severe stress during experimental and clinical protocols where the maintenance of blood pressure is challenged.

Heart period assessed by RR interval and SBP interact in a closed loop, SBP changes induce RR changes through activation of baroreflex, and RR changes cause SBP variations according to diastolic runoff and Starling's law. The study of arterial baroreflex control of HR was first addressed by classical techniques in time and frequency domain, secondly considering an open loop relation between ABP and RR. Later, methods that take into account a closed loop were used to assess arterial baroreflex, and the causal relationship between SBP and RR interval was also evaluated by Granger causality test, i.e. F test.

Cardiopulmonary baroreflex and its relationship with arterial baroreflex were assessed by black-box models, focused on RR variability, PP variability and SV variability, unraveling the contribution of both baroreflex mechanisms during specific maneuvers.

The data considered in this thesis can be divided in two groups; data from patients that underwent major surgeries and data from healthy volunteers that participated in a study where a LBNP procedure was carried out before and on day 50 of HDBR.

Data from surgery patients were analyzed with two main goals. The first one was the evaluation of the baroreflex control during three different epochs: baseline, anesthetic procedure and post-intubation; taking into account the causal relationship between HR and ABP and comparing baroreflex responses between hypertensive and normotensive patients. The second goal was to assess the baroreflex responses to volume loading by means of fluid infusion, a common procedure performed during surgeries. In the context of this study the LBNP maneuver, which leads to fluid removal, was also explored before and after a long duration bed rest procedure.

The novel contribution of this thesis lies on the analysis approaches used to assess arterial and cardiopulmonary baroreflexes and in their application to different experimental conditions.

To our knowledge, the analysis of arterial baroreflex during anesthesia induction presented in chapter 2 is the first study in which the autonomic response to propofol anesthesia induction of CH and NH patients was compared employing four different mathematical techniques for the assessment of BRS. The robustness of the proposed approach relies mainly on the quantification of the causality in the relationship between SBP and HR and on the careful selection of steady-state and stationary time series to avoid transitory trends, which may lead to misleading results.

Impairment in cardiac neural regulation in hypertension is well known (Grassi et al., 1998; Head et al., 1994) and the low values of BRS indicate a considerable risk of cardiac complications (Head et al., 1994). Results of arterial baroreflex control during anesthesia induction are consistent with the reported impairment of baroreflex in hypertensive patients, which resulted unable to maintain ABP after the intubation maneuver and allowed a further ABP drop. From these results hypertensive patients appear prone to a higher risk of perioperative hypotension than non-hypertensive patients. The perioperative period is crucial for possible hypotensive episodes. A continuous monitoring of blood pressure in

chronic hypertensive patients is suggested so to prompt intervene with vasopressor to restore the ABP to safe level.

The main innovation presented in the study of chapter 2 is the systematic analysis of ABP and HR recordings during major surgery with a sound mathematical approach. As a consequence, results could pave the way for additional analysis of data collected in surgical patients affected by other cardiovascular pathologies, geared towards quantifying the status of their autonomic control of circulation under anesthesia.

In chapter 3, control of HR by arterial and cardiopulmonary baroreflexes was investigated in healthy volunteers enrolled in an experimental study envolving both mild LBNP maneuver and long duration HDBR. RR variability was predicted from SBP, CVP and respiration by means of a black box prediction model. The novelty in this study is the inclusion of the relationship between RR and CVP in the prediction model, allowing the quantification of the proportional role of the "reverse" Bainbridge reflex with respect to the arterial baroreflex, and with respect to respiratory sinus arrhythmia in response to the rapid onset of mild LBNP. Furthermore, this quantitative analysis was applied to compare the variations from spontaneous oscillations due to LBNP and the same variations under the adaptation to exposure to simulated microgravity by HDBR. Therefore, this analysis provides deeper insight into the orthostatic stress regulation mechanisms.

An interesting finding of this research is that the "reverse" Bainbridge reflex was elicited during mild LBNP, but its limited relevance tended to disappear in the presence of cardiovascular deconditioning due to prolonged bed rest. This finding was explored by means of the impulse response (CVP   RR) constructed using Laguerre expansion.

The predominant role of arterial baroreflex on control of HR, found in this research, was consistent with the results of (Aletti et al., 2012) in a study on the regulation of afterload by means of a model of DBP variability. Therefore, it is possible to conclude that mild LBNP does involve the cardiopulmonary baroreflex in mediating the regulation of vascular resistance, and also HR according to a "reverse" Bainbridge mechanism; however, this small contribution tends to become even smaller in simulated weightlessness conditions.

The results of the RR variability model, i.e. the contribution of CVP and respiration to the prediction of RR variability, suggested that the role of the cardiopulmonary and respiratory mediated mechanisms is limited, with respect to the regulation of HR in a

condition of reduced circulating volumes, possibly because of tachycardia induced reduction in HRV.

In addition, estimation of BRS was carried out through a bivariate model, during LBNP maneuver before and on day 50 of HDBR. The results of this analysis suggest that BRS in the LF range is reduced in bed rest, and these changes may be due primarily to a reduction in plasma volume associated with bed rest, which impacts the physiological responses of autonomic control of circulation.

Chapter 4 showed an explorative study where the analysis of baroreflex responses to changes in central volume was addressed. During major surgeries, maintenance of hemodynamic stability is a primary goal; to achieve this objective some maneuvers as fluid infusions are carried out, aiding to maintain ABP. Fluids are primarily administered to reverse hypovolemia. Hypovolemia may be due to external fluid losses caused by bleeding or losses from the gastrointestinal or urinary tracts, or internal losses due to extravasation of blood or exudation of body fluids. Baroreflex responses to fluid removal are difficult to study in the same surgical scenery; thus, the analysis of data from a LBNP protocol was addressed, since LBNP is a maneuver that might be a useful surrogate to study hemodynamic effects associated with severe hemorrhage in humans (Convertino et al., 2008; Cooke et al., 2004).

Central blood volume is an important factor in the ABP regulation, because central volume is related to preload and SV by means of Frank-Starling mechanism of the heart, which establish that the greater the heart muscle is stretched during filling, the greater is the force of contraction and the greater the quantity of blood pumped into the aorta. From this fact and from the knowledge that cardiopulmonary baroreceptors primarily monitors and regulates cardiac filling volume, the model of PP variability in function of relationship with CVP to represent ventricular contractility is justified. Nevertheless, is important to consider that the use of the measurement of CVP as a relative indicator of the status of central blood volume requires that the cardiac and pulmonary compliances remain fixed and unvaried (Pawelczyk et al., 1994; Ogoh et al., 2006). Another important consideration is that SV, which is the variable directly related with ventricular contractility, was not a direct measurement. Therefore, for the model of PP variability prediction, PP was used as surrogate of SV, and arterial compliance needs to be considered constant.

In the framework of the study related to the reduction of circulating volume, assessment of a decrease in venous return through graded LBNP maneuver was carried out. A decrease in the gain of cardiopulmonary baroreflex control of ventricular contractility was an expected result to volume reduction, as was showed in an example of chapter 4 (figure 4.5).

A large role of afterload modulation of cardiac ejection, with respect to cardiopulmonary baroreflex control of ventricular contractility and with respect to mechanical modulation of venous return by respiration was exhibited by a larger contribution of DBP in the variability prediction of PP, while a small contribution of CVP in the variability prediction of PP suggests that the cardiopulmonary baroreflex control of ventricular contractility was less effective during LBNP experiment and during long duration bed rest. This finding was in agreement with the results of (Jacobsen et al., 1993; Aletti et al., 2012) which also suggested a predominant role of the arterial baroreflex branch during orthostatic stress.

Results of variability prediction of SV were in average similar to the results obtained by the PP prediction model; a decrease in the gain of cardiopulmonary baroreflex control of ventricular contractility was also found in some subjects and the major contribution in the variability prediction model of SV was the contribution of DBP i.e. afterload modulation of cardiac ejection. However, is important take into account that SV is an estimated measurement, thus a more precise comparison between prediction models of PP and SV variability would be carried out considering more direct measurements of SV.

Some individual trends resulted as expected, showing a decrease of the gain of the $PP_{/CVP}$ filter with incremental LBNP intensities. Differences in the expected behavior of the gain of the $PP_{/CVP}$ filter may be due to the short length of some recordings, which can produce a misleading estimation. The analysis of a larger population, with more than 2 min of recordings, could lead to more accurate results.

In the second part of chapter 4, the same physiological problem was investigated in the context of intra-surgical volume loading procedures. Fluid infusion during major surgery is a routine maneuver aimed at maintaining ABP in order to prevent cardiovascular instability and to prevent or react to hypotensive episodes. Therefore, the study of baroreflex responses during this maneuver provides important information on cardiovascular adaptations to increased volume.

Baroreflex responses to fluid infusion were assessed by the same variability model considered before. An increase of heart contractility was found as the result of the response of cardiopulmonary baroreflex control of ventricular contractility to fluid infusion; this result was exhibited by the increase in the gain of the $PP_{/CVP}$ component corresponding to cardiopulmonary baroreflex control of ventricular contractility (example of figure 4.12). Therefore, ventricular contractility was enhanced to improve cardiac performance when volume was increased. A significant decrease in RR with fluid infusion was found, coinciding with results of (Barbieri et al., 2002), that reported the presence of a Bainbridge reflex (hypervolemia-induced tachycardia) at moderately elevated levels of central volume, induced by 500 ml of normal saline infusion. They also observed a significant drop in HF power of the RR interval spectrum, indicating a reduction in vagal modulation of HR. The absence of significant changes in frequency domain in our study may be due to differences in fluid infusions, since infusions of 100 ml and 500 ml were analyzed.

The significant increase in the contribution of CVP in the prediction of PP variability in the phase of fluid infusion suggests an increase in heart contractility elicited by an increase in cardiopulmonary baroreflex control of ventricular contractility, while the role of afterload modulation of cardiac ejection was reduced by volume increase procedure. Although these findings were not evidenced by the statistical analysis of differences in the estimated gains before and after fluid infusions, some patients were characterized by an increasing trend in cardiopulmonary baroreflex gain. Differences in the trend of patients may be due to the analysis of short length time series.

5.1 Limits of the study

The main limitations of this thesis are the relatively low number of subjects and the short length of time series used in the analysis.

Limitations regarding data from major surgeries are the heterogeneity of surgical procedures, the pathological condition previous to surgery and the prescribed medical treatment. In addition, finding isolated fluid infusion maneuvers is a difficult process, since fluid therapy during surgery is not performed as a purely independent maneuver: other drugs, such as noradrenaline or atropine, are routinely and continuosly administered, the period between fluid infusions can last less than 3 minutes, and the occurrence of surgery

complications is uncontrolled. Because of all these factors, selection of controlled and specific maneuvers is challenging.

Another limitation of this data is the absence of higher LBNP levels up to the tolerance threshold. Assessing higher LBNP levels under the same analysis approach could provide a full understanding of orthostatic intolerance. The protocol considered in this thesis included -30 mmHg which can be a model of moderate hemorrhage (Cooke et al., 2004). Since no stronger stimulus was applied, the presented results may be representative of responses to mild LBNP and of the transition between a non hypotensive and a potentially hypotensive stimulus.

5.2   Impact and future developments

The present study has analyzed different methods and models for the assessment of baroreflex sensitivity during clinical and experimental protocols that severely challenge the autonomic control of circulation.

Regarding the first part of this thesis, estimation of BRS during anesthesia induction provides a robust approach that considers causal relationships between SBP and RR interval and selection of steady-state and stationary time series. Furthermore, the importance of analyzing BRS through a mathematically rigorous and robust procedure consists in the availability of additional information to guide therapy and anesthesia in uncontrolled hypertensive patients, who are prone to a high rate of hypotension events during induction (Howell et al., 2004), and whose monitoring during anesthesia is more challenging than in normotensive patients.

In this thesis, the potential of investigating autonomic nervous system control of circulation, under surgery maneuvers such as anesthesia induction or fluid infusion, was shown. Gaining knowledge on the autonomic status of a patient undergoing major surgery could aid in the administration of the proper therapy to ensure hemodynamic stability and to prevent unexpected and potentially harmful blood pressure drops.

Future studies are needed in order to standardize and validate the proposed approaches in a larger population. Direct comparisons with neural and hemodynamic recordings would be necessary in order to validate the physiological meaning attributed to the proposed decomposition of PP. For the validation, invasive data from animal studies in controlled

experiments may prove to be more useful than working on patient data characterized by large variability. However, the goal would remain to develop reliable indices for guiding therapy in clinical settings such as the OR or the ICU.

The quantification of the "reverse" Bainbrigde reflex could be a prospective index useful in the prevention of hypotension during anesthetic maneuvers, since some authors have suggested that the decrease in HR during spinal anesthesia is caused by a reduction in venous return hinting that the Bainbridge reflex is the most important determinant of HR (Greene et al., 1958; Carpenter et al., 1992). This quantification of the "reverse" Bainbridge and the quantification of mechanisms that affect HRV, i.e. arterial baroreflex, cardiopulmonary baroreflex and RSA, by means of the prediction model of RR, and the quantification of gain values of the prediction model of PP variability, in critical patients might represent potential indices to guide therapy, particularly in the prevention of hypotensive episodes and in the fluid management. For example, if the presence of Bainbridge reflex can be revealed during volume loading of a patient, this should be a sign of volume overload and other maneuvers should be taken.

The integration of robust estimation of BRS and gain estimation or contribution of arterial and cardiopulmonary baroreflexes may be used to interpret variability of central volumes and to track heart performance under stress conditions such as anesthesia and surgery, supporting the decision making process of anesthesiologists, constantly faced with the challenge of identifying the optimal strategy to stabilize volumes and pressures during surgery. Clearly, clinical validation is necessary.

The analyses from second part of this thesis, focused on the quantification of the proportional role of arterial vs. cardiopulmonary baroreflex on control of HR variability, and of the contribution of cardiopulmonary baroreflex control of heart contractility, contributes to elucidate the mechanisms of heart function alterations in the presence of unloading of arterial and cardiopulmonary baroreceptors due to LBNP and long duration HDBR, or in the opposite scenario of volume increase through fluid infusion maneuver.

Another field of application of this analysis is the study of orthostatic intolerance, where treatment of this condition sometimes includes increase of volume (Vernikos et al., 1994). Thus, the larger role of arterial baroreflex on ABP maintenance during HDBR and the reduction of the role of cardiopulmonary baroreflex found in the analysis of this thesis can contribute to understand the response mechanisms of this condition in conjuction with

the evidence of increase of ventricular contractility controlled by cardiopulmonary baroreflex in situations of volume expansion.

Moreover, the assessment of the proposed approach to LBNP procedure incorporating higher levels could lead to better integration of the presented results, taking into account healthy and pathological subjects.

In the framework of exploring baroreflex responses to cardiovascular stress conditions, evaluation of TPR baroreflex could contribute to a more complete picture of the baroreflex functioning. An explorative study based on the work of (Mukkamala et al., 2003) is shown as appendix of this thesis.

Further development could entail the evaluation of nonlinear models. Closed-loop models have included linear approaches, considering the assumption that the contributions of nonlinear components in cardiovascular fluctuations are small. However, several authors have provided evidence that nonlinear dynamics are present, for example in HRV (Kanters et al., 1996). In this context, a closed-loop nonlinear analysis of ABP variability could provide a better understanding of the ABP control mechanisms. For example, exploring the method proposed by Wang et al. (2007), who used a closed-loop nonlinear system based on vector optimal parameter search and the constrained optimal parameter search.

Appendix A. Cardiopulmonary and arterial total peripheral resistance baroreflexes

Introduction

Circulatory baroreflex pathways are less understood than HR baroreflex; however, they may be more significant to ABP regulation than the cardiac baroreflex pathways. The TPR baroreflex, in particular, may be the most important short-term contributor to ABP regulation because TPR affects ABP directly via Ohm's law and indirectly via venous return (Mukkamala et al., 2003).

Since the main goal is to unravel the relationship of arterial and cardiopulmonary baroreflexes in their combined response to specific maneuvers as long duration bed rest and the effect of LBNP experiment; TPR baroreflexes were estimated through the approach proposed by (Mukkamala et al., 2003), which consists in a system identification method to quantify the static gains of both arterial TPR baroreflex and the cardiopulmonary TPR baroreflex from beat-to-beat measurements of ABP and CO.

Methods

The subset of data described in chapter 3 was used also in this analysis. In addition to signals of ABP, HR, CVP and respiration, SV and CO were analyzed as well. CO was estimated from the Modelflow method (Wesseling et al. 1993), the computed aortic flow waveform per beat provided left ventricular SV and consequently CO, by multiplying SV by instantaneous HR.

Estimation of arterial and cardiopulmonary TPR baroreflex gain values

In order to study TPR baroreflex mechanism, the system identification analysis proposed by (Mukkamala et al., 2003) was implemented.

The system identification considers two transfer functions (CO → ABP and SV → ABP) and the perturbing noise source. The involved physiological models are:

CO → ABP encompasses the dynamic properties of the arterial TPR baroreflex and the systemic arterial tree. An increase in CO would initially cause ABP to increase via the

systemic arterial tree. This would, in turn, excite the arterial TPR baroreflex/systemic arterial tree loop to decrease TPR so as to maintain ABP (Mukkamala et al., 2006a).

SV ABP encompasses the dynamic properties of the arterial TPR baroreflex and cardiopulmonary TPR baroreflex, as well as the inverse heart-lung unit and systemic arterial tree. An increase in SV would indicate that an increase in CVP had occurred through the inverse heart-lung unit. This CVP increase would excite the cardiopulmonary TPR baroreflex to decrease TPR, which would then stimulate the arterial TPR baroreflex/systemic arterial tree loop to increase TPR and maintain ABP.

Identification of the physiological systems and noise source was implemented by means of a dual-input, autoregressive exogenous input (ARX) model:

$$DBP\,(i) = \sum_{j=1}^{p} a_j \cdot DBP\,(i-j) + \sum_{j=0}^{q} b_j \cdot CO\,(i-j) + \sum_{j=0}^{r} c_j \cdot SV\,(i-j) + W\,(i) \tag{A.1}$$

where W is the residual error, coefficients (a_j, b_j, c_j) specify the CO ABP and SV ABP impulse responses, whereas the residual error together with the set of parameters a_j define the power spectrum of N_{ABP}. DBP was used to represent ABP since it is classically related to TPR, as outlined in Windkessel modeling of the arterial tree (Mukkamala et al., 2006b). The model orders *p,q,r* were determined by AIC and it were in the range between 8 and 12. G_A and G_C were estimated as follows:

$$G_A = \frac{\sum_{j=0}^{q} b_j + \sum_{j=1}^{p} a_j - 1}{\sum_{j=0}^{q} b_j}\,; \qquad G_C = \frac{\sum_{j=0}^{r} c_j}{\sum_{j=0}^{q} b_j} \tag{A.2}$$

Mukkamala et al. proposed the estimation of G_A and G_C values rather than the entire TPR baroreflex impulse responses (Mukkamala et al., 2006a). Since G_A and G_C are equivalent to the areas of the corresponding TPR baroreflex impulse responses.

Results and discussion

Arterial and cardiopulmonary TPR baroreflex gains

The mean values of CO, SV and TPR are shown in table A.1. CO was significantly reduced in baseline on day 50 of HDBR in comparison with pre-HDBR condition, while SV was significantly smaller after bed rest with respect to pre-bed rest condition in each of the four epochs of LBNP experiment. TPR was determined from (MAP–CVP)/ CO and no

significant changes were found before and after bed rest during LBNP maneuver; however, an increase of TPR can be appreciated with increasing LBNP intensities, while CVP decreased, as is shown in the example of figure A.1, which hints that cardiopulmonary TPR baroreflex was active during high levels of LBNP before and during long duration bed rest.

Regarding arterial and cardiopulmonary TPR baroreflexes, no significant differences were found in the estimation of G_A and G_C; however, at baseline G_A and G_C showed smaller values during HDBR, hinting that arterial and cardiopulmonary TPR baroreflexes were impaired due to cardiovascular deconditioning caused by bed rest. This result is consistent with the study of (Xiao et al., 2002), where a significant decrease in the static gain of the arterial TPR baroreflex was found, they followed the same identification method but they only studied the effect of 16 days of 4-degree HDBR in healthy volunteers, while in the present study the effect of LBNP experiment was also explored.

The gain of arterial TPR baroreflex (G_A) was higher than the gain of cardiopulmonary TPR baroreflex at baseline before bed rest, while during HDBR the difference between G_A and G_C decreased and the gain values were very close (table A.2).

In successive phases, where LBNP intensity increased, trend of G_A showed higher gain values before bed rest than during HDBR condition; and G_C tended to remain stable between both conditions. This result may suggest that arterial TPR baroreflex was mostly affected by bed rest with increasing LBNP levels with respect to cardiopulmonary TPR baroreflex (figure A.2).

A misleading estimation may be the reason of differences in trend of gain values, due to short length time series considered for analysis, since work of (Mukkamala et al., 2003) used time series of 6 minutes.

Study of the effect of simulated or actual microgravity on the cardiovascular control system is quite outspread; however, few works have studied the role of TPR baroreflex function in this maneuver (Fritsch-Yelle et al., 1996; Waters et al., 2002; Xiao et al., 2002; Yuan et al., 2012). Fritsch-Yelle et al. studied cardiovascular responses to upright posture in astronauts before and after spaceflights reporting that average TPR increased less after spaceflight than before spaceflight. This result implies that TPR baroreflex static gain was blunted after spaceflight.

Table A.1. Cardiac output (CO), stroke volume (SV) and total peripheral resistance (TPR) mean values before (PRE) and during bed rest (HDBR), in each of the four experimental epochs of the continuous LBNP maneuver

		BL	-10	-20	-30
CO, l/min[a]	**PRE**	$4.72 \pm 0.50^{\#}$	4.52 ± 0.45	4.34 ± 0.56	4.23 ± 0.63
	HDBR	4.25 ± 0.44	4.12 ± 0.42	3.94 ± 0.46	3.96 ± 0.75
SV, l/beat[a,b]	**PRE**[‡]	$0.074 \pm 0.006^{\#}$	$0.073 \pm 0.006^{\#}$	$0.066 \pm 0.008^{\#}$	$0.061 \pm 0.010^{\#\S}$
	HDBR[‡]	0.060 ± 0.009	0.056 ± 0.010	0.049 ± 0.009	$0.046 \pm 0.012^{\S}$
TPR, mmHg·min/l	**PRE**	18.57 ± 2.77	19.28 ± 2.54	19.88 ± 2.67	20.68 ± 3.16
	HDBR	20.26 ± 3.79	20.87 ± 3.85	21.65 ± 3.97	21.81 ± 5.67

Values are expressed as mean ± SD. [a]Two-way ANOVA row (effect of bed rest) factor, p-value < 0.05. [b]Two-way ANOVA column (effect of LBNP) factor, p-value < 0.05. [‡]One-way ANOVA, p-value < 0.05. [§]significant post-hoc comparison between each LBNP level and BL (in PRE and HDBR condition). [#]Paired t-test between the same LBNP phase (PRE vs HDBR) p-value < 0.05.
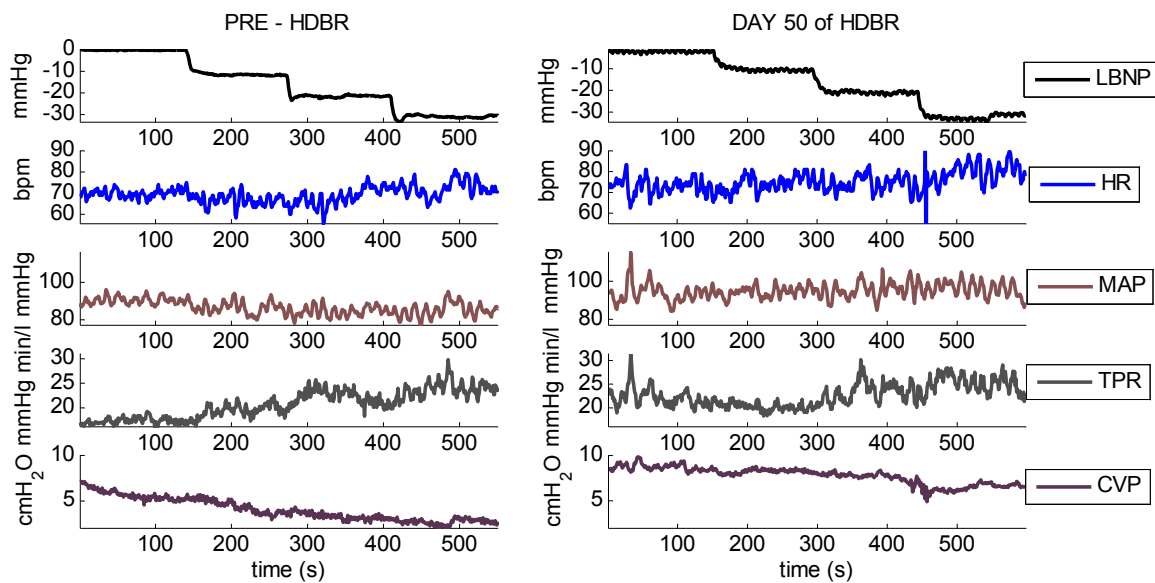

Figure A.1 Beat-by-beat hemodynamic series from one subject during lower body negative pressure (LBNP) experiment before bed rest and on day 50 of HDBR. HR, heart rate; MAP, mean arterial pressure; TPR, total peripheral resistance; CVP, central venous pressure.

Table A.2. Estimated gains of arterial and cardiopulmonary TPR baroreflexes (G_A, G_C) before (PRE) and during bed rest (HDBR), in each of the four experimental epochs of the continuous LBNP maneuver.

		BL	-10	-20	-30
G_A	PRE	-2.05 (-3.37, 0.78)	-1.41 (-1.82,-1.31)	-0.98 (-1.88, 0.38)	-1.00 (-2.09,-0.20)
	HDBR	-0.59 (-1.57,-0.18)	-0.98 (-1.70,-0.33)	-0.42 (-0.49,-0.06)	-0.93 (-1.11,-0.49)
G_C	PRE[‡]	-1.18 (-2.16,-0.45)	-1.21 (-1.41,-0.45)	-0.42 (-1.12,-0.36)	-1.18 (-2.25,-0.44)
	HDBR	-0.57 (-0.92,-0.38)	-1.38 (-1.62,-0.76)	-0.48 (-1.05,-0.25)	-1.02 (-1.45,-0.47)

Values are expressed as median (25th percentile, 75th percentile).
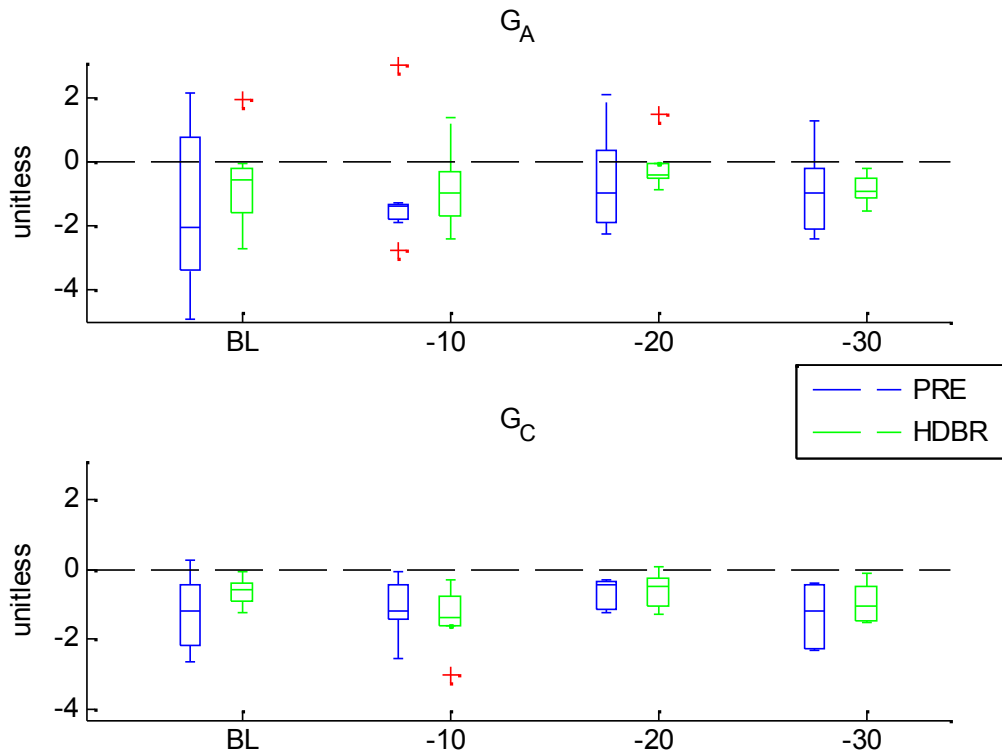

Figure A.2. Estimation of arterial (GA) and cardiopulmonary (GC) TPR baroreflex gains, during baseline (BL) and three levels (-10mmHg, -20mmHg, -30mmHg) of LBNP procedure before (PRE) and on day 50 of bed rest (HDBR).

Appendix B. Black box models

A black-box model of a system is one that does not use any particular prior knowledge of the character or physics of the relationships involved.

BLACK-BOX MODELS: BASIC FEATURES

To bring out the basic features of a black-box estimation problem, a simple example is shown. Suppose the problem is to estimate an unknown function $g_o(x)$, -1 x 1. The observations are noise measurements $y(k)$ at points x_k

$$y(k) = g_0(x_k) + e(k) \tag{B.1}$$

The purpose is to know where looking for g. For example if g is a third order polynomial. This would lead to grey box model structure

$$g(x, \theta) = \theta_1 + \theta_2 x + \theta_3 x^2 + \ldots + \theta_n x^{n-1} \tag{B.2}$$

with $n=4$ and θ would be estimated from the observations y, using e.g. the classical least squares method.

If no structural information about g is available, it is necessary to assume something about g, e.g. it is an analytical function, in this situation (B.2) can be also used, but as black box model. If g is assumed as analytical function, it can be approximated arbitrarily well by a polynomial. The necessary order n would not be known, and we would have to find a good value of it using some suitable scheme. There are several alternatives in this black-box situation: rational approximations, Fourier series expansions or approximate the function by piecewise constant functions.

Therefore, the basic steps of black box modeling are as follows:

1. Choose the "type" of model structure class. (For example: Fourier transform, rational function, or piecewise constant.)
2. Determine the "size" of this model (i.e. the number of parameters, n). This will correspond to how "fine" the approximation is.
3. Use observed data both to estimate the numerical values of the parameters and to select a suitable value of n.

A general model structure for the observations is:

$$\hat{y}(k|) = g(x_k,) \tag{B.3}$$

Information taken from: Ljung, Black-box models from input.output measurementes. IEEE Instrumentation and Measurement Technology Conference, Budapest Hungary. 2001; 138-146.

$\hat{y}(k|\theta)$ is the predicted value of the $y(k)$ assuming that the function can be described by the parameter vector θ.

ESTIMATION TECHNIQUES AND BASIC PROPERTIES.

Criterion of Fit

It suggests itself that the basic least-squares like approach is a natural approach, even when the predictor $\hat{y}(k|\theta)$ is a more general function of θ:

$$\hat{}_N = \arg \quad \min V_N(\theta, Z^N) \tag{B.4}$$

where
$$V_N(\theta, Z^N) = \frac{1}{N} \sum_{t=1}^{N} \|y(t) - \hat{y}(t|\theta)\|^2 \tag{B.5}$$

We shall also use the following notation for the discrepancy between measurement and predicted value

$$\varepsilon(t, \theta) = y(t) - \hat{y}(t|\theta) \tag{B.6}$$

if the noise source in the system is supposed to be a Gaussian sequence of independent random variables $\{e(t)\}$ then (B.4) becomes the Maximum Likelihood Estimate (MLE).

If $\hat{y}(k|\theta)$ is a linear function of θ the minimization problem (B.4) is easily solved. In more general cases the minimization will have to be carried out by iterative (local) search for the minimum:

$$\theta_N^{i+1} = \theta_N^i + \mu f(Z^N, \theta_N^i) \tag{B.7}$$

where f typically is related to the gradient of V_N, like the Gauss-Newton direction.

It is also quite useful work with a modified criterion

$$W_N(\theta, Z^N) = V_N(Z^N) + \delta\|\theta\|^2 \tag{B.8}$$

with V_N defined by (B.5). This is known as regularization.

Convergence as N

Properties of the estimate resulting from (B.5) depend on the properties of the data record Z^N. It is an important aspect of the general identification method (B.5) that the asymptotic properties of the resulting estimate can be expressed in general terms for arbitrary model parameterizations.

The first basic result is the following one:

$$\theta_N \to \theta^* \text{ as } N \to \infty \quad \text{where} \quad \theta^* = \arg \quad \min_{\theta} E \quad \|\varepsilon(t, \theta)\|^2 \tag{B.9}$$

That is, as more and more data become available, the estimate converges to that value θ^*, that would minimize the expected value of the "norm" of the prediction errors. This is

in a sense *the best possible approximation* of the true system that is available within the model structure. The expectation E in (B.9) is taken with respect to all random disturbances that affect the data and it also includes averaging over the' "input properties". This means, in particular, that θ^* will make $\hat{y}(t|\theta^*)$ a good approximation of $y(t)$ with respect to those aspects of the system that are enhanced by the conditions at hand, when the data were collected.

Asymptotic Distribution

If $\{\varepsilon(t|\theta^*)\}$ is approximately white noise, then the random vector $\overline{N}(\hat{\theta}_N - \theta)$ converges in distribution to the normal distribution with zero mean and the covariance matrix of θ_N is approximately given by

$$P_\theta = \lambda \left[E\psi(t)\psi^T(t) \right]^{-1} \tag{B.10}$$

where

$$\lambda = E\varepsilon^2(t, \theta^*)$$
$$\psi(t) = \frac{dE}{d\theta} \hat{y}(t|\theta)\Big|_{\theta=\theta^*} \tag{B.11}$$

This means that the convergence rate of $\hat{\theta}_N$, towards θ^* is $1/\sqrt{N}$.

CHOICE OF TYPE AND SIZE OF MODEL

Bias-Variance Trade-off

The obtained model $g(x, \hat{\theta}_N)$, will be in error in two ways:

1. First, there will be a discrepancy between the limit model $g(x, \theta^*)$ and the true function $g_o(x)$, since our structure assumptions are not correct, e.g. the function is not piecewise constant. This error is called a *bias error*, or a *model mismatch error.*

2. Second, there will be a discrepancy between the actual estimate $\hat{\theta}_N$ and the limit value. This is due to the noise corrupted measurements (the term $e(k)$ in (B.1)). This error will be called a *variance error*, and can be measured by the: covariance matrix (B.10).

An Expression for the Expected Mean-Square Error

Let us measure the (average) fit between any model (B.3) and the true system as

$$\overline{V}(\theta) = E\left|y(t) - \hat{y}(t|\theta)\right|^2 \tag{B.12}$$

Expectation E is over the data properties. The fit $\overline{V}$ will depend, not only on the model and the true system, but also on data properties.

The estimated model parameter $\hat{\theta}_N$, is a random variable, because it is constructed from observed data, that can be described as random variables. To evaluate the model fit, we then take the expectation of $\bar{V}(\hat{\theta}_N)$ with respect to the estimation data. That gives the measure

$$F_N = E\bar{V}(\hat{\theta}_N) \tag{B.13}$$

The rather remarkable fact is that if F_N is evaluated for data with the same properties as those of the estimation data, then, asymptotically in N,

$$F_N \approx \bar{V}(\theta^*)\left(1 + \frac{\dim \theta}{N}\right) \tag{B.14}$$

Here θ^* is the value that minimizes the expected value of the criterion (B.5). The notation *dim* θ means the number of estimated parameters. The result also assumes that the model structure is successful in the sense that $\varepsilon(t)$ is approximately white noise.

It is quite important to note that the number *dim* θ in (B.14) will be changed to the number of eigenvalues of $\bar{V}''(\theta)$ (the Hessian of $\bar{V}$) that are larger than δ in case the regularized loss function (B.8) is minimized to determine the estimate. We can think of this number as the efficient number of parameters. In a sense, we are "offering" more parameters in the structure, than are actually "used" by the data in the resulting model.

The expression (B.14) clearly shows the trade off between variance and bias. The more parameters used by the structure (corresponding to a higher dimension of θ and/or a lower value of the regularization parameter δ) the higher the variance term, but at the same the lower the fit $\bar{V}(\theta^*)$. The trade off is thus to increase the efficient number of parameters only to that point that the improvement of fit per parameter exceeds $\bar{V}(\theta^*)/N$. This can be achieved by estimating F_N in (B.13) by evaluating the loss function at $\hat{\theta}_N$ for a validation data set. It can also be achieved by Akaike (or Akaike-like) procedures, balancing the variance term in (B.14) against the fit improvement.

LINEAR BLACK-BOX MODELS

Linear Models and Estimating Frequency Functions

A linear system is uniquely defined and described by its *frequency function* $G(e^{iw})$ i.e. the Fourier transform of its impulse response. We could therefore link estimation of linear systems directly to the function estimation problem (B.l), taking $x_k = e^{iwk}$ and allowing g to

be complex-valued. With observations of the input-output being directly taken from, or transformed to the frequency domain (*y* would here be uncertain observations of the frequency response at certain frequencies) we have a straightforward function estimation problem.

Time-domain Data and General Linear Models

If the observations *y* to be used for the model fit are input-output data in the time domain, we proceed as follows: Assume that the data have been generated according to

$$y(t) = G(q, \theta) \, u(t) + H(q, \theta) \, e(t) \tag{B.15}$$

where *e* is white noise (unpredictable), *q* is the forward shift operator and *H* is monic (that is, its expansion in q^{-1} starts with the identity matrix). We also assume that *G* contains a delay. Rewrite (B.15) as

$$y(t) = [I - H^{-1}(q, \theta)] + H^{-1}(q, \theta) \, G(q, \theta) \, u(t) + e(t) \tag{B.16}$$

Linear Input-output Black-box models

In the black-box case, a very natural approach is to describe *G* and *H* in (B.15) as rational transfer functions in the shift (delay) operator with unknown numerator and denominator polynomial. We would then have

$$G(q, \ ) = \frac{B(q)}{F(q)} = \frac{b_1 q^{-nk} + b_2 q^{-nk-1} + \cdots + b_{nb} q^{-nk-nb+1}}{1 + f_1 q^{-1} + \cdots + f_{nf} q^{-nf}} \tag{B.17}$$

Then

$$\eta(t) = G(q, \theta) \, u(t) \tag{B.18}$$

$$\eta(t) + f_1 \eta(t-1) + \ldots + f_{nf} \eta(t-nf) = b_1 u(t-nk) + \ldots + b_{nb} u(t-(nb+nk-1)) \tag{B.19}$$

In the same way the disturbance transfer function can be written

$$H(q, \ ) = \frac{C(q)}{D(q)} = \frac{1 + c_1 q^{-1} + \ldots + c_{nc} q^{-nc}}{1 + d_1 q^{-1} + \ldots + d_{nd} q^{-nd}} \tag{B.20}$$

The parameter vector θ thus contains the coefficients b_i, c_i, d_i, and f_i of the transfer functions. This model is thus described by five structural parameters: *nb, nc, nd, nf*, and *nk* and is known as the *Box-Jenkins* (BJ) model.

A common variant is to use the same denominator for *G* and *H*:

$$F(q) = D(q) = A(q) = 1 + a_1 q^{-1} + \ldots + a_{na} q^{-na} \tag{B.21}$$

Multiplying both sides of (B.17)-(B.20) by *A*(*q*) then gives

$$A(q)\ y(t) = B(q)\ u(t) + C(q)\ e(t) \tag{B.22}$$

This model is known as the *ARMAX model*. The name is derived from the fact that $A(q)y(t)$ represents an Autoregression and $C(q)e(t)$ a Moving Average of white noise, while $B(q)u(t)$ represents an extra input (an exogenous variable).

The special case $C(q)=1$ gives an *ARX* model.

Appendix C. Fluid challenge

Fluid challenge is used in the fluid management of many sick patients. The principle behind the fluid challenge technique is that by giving a small amount of fluid in a short period of time, the clinician can assess whether the patient has a preload reserve that can be used to increase the stroke volume (SV) with further fluids.

The resuscitation of the critically ill patient requires an accurate assessment of the patient's intravascular volume status (cardiac preload) and the likelihood that the patient will respond (increase SV) to a fluid challenge (volume responsiveness). Preload assessment and fluid responsiveness is a routine exercise in critically ill patients, and it becomes of vital importance during hemodynamic management. It can often be challenging in the intensive care unit patient since there is no single clinical gold standard.

From the Frank–Starling law of the heart (figure C.1), an increase in preload will significantly increase SV only if both ventricles are on the ascending portion of the curve. If one or both ventricles lie on the flat portion, then the patient will be regarded as a non-responder; that is, cardiac output (CO) will not increase significantly in response to volume expansion.

Studies in mechanically ventilated patient have demonstrated that pressure variations in respiratory cycle are useful in the assessment of fluid administration. Fluid responsiveness in the mechanically ventilated patient is assessed by static and dynamic indices.

Static indices are preload measurements, such as central venous pressure (CVP) and pulmonary artery occlusion pressure (PAOP). CVP has been traditionally used to guide fluid administration within the operating theatre. However, static preload filling-pressure markers like CVP and PAOP have been shown to correlate poorly with ventricular filling volumes and fluid responsiveness in healthy volunteers and critically ill patients (Lazaridis 2012).

Other static indices are right ventricular end-diastolic volume, left ventricular end-diastolic area, global end-diastolic volume and intrathoracic blood volume. PiCCO, Pulsion Medical Systems through transpulmonary thermodilution can be used to assess the global end-diastolic volume (GEDV), the largest volume of blood contained within the

four heart chambers, and intrathoracic blood volume, which comprises GEDV and pulmonary blood volume.

Dynamic indices, are derived from the respiratory-induced variations in the arterial pressure in the mechanically ventilated patients, in regard to their ability to predict the left ventricular response to volume load. These indices include SV variation, pulse pressure variation, systolic pressure variation, aortic blood velocity, superior vena cava collapsibility index and inferior vena cava distensibilty index.

Stroke volume variation (SVV) is the change in SV during the respiratory cycle, and is calculated by:

$$SVV(\%) = \frac{SV_{max} - SV_{min}}{SV_{mean}} \qquad (C.1)$$

SVV can be assessed continuously by any beat-to-beat CO monitor. Many studies have shown this to be a reliable predictor of fluid responsiveness (Hofer et al., 2008).

Pulse Pressure Variation (PPV). Pulse pressure (difference between systolic and diastolic pressure) is directly proportional to left ventricular SV and inversely related to arterial compliance. The respiratory changes seen in left ventricular SV determine changes in the peripheral pulse pressure during the respiratory cycle (Michard et al., 2007). PPV can be expressed as a percentage using the following equation:

$$PPV(\%) = 2 \cdot \frac{PP_{max} - PP_{min}}{PP_{max} - PP_{min}} \qquad (C.2)$$

where PP_{max} and PP_{min} are the maximal and minimal values within one respiratory cycle. Measurement of PPV can be used to predict preload non-responders in those with a PPV<13%. Also, high baseline PPV values correlate well with subsequent increase in cardiac index.

Systolic Pressure Variation (SPV) induced by intermittent positive pressure ventilation results from changes in aortic transmural pressure secondary to changes in left ventricular SV, and changes in extramural pressure caused by changes in pleural pressure. For this reason, SPV is a less specific indicator of left ventricular SV and less useful in predicting fluid responsiveness. SPV is the difference between the maximal and minimal values of systolic pressure over a single respiratory cycle:

$$SPV(mmHg) = SBP_{max} - SBP_{min} \qquad (C.3)$$

SPV can be divided into two components, to discriminate between the effects of the expiratory phase and inspiratory phase: up and down. These require a reference systolic pressure taken during an end-expiratory pause.

down is the difference between the reference systolic pressure and the minimal value of systolic pressure over a single respiratory cycle: down(mmHg)=SBP_{ref} - SBP_{min}. It reflects the expiratory decrease in left ventricular preload and SV related to the inspiratory decrease in right ventricular SV. down appears to be the major component of SPV, and during hemorrhage, its value increases. It predicts fluid responsiveness well because the higher the down value before fluid infusion, the greater the increase in cardiac index post-infusion (Tavernier et al., 1998). up is defined as up(mmHg)=SBP_{max}-$SBP_{ref.}$
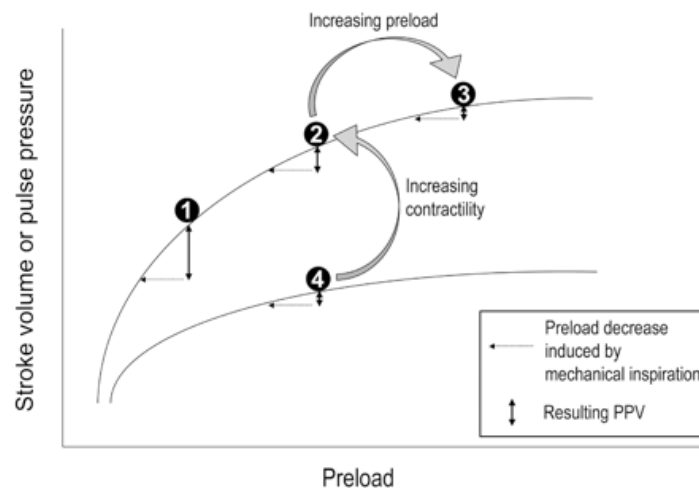

Figure C.1 Determinants of pulse pressure variation (PPV). PPV is a marker of the position on the Frank–Starling curve, not an indicator of blood volume or a marker of cardiac preload. Increasing preload induces a decrease in PPV (from 2 to 3). PPV is mimimal when the heart is operating on the plateau of the Frank–Starling curve (3 and 4). Decreasing preload induces an increase in PPV (from 2 to 1), also increasing contractility (from 4 to 2).

The clinical use of dynamic indices has certain limitations. First of all, these methods may be used only for the assessment of mechanically ventilated patients with no arrhythmias, whose arterial pressure is monitored invasively. Other limitations include a dependency on the delivered tidal volume (Reuter et al., 2003), as well as the fact that the SPV, PPV, and SVV are calculated as the difference between the maximal and minimal values of systolic arterial pressure or SV during mechanical breath. However, the maximal

value is often influenced by an early inspiratory augmentation of left ventricular SV, which is not related to fluid responsiveness (Preisman et al., 2005).

Passive leg raising can be used in the spontaneous breathing patient, but requires the use of a fast response CO measurement, such as transthoracic echo (measuring velocity time interval at the aortic valve as an index of aortic flow).
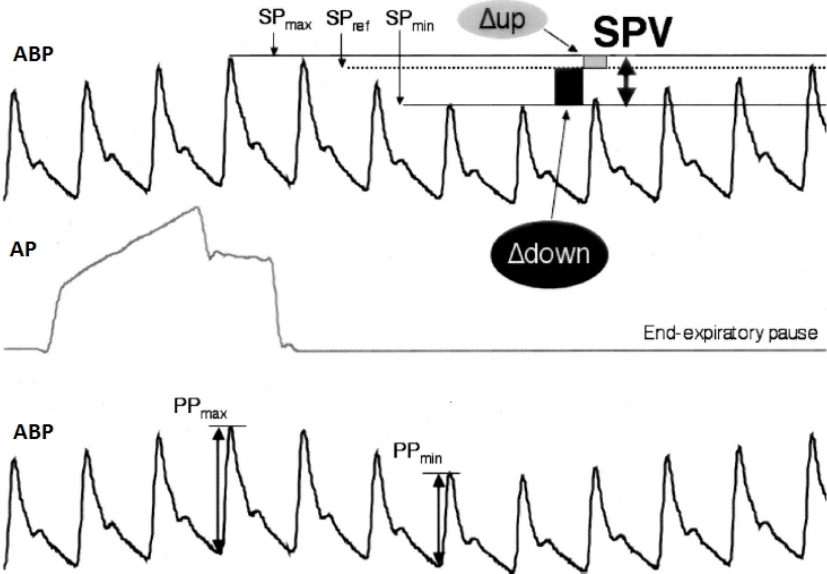

Figure C.2 Fluid responsiveness indices: SPV (Systolic Pressure Variation), PPV (Pulse Pressure Variation), up e down. ABP= Arterial Blood Pressure, AP= Air Pressure.

Bibliography

Abboud F. The sympathetic system in hypertension. State of the art review. Hypertension 1982; 4(3): 208-225.

Aicher SA, Randich A. Antinociception and cardiovascular responses produced by electrical stimulation in the nucleus tractus solitarius, nucleus reticularis ventralis, and the caudal medulla. Pain. 1990; 42(1):103-19.

Akselrod S, Gordon D, Ubel FA, Shannon DC, Berger AC, Cohen RJ. Power spectrum analysis of heart rate fluctuation: a quantitative probe of beat-to-beat cardiovascular control. Science. 1981; 213: 220–222.

Aletti F, Bassani T, Lucini D, Pagani M, Baselli G. Multivariate decomposition of arterial blood pressure variability for the assessment of arterial control of circulation. IEEE Trans Biomed Eng. 2009; 56(7):1781-90.

Aletti F, Ferrario M, Xu D, Greaves DK, Shoemaker JK, Arbeille P, et al. Short-term variability of blood pressure: Effects of lower-body negative pressure and long-duration bed rest. Am J Physiol Regul Integr Comp Physiol. 2012; 303(1):R77-85.

Arbeille P, Kerbeci P, Mattar L, Shoemaker JK, Hughson RL. WISE-2005: tibial and gastrocnemius vein and calf tissue response to LBNP after a 60-day bed rest with and without countermeasures. J Appl Physiol. 2008; 104:938-943.

Baccala LA, Sameshima K, Ballester G, Valle AC, Timo-Iaria. Studying the interaction between brain structures via directed coherence and Granger causality. Appl Signal Process. 1998; 5:40–48.

Bainbridge FA. The influence of venous filling upon the rate of the heart. J Physiol. 1915; 50:65–84.

Barbieri R, Parati G, Saul JP. Closed-versus open-loop assessment of heart rate baroreflex. IEEE Eng Med Biol Mag. 2001; 20: 33-42.

Barbieri R, Triedman JK, Saul JP. Heart rate control and mechanical cardiopulmonary coupling to assess central volume: a systems analysis. Am J Physiol Regul Integr Comp Physiol. 2002; 283: R1210-R1220.

Baselli G, Cerutti S, Badilini F, et al. Model for the assessment of heart period and arterial pressure variability interactions and of respiratory influences. Med Biol Eng Comp. 1994; 32(2):143–52.

Baselli G, Cerutti S, Civardi S, Malliani A, Pagani M. Cardiovascular variability signals: towards the identification of a closed-loop model of the neural control mechanisms. IEEE Trans Biomed Eng. 1988; 35: 1033-1046.

Baselli G, Porta A, Cerutti S, Caiani EG, Lucini D, Pagani M. RR-arterial pressure variability relationships. Auton Neurosci. 2001; 90(1-2):57-65.

Bassani T, Magagnin V, Guzzetti S, Baselli G, Citerio G, Porta A. Testing the involvement of baroreflex during general anesthesia through Granger causality approach. Comput Biol Med. 2012; 42(3):306-12.

Bentzen BH, Grunnet M. Central and peripheral $GABA_A$ receptor regulation of the heart rate depends on the conscious state animal. Adv Pharmacol Sci. 2011; doi:10.1155/2011/578273.

Berdeaux A, Duranteau J, Pussard E, Edouard A, Giudicelli JF. Baroreflex control of regional vascular resistances during simulated orthostatism. Kidney Int. 1992; 41:S29-33.

Berthelsen PG, Eldrup N, Nilsson LB, Rasmussen JP. Thermodilution cardiac output. Acta Anaesthesiol Scand. 2002; 46(9):1103-10.

Bertinieri G, di Rienzo M, Cavallazzi A, Ferrari AU, Pedotti A, Mancia G. A new approach to analysis of the arterial baroreflex. J Hypertens Suppl. 1985; 3(3):S79-81.

Bevegård S, Castenfors J, Lindblad LE. Effect of changes in blood volume distribution on circulatory variables and plasma renin activity in man. Acta Physiol Scand. 1977; 99(2):237-45.

Blasi A, Jo J, Valladares E, Juarez R, Baydur A, Khoo MCK. Autonomic cardiovascular control following transient arousal from sleep: a time-varying closed-loop model. IEEE Trans Biomed Eng. 2006; 53:74-82.

Boettcher DH, Zimpfer M, Vatner SF. Phylogenesis of the Bainbridge reflex. Am J Physiol. 1982; 242:R244-6.

Brown AM. Receptors under pressure. an update on baroreceptors. Circ Res. 1980; 46(1):1-10.

Brown CM, Hecht MJ, Neundörfer B, Hilz MJ. Effects of lower body negative pressure on cardiac and vascular responses to carotid baroreflex stimulation. Physiol Res. 2003; 52(5):637-45.

Buckey JC Jr, Lane LD, Levine BD, Watenpaugh DE, Wright SJ, Moore WE, GaVney FA, Blomqvist CG. Orthostatic intolerance after spaceflight. J Appl Physiol. 1996; 81:7-18.

Butler GC, Xing HC, Northey DR, Hughson RL. Reduced orthostatic tolerance following 4 h head-down tilt. Eur J Appl Physiol Occup Physiol. 1991; 62:26–30.

Carpenter RL, Caplan RA, Brown DL, Stephenson C, Wu R. Incidence and risk factors for side effects of spinal anesthesia. Anesthesiology. 1992; 76(6):906-16.

Cavalcanti S, Belardinelli E. Modeling of cardiovascular variability using a differential delay equation. IEEE Trans Biomed Eng. 1996; 43(10):982-9.

Chapleau M, Li Z, Meyrelles S, Ma X, Abboud F. Mechanisms determining sensitivity of baroreceptor afferents in health and disease. Ann NY Acad Sci. 2001; 940:1-19.

Chen X, Kim JK, Sala-Mercado JA, Hammond RL, Elahi RI, Scislo TJ, Swamy G, O'Leary DS, Mukkamala R. Estimation of the total peripheral resistance baroreflex impulse response from spontaneous hemodynamic variability. Am J Physiol Heart Circ Physiol. 2008; 294(1):H293-301.

Chen Z, Purdon PL, Harrell G, Pierce ET, Walsh J, Brown EN, Barbieri R. Dynamic assessment of baroreflex control of heart rate during induction of propofol anesthesia using a point process method. Ann Biomed Eng. 2011; 39 (1):260-76.

Chung E, Chen G, Alexander B, Cannesson M. Non-invasive continuous blood pressure monitoring: A review of current applications. Frontiers of medicine. 2013; 7(1):91-101.

Convertino VA, Doerr DF, Eckberg DL, Fritsch JM, Vernikos-Danellis J. Head-down bed rest impairs vagal baroreflex responses and provokes orthostatic hypotension. J Appl Physiol. 1990; 68: 1458–1464.

Convertino VA, Ryan KL, Rickards CA, Salinas J, McManus JG, Cooke WH, Holcomb JB. Physiological and medical monitoring for en route care of combat casualties. J Trauma. 2008; 64(4 Suppl): S342-53.

Convertino VA. Clinical aspects of the control of plasma volume at microgravity and during return to one gravity. Med Sci Sports Exerc. 1996; 28: S45-S52.

Convertino VA. Lower body negative pressure as a tool for research in aerospace medicine and military medicine. J Gravit Physiol. 2001; 8(2):1-14.

Cooke WH, Ryan KL, Convertino VA. Lower body negative pressure as a model to study progression to acute hemorrhagic shock in humans. J Appl Physiol. 2004; 96(4):1249-61.

Cooper VL, Hainsworth R. Carotid baroreceptor reflexes in humans during orthostatic stress. Exp Physiol. 2001; 86(5):677-81.

Crystal GJ, Salem MR. The bainbridge and the "reverse" bainbridge reflexes: History, physiology, and clinical relevance. Anesth Analg. 2012; 114(3):520-32.

Cullen PM, Turtle M, Prys-Roberts C, Way WL, Dye J. Effect of propofol anesthesia on baroreflex activity in humans. Anesth Analg. 1987; 66:115–120.

De Boer R.W, Karemaker J.M, Strackee J. Hemodynamic fluctuations and baroreflex sensitivity in humans: a beat-to-beat model. Am. J. Physiol. Heart Circ. Physiol. 1987; 253, H680–H689.

Desai TH, Collins JC, Snell M, Mosqueda-Garcia R. Modeling of arterial and cardiopulmonary baroreflex control of heart rate. Am J Physiol. 1997; 272(5 Pt 2):H2343-52.

Di Rienzo M, Parati G, Radaelli A, Castiglioni P. Baroreflex contribution to blood pressure and heart rate oscillations: Time scales, time-variant characteristics and nonlinearities. Phil Trans R Soc A. 2009; 367(1892):1301-18.

Dorantes-Mendez G, Aletti F, Toschi N, Canichella A, Dauri M, Coniglione F, Guerrisi M, Signorini MG, Cerutti S, Ferrario M. Baroreflex sensitivity variations in response to propofol anesthesia: comparison between normotensive and hypertensive patients. J Clin Monit Comput. 2013a; 27(4):417-26.

Dorantes-Mendez G, Aletti F, Toschi N, Coniglione F, Dauri M, Guerrisi M, Baselli G, Signorini MG, Cerutti S, Ferrario M. Effects of propofol anesthesia induction on autonomic cardiovascular control. 7th International Workshop on Biosignal Interpretation, Italy, 2012a.

Dorantes-Mendez G, Aletti F, Toschi N, Canichella A, Coniglione F, Sabato E, della Badia Giussi F, Dauri M, Sabato AF, Guerrisi M, Baselli G, Signorini MG, Cerutti S, Ferrario M. Estimation of baroreflex sensitivity during anesthesia induction with propofol. Conf Proc IEEE Eng Med Biol Soc. 2011; 2011:3788-91.

Dorantes-Mendez G, Aletti F, Toschi N, Guerrisi M, Coniglione F, Dauri M, Baselli G, Signorini MG, Cerutti S, Ferrario M. Effects of propofol anesthesia induction on the relationship between arterial blood pressure and heart rate. Conf Proc IEEE Eng Med Biol Soc. 2012b; 2012:2835-8.

Dorantes-Mendez G, Ferrario M, Baselli G, Arbeille P, Shoemaker JK, Greaves DK, Hughson RL, Aletti F. Comparison of baroreflex sensitivity gain during mild lower body negative pressure in presence and absence of long duration bed rest. Comput Cardiol. 2013b.

Ebert TJ. Sympathetic and hemodynamic effects of moderate and deep sedation with propofol in humans. Anesthesiology. 2005; 103(1): 20-4.

Eckberg DL, Fritsch JM. Influence of ten-day head-down bedrest on human carotid baroreceptor-cardiac reflex function. Acta Physiol Scand Suppl. 1992; 604:69-76.

Epstein M. Cardiovascular and renal effects of head-out water immersion in man: application of the model in the assessment of volume homeostasis. Circ Res. 1976; 39(5):619-28.

Faes L, Nollo G. Assessing frequency domain causality in cardiovascular time series with instantaneous interactions. Methods Inf Med. 2010; 49(5):453-7.

Ferrario M, Aletti F, Dorantes Mendez G, Toschi N, Guerrisi M, Canichella A, Cerutti S, Della Badia Giussi F, Sabato E, Coniglione F, Dauri M, Sabato AF. Intraoperative monitoring of cardiovascular autonomic control responsiveness. Journal of Critical Care 27(3), 10th International Conference on Complexity in Acute Illness (ICCAI), 2011.

Ferretti G, Iellamo F, Pizzinelli P, et al. Prolonged head down bed rest-induced inactivity impairs tonic autonomic regulation while sparing oscillatory cardiovascular rhythms in healthy humans. J Hypertens. 2009; 27(3):551-61.

Floras JS, Butler GC, Ando SI, Brooks SC, Pollard MJ, and Picton P. Differential sympathetic nerve and heart rate spectral effects of nonhypotensive lower body negative pressure. Am J Physiol Regul Integr Comp Physiol. 2001; 281: R468-R475.

Foëx P and Sear J. The surgical hypertensive patient. Continuing Education in Anaesthesia, Critical Care & Pain. 2004; 4(5):139-43.

Fox SI. Human Physiology 12th ed. 2006. The McGraw-Hill.

Freeman R. Assessment of cardiovascular autonomic function. Clinical Neurophysiology. 2006; 117(4):716-30.

Fritsch-Yelle JM, Whitson PA, Bondar RL, Brown TE. Subnormal norepinephrine release relates to presyncope in astronauts after spaceflight. J Appl Physiol. 1996; 81(5):2134-41.

Fu Q, Shibata S, Hastings JL, Prasad A, Palmer MD, Levine BD. Evidence for unloading arterial baroreceptors during low levels of lower body negative pressure in humans. Am J Physiol Heart Circ Physiol. 2009; 296(2):H480-8.

Gauer OH, Sieker HO. The continuous recording of central venous pressure changes from an arm vein. Circ Res. 1956; 4:74-78.

Goepfert MS, Reuter DA, Akyol D, Lamm P, Kilger E, Goetz AE. Goal-directed fluid management reduces vasopressor and catecholamine use in cardiac surgery patients. Intensive Care Med. 2007; 33(1):96-103.

Grassi G, Cattaneo BM, Seravalle G, Lanfranchi A, Mancia G. Baroreflex control of sympathetic nerve activity in essential and secondary hypertension. J Hypertens. 1998; 31:68-72.

Grassi G, Seravalle G, Quarti-Trevano F, Dell'Oro R, Arenare F, Spaziani D, Mancia G. Sympathetic and baroreflex cardiovascular control in hypertension-related left ventricular dysfunction. Hypertension. 2009; 53(2):205-9.

Greene N. Preanesthetic blood pressure determinations. Anesth Analg. 1963; 42(2):454-462.

Greene NM. Physiology of Spinal Anesthesia. Baltimore: Williams and Wilkins, 1958.

Grocott MP, Mythen MG, Gan TJ. Perioperative fluid management and clinical outcomes in adults. Anesth Analg. 2005; 100(4):1093-106.

Guinet P, Schneider SM, Macias BR, Watenpaugh DE, Hughson RL, Le Traon AP, Bansard JY, Hargens AR. WISE-2005: effect of aerobic and resistive exercises on orthostatic tolerance during 60 days bed rest in women. Eur J Appl Physiol. 2009; 106:217–227.

Guyenet PG. The sympathetic control of blood pressure. Nat Rev Neurosci. 2006; 7(5):335-46.

Guyton AC, Hall J. Textbook of medical physiology. 11th ed. 2006. Elsevier Saunders.

Guyton, A. C., Coleman, T. G. & Granger, H. J. Circulation: overall regulation. Annu. Rev. Physiol. 1972; 34:13-46.

Haider AW, Larson MG, Franklin SS, Levy D; Framingham Heart Study. Systolic blood pressure, diastolic blood pressure, and pulse pressure as predictors of risk for congestive heart failure in the Framingham Heart Study. Ann Intern Med. 2003; 138(1):10-6.

Hainsworth R. Reflexes from the heart. Physiol. Reviews 1991; 71(3):617-658.

Head GA Cardiac baroreflexes and hypertension. Clin Exp Pharmacol Physiol. 1994; 21(10):791-802.

Hisdal J, Toska K, Flatebo T, Walloe L. Onset of mild lower body negative pressure induces transient change in mean arterial pressure in humans. Eur J Appl Physiol. 2002; 87(3):251-6.

Hisdal J, Toska K, Walloe L. Beat-to-beat cardiovascular responses to rapid, low-level LBNP in humans. Am J Physiol Regul Integr Comp Physiol. 2001; 281(1):R213-21.

Hodges GJ, Mattar L, Zuj KA, Greaves DK, Arbeille PM, Hughson RL, Shoemaker JK. WISE-2005: prolongation of left ventricular pre-ejection period with 56 days head-down bed rest in women. Exp Physiol. 2010; 95:1081-1088.

Hofer CK, Senn A, Weibel L, Zollinger A. Assessment of stroke volume variation for prediction of fluid responsiveness using the modified FloTrac and PiCCOplus system. Crit Care. 2008; 12(3):R82.

Howell SJ, Sear JW, Foëx P. Hypertension, hypertensive heart disease and perioperative cardiac risk. Br J Anaesth. 2004; 92(4):570-83.

Hughson R, O'Leary D, Shoemaker JK, Lin D, Topor Z, Edwards M, et al. Searching for the vascular component of the arterial baroreflex. Cardiovascular Engineering: An International Journal. 2004; 4(2):155-162.

Hughson RL, Yamamoto Y, Blaber AP, Maillet A, et al. Effect of 28-day head-down bed rest with countermeasures on heart rate variability during LBNP. Aviat Space Environ Med. 1994; 65(4):293-300.

Hyndman BW, Kitney RI, Sayers BM. Spontaneous rhythms in physiological control systems. Nature. 1971; 233(5318):339-41.

Imholz BPM, Wieling W, van Montfrans GA, Wesseling KH. Fifteen years experience with finger arterial pressure monitoring: Assessment of the technology. Cardiovasc Res. 1998; 38(3):605-16.

Iwasaki KI, Zhang R, Zuckerman JH, Pawelczyk JA, Levine BD. Effect of head-down-tilt bed rest and hypovolemia on dynamic regulation of heart rate and blood pressure. Am J Physiol Regul Integr Comp Physiol. 2000; 279(6):R2189-99.

Jacobsen TN, Morgan BJ, Scherrer U, Vissing SF, et al. Relative contributions of cardiopulmonary and sinoaortic baroreflexes in causing sympathetic activation in the human skeletal muscle circulation during orthostatic stress. Circ Res. 1993; 73:367-78.

Johnson JM, Rowell LB, Niederberger M, Eisman MM. Human splanchnic and forearm vasoconstrictor responses to reductions of right atrial and aortic pressures. Circ Res. 1974; 34(4):515-24.

Kanters JK, Højgaard MV, Agner E, Holstein-Rathlou NH. Short- and long-term variations in non-linear dynamics of heart rate variability. Cardiovasc Res. 1996; 31(3):400-9.

Keyl C, Schneider A, Dambacher M, Wegenhorst U, Ingenlath, M, Gruber M, Bernardi L. Dynamic cardiocirculatory control during propofol anesthesia in mechanically ventilated patients. Anesth Analg. 2000; 91(5):1188-95.

Khoo MCK. Physiological control systems: analysis, simulation and estimation. Piscataway, NJ: Wiley/IEEE Press; 2000.

Kimmerly DS, Shoemaker JK. Hypovolemia and neurovascular control during orthostatic stress. Am J Physiol Heart Circ Physiol. 2002; 282(2):H645-55.

Krasowski MD, Harrison NL. General anaesthetic actions on ligand-gated ion channels. Cell Mol Life Sci. 1999; 55(10):1278-1303.

La Rovere MT, Maestri R, Robbi E, Caporotondi A, Guazzotti G, Febo O, Pinna GD. Comparison of the prognostic values of invasive and noninvasive assessments of baroreflex sensitivity in heart failure. J Hypertens. 2011; 29(8):1546-52.

La Rovere MT, Pinna GD, Raczak G. Baroreflex sensitivity: measurement and clinical implications. Ann Noninvasive Electrocardiol. 2008; 13(2):191-207.

Lamia B, Chemla D, Richard C, Teboul JL. Clinical review: Interpretation of arterial pressure wave in shock states. Critical Care. 2005; 9(6):601-6.

Lazaridis C. Advanced hemodynamic monitoring: principles and practice in neurocritical care. Neurocrit Care. 2012; 16(1):163-9.

Levine BD, Zuckerman JH, Pawelczyk JA. Cardiac atrophy after bed-rest deconditioning: a nonneural mechanism for orthostatic intolerance. 1997; Circulation 96:517–525.

Lollgen H, Dirschedl P, Koppenhagen K, Klein KE. Cardiac factors in orthostatic hypotension. Acta Astronaut. 1992; 27:93-5.

Mancia G, Mark AL. A. Arterial baroreflexes in humans. In Handbook of physiology, the cardiovascular system, peripheral circulation and organ blood flow. 1983; Bethesda, MD: American Physiological Society.

Marik P, Monnet X, Teboul J. Hemodynamic parameters to guide fluid therapy. Ann Intensive Care. 2011; 1:1.

Mark AL, Mancia G. Cardiopulmonary baroreflexes in humans. In: Handbook of Physiology. The cardiovascular system. Peripheral circulation and organ blood flow. Bethesda,MD. Am. Physiol. Soc. 1983 sect.2, vol. III, pt. 2, chapt. 21, 795-813.

Marmarelis VZ. Identification of nonlinear biological systems using Laguerre expansion of kernels. Ann Biomed Eng. 1993; 21:573-89.

Mathews L, Singh KR. Cardiac output monitoring. Ann Card Anaesth. 2008; 11:56-68.

Matsukawa T, Gotoh E, Hasegawa O, Shionoiri H, Tochikubo O, Ishii M. Reduced baroreflex changes in muscle sympathetic nerve activity during blood pressure elevation in essential hypertension. J Hypertens. 1991; 9:537–542.

Michard F, Lopes MR, Auler JO Jr. Pulse pressure variation: beyond the fluid management of patients with shock. Crit Care. 2007; 11(3):131.

Michard F, Teboul JL. Predicting fluid responsiveness in ICU patients: a critical analysis of the evidence. Chest. 2002; 121:2000–2008.

Middlekauff HR, Nitzsche EU, Hamilton MA, et al. Evidence for preserved cardiopulmonary baroreflex control of renal cortical blood flow in humans with advanced heart failure. A positron emission tomography study. Circulation. 1995; 92(3):395-401.

Moffitt JA, Foley CM, Schadt JC, Laughlin MH, and Hasser EM. Attenuated baroreflex control of sympathetic nerve activity after cardiovascular deconditioning in rats. Am J Physiol Regulatory Integrative Comp Physiol. 1998; 274: R1397–R1405.

Monnet X, Teboul J. Passive leg raising. Intensive Care Med. 2008; 34(4): 659-63.

Mukkamala R, Kim J, Li Y, Sala-Mercado J, Hammond R, Scislo T, et al. Estimation of arterial and cardiopulmonary total peripheral resistance baroreflex gain values: Validation by chronic arterial baroreceptor denervation. Am J Physiol Heart Circ Physiol. 2006a; 290(5):H1830-6.

Mukkamala R, Reisner AT, Hojman HM, Mark RG, Cohen RJ. Continuous cardiac output monitoring by peripheral blood pressure waveform analysis. IEEE Trans Biomed Eng. 2006b; 53(3):459-67.

Mukkamala R, Toska K, Cohen RJ. Noninvasive identification of the total peripheral resistance baroreflex. Am J Physiol Heart Circ Physiol. 2003; 284(3):H947-59.

Nollo G, Faes L, Porta A, Antolini R, Ravelli F. Exploring directionality in spontaneous heart period and systolic pressure variability interactions in humans: implications in the evaluation of baroreflex gain. Am J Physiol Heart Circ Physiol. 2005; 288(4):H1777-85.

Ogawa Y, Iwasaki K, Shibata S, Kato J, Ogawa S, Oi Y. Different effects on circulatory control during volatile induction and maintenance of anesthesia and total intravenous anesthesia: autonomic nervous activity and arterial cardiac baroreflex function evaluated by blood pressure and heart rate variability analysis. J Clin Anesth. 2006; 18: 87–95.

Ogoh S, Brothers RM, Barnes Q, Eubank WL, Hawkins MN, Purkayastha S, O-Yurvati A, Raven PB. Cardiopulmonary baroreflex is reset during dynamic exercise. J Appl Physiol. 2006; 100(1):51-9.

Pagani M, Lombardi F, Guzzetti S, Rimoldi O, et al. Power spectral analysis of heart rate and arterial pressure variabilities as a marker of sympatho-vagal interaction in man and conscious dog. Circ Res. 1986; 59(2):178-93.

Parati G,Esler M. The human sympathetic nervous system: Its relevance in hypertension and heart failure. Eur Heart J. 2012; 33(9):1058-66.

Patton D, Triedman J, Perrott M, Vidian A, Saul J. Baroreflex gain: characterization using autoregressive moving average analysis. Am J Physiol Heart Circ Physiol. 1996; 270(4):H1240–9.

Pawelczyk JA, Matzen S, Friedman DB, and Secher NH. Cardiovascular and hormonal responses to central hypovolaemia in humans. In: Blood Loss and Shock, edited by Secher NH, Pawelzyk JA, and Ludbrook J. Boston, MA: Little, Brown, pt. 1, chapt. 3, p. 25–36, 1994.

Pawelczyk JA, Raven PB. Reductions in central venous-pressure improve carotid baroreflex responses in conscious men. Am J Physiol. 1989; 257(5):H1389-95.

Pinsky MR, Payen D. Functional hemodynamic monitoring. Crit Care. 2005; 9:566–572.

Porta A, Furlan R, Rimoldi O, Pagani M, Malliani A, van de Borne P. Quantifying the strength of the linear causal coupling in closed loop interacting cardiovascular variability signals. Biol Cybern. 2002; 86(3):241-51.

Prabhu M. Cardiac output measurement. Anaesthesia and Intensive Care Medicine. 2007; 8(2):63-6.

Preisman S, Kogan S, Berkenstadt H, Perel A. Predicting fluid responsiveness in patients undergoing cardiac surgery: functional haemodynamic parameters including the Respiratory Systolic Variation Test and static preload indicators. Br. J. Anaesth. 2005; 95 (6): 746-755.

Prys-Roberts C, Meloche R, Foex P, Ryder A. Studies of anaesthesia in relation to hypertension I: Cardiovascular responses of treated and untreated patients. Br J Anaesth. 1971; 43(2); 122-137.

Ray C, Saito M. The cardiopulmonary baroreflex. In Exercise and circulation in health and disease, edited by Saltin B, Boushel R. Human Kinetics, Champaign, IL, USA. 2000; 43–51.

Raymundo H, Scher AM, O'Leary DS, and Sampson PD. Cardiovascular control by arterial and cardiopulmonary baroreceptors in awake dogs with atrioventricular block. Am J Physiol Heart Circ Physiol. 1989; 257: H2048–H2058.

Rhodes A, Sunderland R. Arterial pulse power analysis, the LiDCO™ plus system. In: Pinsky MR, Pyen D, editors. Functional Hemodynamics. Berlin: Springer Verlag; 2005. p. 183-92.

Robbe HW, Mulder LJ, Ruddel H, Langewitz WA. Assessment of baroreceptor reflex sensitivity by means of spectral analysis. Hypertension. 1987; 10:538-543.

Robinson BJ, Ebert TJ, O'Brien TJ, Colinco MD, Muzi M. Mechanisms whereby propofol mediates peripheral vasodilation in humans. Sympathoinhibition or direct vascular relaxation? Anesthesiology. 1997; 86(1):64-72.

Robinson T, Potter J. Cardiopulmonary and arterial baroreflex-mediated control of forearm vasomotor tone is impaired after acute stroke. Stroke. 1997; 28(12):2357-62.

Rouby JJ,Andreev A,Léger P,Arthaud M,Landault C,Vicaut E,Maistre G,Eurin J,Gandjbakch I,Viars P. Peripheral vascular effects of thiopental and propofol in humans with artificial hearts. Anesthesiology. 1991; 75(1):32-42.

Samain E, Marty J, Gauzit R, Bouyer I, Couderc E, Farinotti R, Desmonts JM. Effects of propofol on baroreflex control of heart rate and on plasma noradrenaline levels. Eur J Anaesthesiol. 1989; 6(5):321-6.

Sato M, Tanaka M, Umehara S, Nishikaw T. Baroreflex control of heart rate during and after propofol infusion in humans. Br J Anaesth. 2005; 94: 577–81.

Saul JP, Berger RD, Albrecht P, Stein SP, Chen MH, Cohen RJ. Transfer function analysis of the circulation: unique insights into cardiovascular regulation. Am J Physiol. 1991; 261:H1231-45.

Scheer B, Perel A, Pfeiffer UJ. Clinical review: Complications and risk factors of peripheral arterial catheters used for haemodynamic monitoring in anaesthesia and intensive care medicine. Crit Care. 2002; 6(3):199-204.

Seidel H, Herzel H. Bifurcations in a nonlinear model of the baroreceptor–cardiac reflex. Physica D. 1998; 115(1-2):145–160.

Sellgren J, Ejnell H, Elam M, Pontén J, Wallin BG. Sympathetic muscle nerve activity, peripheral blood flows, and baroreceptor reflexes in humans during propofol anesthesia and surgery. Anesthesiology. 1994; 80 (3):534-44.

Sesso HD, Stampfer MJ, Rosner B, Hennekens CH, Gaziano JM, Manson JE, Glynn RJ. Systolic and diastolic blood pressure, pulse pressure, and mean arterial pressure as predictors of cardiovascular disease risk in Men. Hypertension. 2000; 36(5):801-7.

Sevre K, Lefrandt JD, Nordbly G, Os I, Mulder M, Gans ROB, Rostrup M, Smit A. Autonomic function in hypertension and normotensive subjects. Hypertension. 2001; 37:1351–1356.

Sigaudo-Roussel D, Custaud MA, Maillet A, Guell A, Kaspranski R, Hughson RL, Gharib C, Fortrat JO. Heart rate variability after prolonged spaceflights. Eur J Appl Physiol. 2002; 86:258-265.

Smyth HS, Sleight P, Pickering GW. Reflex regulation of the arterial pressure during sleep in man. A quantitative method of assessing baroreflex sensitivity. Circ Res. 1969; 24(1): 109–121.

Soderstrom T, Stoica P. System identification. Prentice Hall, Englewood Cliffs, NJ. 1988.

Sun JX, Reisner AT, Saeed M, Mark RG. Estimating Cardiac Output from Arterial Blood Pressure Waveforms: a Critical Evaluation using the MIMIC II Database. Computers in Cardiology. 2005; 32:295-298.

Sundlof G, Wallin BG. Effect of lower body negative pressure on human muscle nerve sympathetic activity. J Physiol. 1978; 278: 525–532.

Tavernier B, Makhotine O, Lebuffe G, Dupont J, Scherpereel P. Systolic pressure variation as a guide to fluid therapy in patients with sepsis-induced hypotension. Anesthesiology 1998; 89: 1313–21.

Taylor JA, Halliwill JR, Brown TE, Hayano J, Eckberg DL. Nonhypotensive hypovolemia reduces ascending aortic dimensions in humans. J Physiol-London. 1995; 483(1):289-98.

TenVoorde B.J, Kingma R. A baroreflex model of short term blood pressure and heart rate variability. Stud. Health Technol Inform. 2000; 71:179–200.

Thomas GD. Neural control of the circulation, Adv Physiol Educ. 2011; 35(1):28-32.

Thompson CA, Ludwig DA, Convertino VA. Carotid baroreceptor influence on forearm vascular-resistance during low-level lower-body negative-pressure. Aviat Space Environ Med. 1991; 62(10):930-3.

Thompson CA, Tatro DL, Ludwig DA, Convertino VA. Baroreflex responses to acute changes in blood volume in humans. Am J Physiol. 1990; 259(4):R792-8.

Toschi N, Canichella A, Coniglione F, Sabato E, Della Badia F, Dauri M. Intraoperative haemodynamic monitoring: A pilot study on integrated data collection, processing and modelling for extracting vital signs and beyond. Applied Sciences in Biomedical and Communication Technologies (ISABEL) 3rd International Symposium. 2010.

Triedman JK, Cohen RJ, Saul JP. Mild hypovolemic stress alters autonomic modulation of heart rate. Hypertension. 1993; 21: 236-247.

Vallais F, Baselli G, Lucini D, Pagani M, Porta A. Spontaneous baroreflex sensitivity estimates during graded bicycle exercise: a comparative study. Physiol Meas. 2009; 30(2): 201-13.

Varon J, Mark P E. Perioperative hypertension management. Vascular health and risk management. 2008; 4(3):615-627.

Vatner SF, Boettcher DH, Heyndrickx GR, McRitchie RJ. Reduced baroreflex sensitivity with volume loading in conscious dogs. Circ Res. 1975; 37: 236-242.

Vatner SF, Zimpfer M. Bainbridge reflex in conscious, unrestrained, and tranquilized baboons. Am J Physiol. 1981; 240(2):H164-7.

Vernikos J and Convertino VA. Advantages and disadvantages of fludrocortisone or saline load in preventing post-spaceflight orthostatic hypotension. Acta Astronaut. 1994; 33: 259–266.

Victor RG, Leimbach WN Jr. Effects of lower body negative pressure on sympathetic discharge to leg muscles in humans. J Appl Physiol. 1987; 63(6):2558-62.

Wang H, Ju K, Chon KH. Closed-loop nonlinear system identification via the vector optimal parameter search algorithm: application to heart rate baroreflex control. Med Eng Phys. 2007; 29(4):505-15.

Waters WW, Ziegler MG, Meck JV. Postspaceflight orthostatic hypotension occurs mostly in women and is predicted by low vascular resistance. J Appl Physiol. 2002; 92(2):586-94.

Weisenberg M, Sessler D I, Tavdi M, Gleb M, Ezri T, Dalton J E, et al. Dose-dependent hemodynamic effects of propofol induction following brotizolam premedication in hypertensive patients taking angiotensin-converting enzyme inhibitors. J Clin Anesth. 2010; 22(3): 190-195.

Wessel N, Voss A, Malberg H, Ziehmann C, Voss HU, Schirdewan A, Meyerfeldt U, Kurths J. Nonlinear analysis of complex phenomena in cardiological data. Herzschr Elektrophys. 2000; 11:159-173.

Wesseling KH, Jansen JR, Settels JJ, Schreuder JJ. Computation of aortic flow from pressure in humans using a nonlinear, three-element model. J Appl Physiol. 1993; 74(5):2566-73.

Wesseling KH, Settels JJ. Baromodulation explains short-term blood pressure variability. In: Psychophysiology of cardiovascular control. Models, methods and data. Plenum Publishing Corporation. 1985; 69-97.

Wesseling KH. A century of noninvasive arterial pressure measurement: from Marey to Peñáz and Finapres. Homeostasis. 1995; 36:50–66.

Wolthius R, Bergman S, Nicogossian A. Physiological effects of locally applied reduced pressure in man. Physiol Rev. 1974; 54:566-595.

Wyller VB, Barbieri R, Saul JP. Blood pressure variability and closed-loop baroreflex assessment in adolescent chronic fatigue syndrome during supine rest and orthostatic stress. Eur J Appl Physiol. 2011; 111(3):497-507.

Xiao X, Mukkamala R, Sheynberg N, Williams GH, Cohen RJ. Effects of prolonged bed rest on the total peripheral resistance baroreflex. Comput Cardiol. 2002; 29:53-6.

Xu H, Aibiki M, , Yokono S, Ogli K. Dose-dependent effects of propofol on renal sympathetic nerve activity, blood pressure and heart rate in urethane-anesthetized rabbits. Eur J Pharmacol. 2000; 387(1) 79-85.

Yuan M, Coupé M, Bai Y, Gauquelin-Koch G, Jiang S, Aubry P, Wan Y, Custaud MA, Li Y, Arbeille P. Peripheral arterial and venous response to tilt test after a 60-day bedrest with and without countermeasures (ES-IBREP). PLoS One. 2012; 7(3):e32854.

Zhuo H, Ichikawa H, Helke CJ. Neurochemistry of the nodose ganglion. Prog Neurobiol. 1997; 52(2):79-107.

Zong W, Heldt T., Moody G.B., Mark R.G. An open-source algorithm to detect onset of arterial blood pressure pulses. Computers in Cardiology. 2003; 30:259-262.